AFCRL - 69-0393

A PROGRAM TO ACQUIRE ENVIRONMENTAL FIELD DATA IN FOUR AREAS IN A HUMID SUBTROPIC ENVIRONMENT

John E. Walker
Cornell Aeronautical Laboratory, Incorporated
Buffalo, New York, 14221

Contract No. F 19628-68-C0339

Project No. 7628
Task No. 762803
Work Unit No. 76280301

FINAL REPORT

Period Covered: 1 May 1968 - 31 August 1969

November 1969

Carlton Molineux
Terrestrial Sciences Laboratory

Prepared
For

Air Force Cambridge Research Laboratories
Office of Aerospace Research
United States Air Force
Bedford, Massachusetts 01730

AFCRL - 69-0393

A PROGRAM

TO

ACQUIRE ENVIRONMENTAL FIELD DATA

IN

FOUR AREAS IN A HUMID SUBTROPIC ENVIRONMENT

John E. Walker
Cornell Aeronautical Laboratory, Incorporated
Buffalo, New York, 14221

Contract No. F 19628-68-C0339

Project No. 7628
Task No. 762803
Work Unit No. 76280301

FINAL REPORT

Period Covered: 1 May 1968 - 31 August 1969

November 1969

Carlton Molineux
Terrestrial Sciences Laboratory

Prepared
For

Air Force Cambridge Research Laboratories
Office of Aerospace Research
United States Air Force
Bedford, Massachusetts 01730

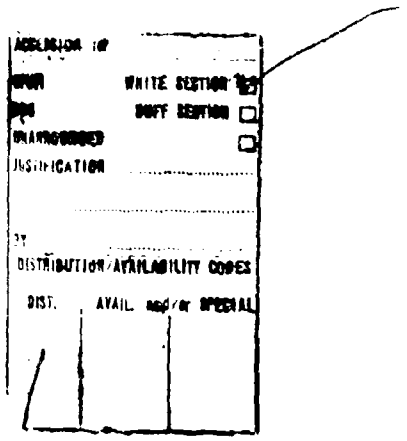

Qualified requestors may obtain additional copies from the Defense Documentation Center. All others should apply to the Clearinghouse for Federal Scientific and Technical Information.

ABSTRACT

Multi-band remote sensing provides a means of obtaining signatures for natural earth objects and backgrounds. The Terrestrial Sciences Laboratory (CRJ), Air Force Cambridge Research Laboratories (AFCRL) collected multiband data from four humid tropical enviroments in Puerto Rico. The Cornell Aeronautical Laboratory, Incorporated (CAL) collected field data and performed a limited quantitative analysis toward the objective of defining terrain signatures. Irradiance, spectral reflectance, surface temperature, soil moisture, soil granularity, air temperature, humidity, wind speed and direction measurements and ground photographs were obtained. The limited analysis resulted in the development of bi-band methodology for determing whether variations in film image density of soil are caused by surface moisture or surface structure. If the ratio of the average exposures (low/high) of two images of soil in the blue region of the spectrum ($\sim .50\mu$) is equal to or greater than their exposure ratios in the near infrared ($\sim 0.80\mu$) the difference is attributable to surface structure; if less, then the cause is surface moisture. The results also suggest that for surface structure, the absolute value of the ratio can be related to the amount of textural difference between the surfaces. It is concluded that an electro-optical multi band analysis system using bi-band techniques can be developed to facilitate the Air Force engineer's task of terrain analysis and at the same time provide him with the tools necessary to extend the utility of multi band remote sensing to obtain spectral signatures for other earth objects and backgrounds.

TABLE OF CONTENTS

LIST OF FIGURES

GLOSSARY OF TERMS

Remote sensing of the terrain is truly a multi discipline art and/or science. It is practised by geologists, geographers, engineers and military intelligence analysts. Research efforts often involve physicists and psychologists as well. Because terms used in one discipline are often used in other disciplines but with different connotations, a glossary of terms is generally useful in reporting results.

This report was prepared by a civil engineer with a background in image interpretation and the physics of image formation, which is reflected in many of the terms used in the report. Therefore, terms which may have different connotations in different disciplines are defined below and underlined in the text.

Alluvial soil, beach sand gravely clay, fine sand silty clay

There is agreement on general descriptor of soils such as alluvial, sand, and gravel but there are also significant geological differences between such soil classes. Therefore, wherever a general term such as this is used in this report, it is cross referenced below to the appropriate appendix in which more specific information can be found.

	Soil	Text Page	Appendix Page
Alluvial soil	Colosco Clay	16,18,21	B-16 Location 7
Beach sand	Palm Sand	16,18,24, 25	B-9, B-10 Location 2
Gravely clay	Yaucoa Clay	23,24,25, 26,28,29	B-28 (Yo)
Fine sand	Guayabo fine sand	23,24,29	
Silty clay	Coloso Clay	25,28,29	B-16 Location 7
Beach sand	Palm Sand	39,40,44, 47	B-9 Location 3
Pasture grass	--	41	B-18

(Note: Species could not be identified because of heavy grazing condition)

MANGROVE

Micron (μ)

The term micron used in this report is a unit of length equal to 10^{-6} meters or 10^{-3} millimeters. It has been commonly used as a measure of the wavelength of energy in parts of the electromagnet spectrum in which remote sensors operate. Because other terms[23] are also used for this same unit of length a conversion table is presented below.

	meters	millimeters	
micron	10^{-6}	10^{-3}	micrometer
millimicron	10^{-9}	10^{-6}	nanometer
angstron	10^{-10}	10^{-7}	--

Pasture grass, mangrove

There is agreement on general descriptors of vegetation but there are also significant botanical differences between such vegetation classes. As is explained in the appendices, species were not determined on this effort, but other details are presented and cross referenced below.

	Text	Appendix
Pasture grass	41,43,46	B-18
Mangrove	43,45	B-14, 15

Stabilized beach

A water deposited sand whose surface has been wholly encroached by vegetation (grasses, vines, woody plants and palm trees) to the degree that no erosion by wind can occur.

Term

Surface Moisture

The area of water surfaces present on a terrain surface and within the area of a ground resolution element of a remote sensor. This water may occur in a wide variety of forms such as: a) puddles filling depressions in the ground surface; b) water trapped between soil grains at the surface or water droplets on vegetation.

Surface moisture is not synomomous with the term soil moisture which image interpreters use to define an image that they judge is a wet soil on the ground. Areas of surface moisture which are on the order of the sign of the ground resolution element of a remote sensor are not recorded as an image which the interpreter can identify. An interpreter

requires on the order of five to ten such elements together before he can recognize an image as a specific ground object.

Surface moisture is not synomomous with the geologic term soil moisture content which refers to the percentage of water in a sample of soil by weight. However, it appears that by using prior geologic knowledge of terrain and bi-band remote sensing techniques reliable relationships may be found between these terms, so that soil moisture content can be determined by remote sensing.

Surface structure

Three dimensional variations in a terrain surface within the area of a ground resolution of a remote sensor. Such variations can be caused by differences in vegetation height and density, the presence of boulders, cobbles, or coconuts, or earth scars made by man. These three dimensional variations in the terrain surface affect both the spectral distribution and the intensity of the average radiance detected by a remote sensor in its ground resolution element. However, they are not recorded as specific images by the remote sensor; and therefore the term surface structure is not synomomous with the image interpreter's term soil texture, i.e., the frequency of change and arrangement of (image) tone as defined in Reference 14. Also it is not synomomous with the texture of soil, as defined in Reference 19, which relates to laboratory sieve analysis and other standard soil tests to determine the distribution of

individual partical sizes in a soil sample. However, it appears that by using prior geologic knowledge of the terrain and bi-band remote sensing techniques reliable relationships may be found between this terms, so that soil texture, in the geologic sense can be determined remotely.

1. INTRODUCTION AND SUMMARY

The United States Air Force has the very important mission of evaluating terrain for engineering properties related to uses such as airfields or support facilities development. Preliminary surveys especially in remote areas are conducted using remote sensor data and photogrammetric and interpretation analysis methods.

Multi-band remote sensing techniques can provide new and more precise information about the terrain to aid in the task of terrain evaluation. Deriving spectral signatures for natural earth objects and backgrounds therefore is a major objective of the USAF, and the ultimate objective of this effort.

On this effort, CAL supported Terrestrial Sciences Laboratory of the Air Force Cambridge Research Laboratories [AFCRL (CRJ)] by acquiring field data from four humid tropical environments in Puerto Rico, which was used in a limited analysis of multi-band remote sensor data collected by AFCRL. The field data contained in the Appendices of this report attest to the successful completion of the support objective.

The most significant result obtained from the limited analysis was the development of a bi band spectral technique to allow the image interpreter to determine whether tonal differences of images of soil were caused by surface moisture or surface structure. This result is considered significant because it represents a step toward being able to measure soil moisture and granularity remotely and thus predict bearing strength for facilities development. It also strengthens CAL's hypothesis that the answer to the successful utilization of multi-band data, remotely sensed, lies in the proper selection of a limited number of spectral bands, of proper band width, whose spectral reflectance ratios are unique. In addition, it extends the usefulness of a bi-band spectral signature technique developed by CAL for the basic surface features, water, vegetation and soil.

The basic concept of spectral signatures is discussed in Section 2,

followed by a brief discussion in Section 3 of the major factors in the remote sensing system which affect the observed spectral signatures. Section 4 contains results of this effort with respect to the major factors described in Section 3 including spectral irradiance, spectral reflectance, and sensor limitations. The development of the gross signatures for water, soil and vegetation is discussed in Section 5 followed by the Results and Conclusions for the effort in Section 6.

Processed ground data collected during the effort and technical details of the analyses are included in Appendices.

2. BASIC CONCEPT OF SPECTRAL SIGNATURES

The remote sensor can only record the true energy per unit area from an object as measured by ground instrumentation when the two measurement systems have identical sensitivities, have identical geometries of source, objects and detector, and have identical attenuations by outside forces such as the atmosphere. Since these conditions rarely exist in practice, the energy recorded by the remote sensor is referred to here as the apparent energy reflected or emitted by the ground object or background.

What the interpreter observes as image tone or density is a spatially distributed and modulated representation of this energy. CAL has demonstrated in a previous program quantitatively that the tone or density of an image can be related to the average reflected energy from ground objects using appropriate controls. Laboratory measurements of object surface spectral reflectance (Refs. 1-5) have shown that differences in reflectance do occur in nature between ground objects and backgrounds pertinent to variations in object properties such as soil moisture. Therefore, if the apparent energy is sampled in the appropriate spectral regions and displayed as spatial images which the interpreter can recognize, the interpreter can extract information pertinent to his task more rapidly than presently possible and in greater detail.

For example, the interpreter using a grease pencil, stereoscope, and overlay can outline all the images of tree stands in a scene and by planimetry or the block square method, he can measure the area of ground covered by trees. A comparison of such areas at several sites considered for the development of an airfield could be the deciding factor in site selection.

Laboratory reflectance measurements have established that vegetation has spectrally unique properties in two bands when compared to all other earth objects; namely low reflectance in the chlorophyl absorption band at

approximately 0.65μ and high reflectance in the near infrared band at approximately 0.80μ .

Using these spectral signature bands, CAL developed a methodology of photographically preprocessing photographs taken in these two bands to produce a third photograph which does not image vegetation (Ref. 1). Additional research (Ref. 6) led to the development of an electro-optical preprocessing technique which allowed the interpreter to eliminate areas of vegetation selectively, based upon the absolute value of the reflected spectral energy in these two bands. It was noted that grass and brush areas were separated from tree stands by this technique so that a transparency could be obtained which imaged only the latter. Therefore, areas of tree stands can be determined readily by measuring the transmission of the transparency and the tedious, time-consuming interpretation task of preparing grease pencil overlays for mechanical measurements of area can be eliminated.

The same methodology indicated above for vegetation was also applied to images of soil (including rock outcrops) and water bodies, the other two primary natural objects or backgrounds which are present on the earth's surface. The results indicated that for the two spectral bands used, transparencies could be generated which would give the area distribution of both soil and water.

The state-of-the-art of developing and utilizing spectral signature data is in its infancy. The effect of the change of the true spectral energy from an object sensed remotely, caused by the remote sensing system components and conditions must be determined before efficient use can be made of the spectral energy. These factors are discussed in detail in the following section of this report. In Section 5 , Spectral Signatures, the basic concept of spectral signatures described above is applied to spectral film obtained on this effort and the significant results with respect to terrain analysis by remote sensing are presented.

3. FACTORS AFFECTING REMOTE SENSING FOR SPECTRAL SIGNATURES

To many, placing a band pass filter on an aerial camera lens yields a spectral, aerial photographic, sensing system that will produce a photograph on which differences in image densities are attributable to the reflectance properties of the ground objects at this wavelength. To illustrate how the validity of this assumption is affected by the other factors, Figure 1 has been prepared to diagram a complete system.

The sun is the source of the energy for the system. Its intensity and spectral distribution have been the subject of much research culminating in a generally agreed upon and useable standard by the scientific community (Ref. 7).

The earth however, is surrounded by an atmosphere which attenuates the energy from the sun as well as the reflected energy returning from ground objects (Ref. 8). These attenuations factors have also been the subject of considerable research (Ref. 9); however, less agreement is found in the scientific community regarding the attenuation effects of the atmosphere than the intensity and spectral distribution of the sun outside our atmosphere.

The reflectance of an object is defined broadly in terms of the ratio of the energy reflected by the object to the energy incident upon it. Since basically the reflected energy produces the image density of the ground object, the density is therefore dependent upon the intensity and spectral distribution of the incident energy. Some objects in an aerial photographic scene will receive direct solar illumination whereas others, because of surrounding taller objects, will receive indirect illumination (shadow areas). The intensity and spectral spectral distribution of the latter is extremely difficult to predict because it is composed primarily of skylight (which depends on cloud conditions) and the light reflected from surrounding objects. Finally, when cloud shadows are present within the scene, objects are illuminated partially

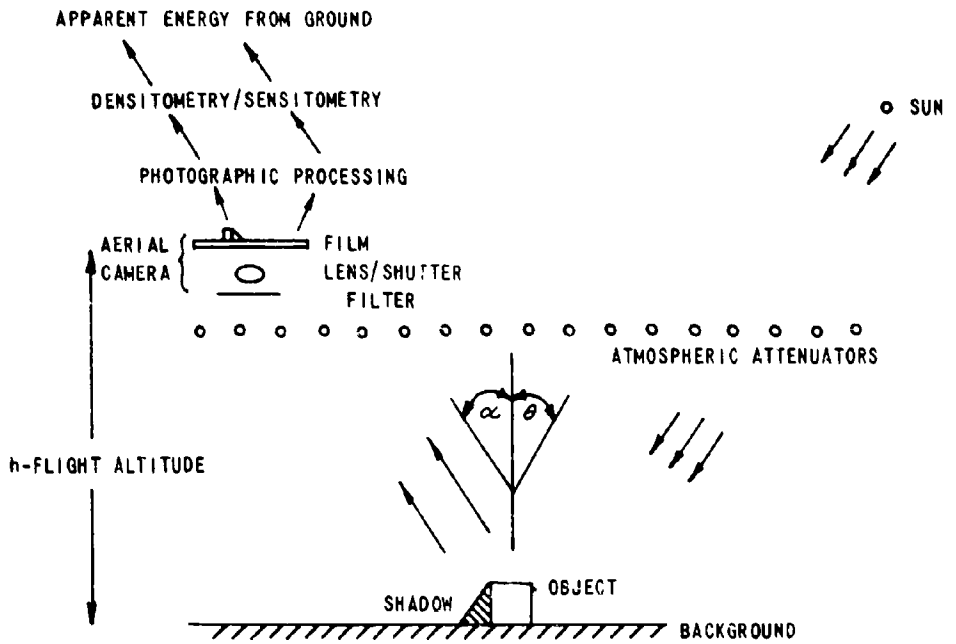

Figure 1 BASIC AERIAL PHOTOGRAPHIC SPECTRAL SYSTEM

by direct illumination and partially by indirect illumination. Again, this is a difficult illumination condition for predicting intensity and spectral distribution. However, if a natural object of known spectral reflectance appears in the photographic scene under each condition of illumination, the differences in reflected energy for cloud and structure shadow conditions relative to direct sunlight could be determined from the densities of the images. As will be discussed in Section 4.2.6, vegetation has been considered in this study as a potential natural standard reflectance reference.

The definition of object reflectance used above is very general. Most real objects reflect energy differently in all directions, depending upon surface geometry and the geometry of the source, object and detector. Real objects are generally not ideal diffuse or specular reflectors. Laboratory measurements of object reflectance are generally standardized, but do not include the in situ geometry of the objects of interest or the specific geometry of source, object and detector for all situations which are likely to be encountered. Therefore, laboratory or even in situ ground measurements of object reflectance are at best a poor standard with which to judge the accuracy or precision of measurements made using an aerial photographic system, as will be discussed further in Section 4.2.1.

Finally, the photographic system itself affects the apparent reflectance of a ground object as derived from its image density.

If the spectral filters are of the interference type employing dielectric coatings, the transmittance peak shifts to shorter wavelengths with increasing off-axis angles. This effect is generally small for objects close to the axis of the system. For objects considerably off axis, corrections can be applied if needed.

Gelatin filters between optical quality glass have essentially no effect on image density in this respect. However, narrow band passes must be achieved by combining two or more filters which can result in internal reflections

which add to the flare light of the system. Gelatin filters unmounted tend to wrinkle, introducing more flare and distortion than the glass-mounted variety.

Lenses have some degree of transmission fall-off as the angle off-axis increases. The effect on image density is small for good quality lenses. Lenses are generally focused for imaging energy received in the red-green portion of the spectrum. Multi-band aerial cameras have independent lenses for each spectral region sensed. Refocusing is required if such lenses are to be used with blue or near infrared energy, in order to match the ground resolution capability of each lens/film combination. Thus the same ground objects will be imaged with the same degree of detail by each lens system and the resultant image densities will be truly related to the object reflectance properties in each spectral band.

The shutter characteristics of the camera are also important if quantitative reflectance data are to be derived from the imagery. The between-the-lens shutter exposes every point in the photographic scene essentially simultaneously, whereas the focal plane shutter exposes a line at a time as it moves across the film format. The latter is undesirable because variations in the speed of the shutter across the format introduces variations in image densities across the format. In some cameras, these variations are severe enough to cause visible density bands on the photographs.

Film processing can also be a source of major error, especially where rewind processing is employed. The relationship between image density and the exposure will vary considerably over the entire length of the roll of film being processed. If continuous processing is used, errors of this nature are minimized.

A scanning microdensitometer is generally used to measure the densities of images of ground objects on the filtered films and is another important consideration in deriving quantitative reflectance data. The scanning slit

aperture size must be selected which is of the proper size to yield an average value of density for the object of interest. If the object is large relative to the ground resolution element of the system and has no internal pattern or structure, aperture size is not critical. However, most natural objects of interest do have structure or internal patterns so that the averaging effect of the aperture selection must be considered.

Obviously, there are many factors which must be considered in a complete aerial spectral sensing system. Some of the factors considered above are also important with respect to scanning systems operating in the infrared and ultraviolet such as the atmospheric attenuations, and film processing. Different factors are also introduced by changing the principle of the sensor system, such as the transfer function of the electronic components of such systems.

Under this research effort, only spectral sensors operating in the visible (0.4 microns to 0.7 microns) near infrared (0.7 to 0.9 microns) and intermediate infrared (3.0 to 5.0 microns) regions of the spectrum have been employed. The factors discussed above were considered in every phase of the effort from the planning of the data collection program through the limited analysis effort.

4. RESULTS PERTINENT TO SPECTRAL SIGNATURES FOR NATURAL EARTH OBJECTS AND BACKGROUNDS

Deining signatures for natural earth objects and backgrounds is the ultimace objective toward which this research effort was directed. It was planned that this effort would produce quality data and techniques for analyses to derive signatures. The data contained in the Appendices of this report and the films from the spectral camera and infrared scanner attest to the successful data collection. Only one other such data bank is known to exist. (Ref. 10) The establishment of spectral signatures for water, soil and vegetation confirms the value of the quantitative analytical techniques for deriving spectral signatures.

4.1 Spectral Irradiance

On this effort CAL measured the relative irradiance changes throughout the test period. Figure 2 shows the results of these measurements compared to a spectral irradiance curve used by others (Ref. 13). The details of how these curves were derived are presented in Appendix A. In deriving ground object spectral reflectance from film image density the difference in density between an object of known reflectance and an object of interest is measured as described in detail in Section 4.2.6. As long as both images are on the same frame of photography and both in sunlight, the irradiance on both is essentially the same, and therefore does not affect the measurement of relative reflectance. However if the image of known reflectance occurs in one frame and the image of interest is on a previous or subsequent frame irradiance conditions could change and thus effect the measure of relative reflectance. The relative change in irradiance not the absolute change is significant. Therefore, the relative changes in spectral irradiance for each wavelength band were determined from the data for Figure 2 for corresponding changes

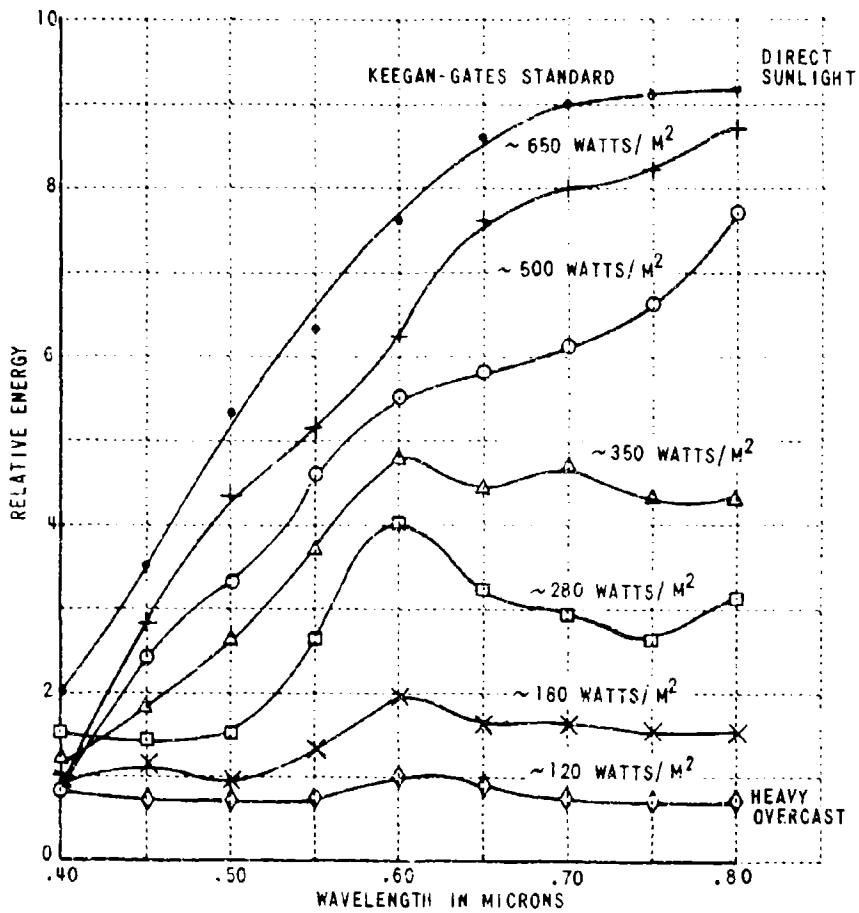

Figure 2 SPECTRAL IRRADIANCE

in total irradiance. As shown in Figure 3 the changes in spectral irradiance tend to follow the 45° correlation line, but variations as large as a factor of 2 occur which could result in errors of the same magnitude in reflectance calculations based upon a one to one correlation between changes in spectral irradiance and total irradiance. In plotting these data it was noted that in the blue region of the spectrum (+) practically all points fell above the one to one correlation line suggesting that corrections to be used in deriving ground object reflectance, and based upon a measurement of a change in total irradiance would always be in one direction. Beyond 0.45μ , each band appeared to be below the correlation line for small changes in total irradiance at low irradiance levels and above the line for changes greater than .50 at high total irradiance levels. Changes in total irradiance greater than .5 at total irradiance levels on the order of 300 watts/ m^2 or less appear to lower the curve for high level irradiance so that all points fall below the correlation line. The only spectral irradiance band in which changes in spectral irradiance correlated well with changes in total irradiance was the .65μ band at high levels of total irradiance. Each set of wavelength dependent data plotted in Figure 3, is replotted in separate figures (A 4 through A 11) in Appendix A.

Because only a limited analysis could be undertaken of the irradiance data collected the statistical validity of the results given above can be challenged.

However, in view of the present trend toward the development of multispectral remote sensing systems for obtaining information pertinent to earth objects and backgrounds, it is necessary that the effects of changes in irradiance be evaluated fully to design a workable analysis system. Therefore it is recommended that research be undertaken to establish the degree to which the results above can be generalized for other geographic areas, times of day and sky conditions.

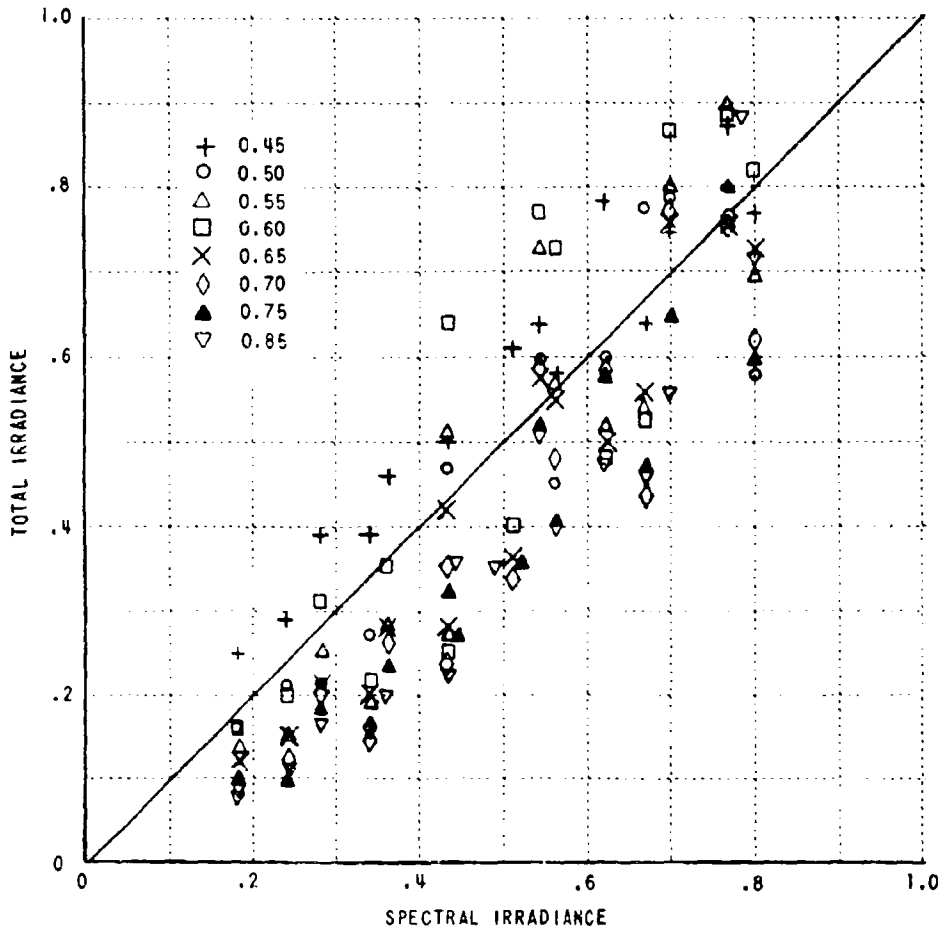

Figure 3 CORRELATION OF TOTAL IRRADIANCE TO SPECTRAL IRRADIANCE

4.2 Spectral Reflectance of Natural Earth Objects and Backgrounds

As pointed out in Section 2, studies over the years have shown that natural earth objects do exhibit spectral reflectance differences which are of significance in terrain analysis. Therefore, many research efforts have been undertaken with the ultimate objective of developing a remote sensing system to exploit these differences. Most of these efforts have concentrated on only one or a few of the numerous factors which affect the image density of an object on aerial film so that results have been highly qualified. By far the greatest number of these efforts concentrated on the measurement of object reflectance. Initially, such measures were made in the laboratory because no field spectrometers existed. Such instruments were built, but correlation of field measures to laboratory measures were infrequent. In 1966, measurements of the reflectance of ground objects from the densities of images on spectrally filtered photographs were made by CAL (Ref. 1). The precision of these measurements was established as $\pm$ 6% of the mean value of reflectance. In addition, this previous effort demonstrated the primary reasons for lack of correlation between measurements of object reflectance from film, in situ and in the laboratory.

The two major factors causing the lack of correlation are inherent differences in the basic geometries of the measuring systems and of the surfaces of the natural objects of interest. Under the present effort, where possible, object reflectance was measured in the laboratory, in situ and from image densities on filtered film exposed in an Itek multiband spectral camera. These data are included in Appendix B.

4.2.1 Geometric Differences in Measurements

Magnesium oxide is the accepted standard for reflectance measurements because its reflectance is high ($\sim$ 98%), it is nearly independent of wavelength and it is nearly a diffuse reflector (i.e., reflections from its surface

obey Lambert's law (Ref. 11).

However, natural earth objects are generally not diffuse reflectors and therefore their reflectance is dependent upon the geometry of the source, object surface and detector. Therefore, measurements of object reflectance (Ref. 12) at all source and detector angles relative to the surface are required to define fully the reflectance properties of an object. The complexity of a device for making such measurements with the precision of existing reflectance instruments and the limited market for its use, has led manufacturers to more or less standardize the geometry of source,surface and detector and utilize an integrating sphere to collect all of the reflected energy from the surface, which yields a single number for total reflectance. Some manufacturers provide a means for deflecting most of the specular component out of the system which then yields a measure of near total diffuse reflectance. The geometry of the natural object, within the ground resolution element of the aerial camera system, influences the apparent reflectance of objects as determined from image density on film.

In general then, the geometry of the small surface areas sampled by the laboratory equipment are not representative of the geometry of the surface areas sampled by the resolution element of a spectral camera system or an in situ field system. Thus strictly on the basis of geometric differences in measuring systems, there is no reason to expect spectral reflectance values determined in the laboratory, in situ, and from aerial image density to correlate well. However, if the factors causing the apparent differences in object conditions are defined, correlations will be possible. Therefore, three basic experiments were conducted on vegetation and soil samples in the laboratory to determine the effect of combinations in a finite sample area and the effect of background on the apparent reflectance of vegetation. These experiments are described briefly in sections 4.2.2, 4.2.3, and 4.2.4.

4.2.2 Soil-Vegetation in Fixed Sample Area

The energy received by an aerial camera and converted to an image density depends on the reflectance properties of objects within the ground resolution element of the system. Assuming the camera system has a ground resolution element of area A_T the total energy reflected by several different objects in the sample area can be expressed as follows:

$$H \cdot \bar{R} \cdot A_T = H \cdot \bar{R}_1 \cdot A_1 + H \cdot \bar{R}_2 \cdot A_2 + \cdots + H \cdot \bar{R}_n \cdot A_n$$

where H = irradiance on area
A = area
R = reflectance

and the subscripts refer to different objects. Then the average reflectance can be expressed as:

$$\bar{R} = \frac{A_1}{A_T} \bar{R}_1 + \frac{A_2}{A_T} \bar{R}_2 + \cdots + \frac{A_n}{A_T} \bar{R}_n$$

To check the validity of this expression, a milk weed leaf was placed in the sample holder of a Beckman DK spectrophotometer and was backed by an alluvial soil sample. The area A_T now becomes the sampling area of the spectrometer. Reflectance was measured with the soil surfa completely covered, 25% exposed, 50% exposed and 75% exposed and finally 100% exposed. The results are shown in Figure 4 where the continuous curves are measured on the Beckman spectrometer and the computed values are shown as points. As can be seen from the figure, excellent agreement is achieved from .5μ - .6μ ; however, considerable disagreement is noted in the far red (0.6μ - 0.7μ) and the near infrared (0.7μ -0.8μ) regions.

A second test was conducted using a beach sand as a backing for a second milkweed leaf sample. Very similar results were obtained as illustrated in Figure 5. Within the visible region of the spectrum (0.4μ -0.7μ) the basic vegetation

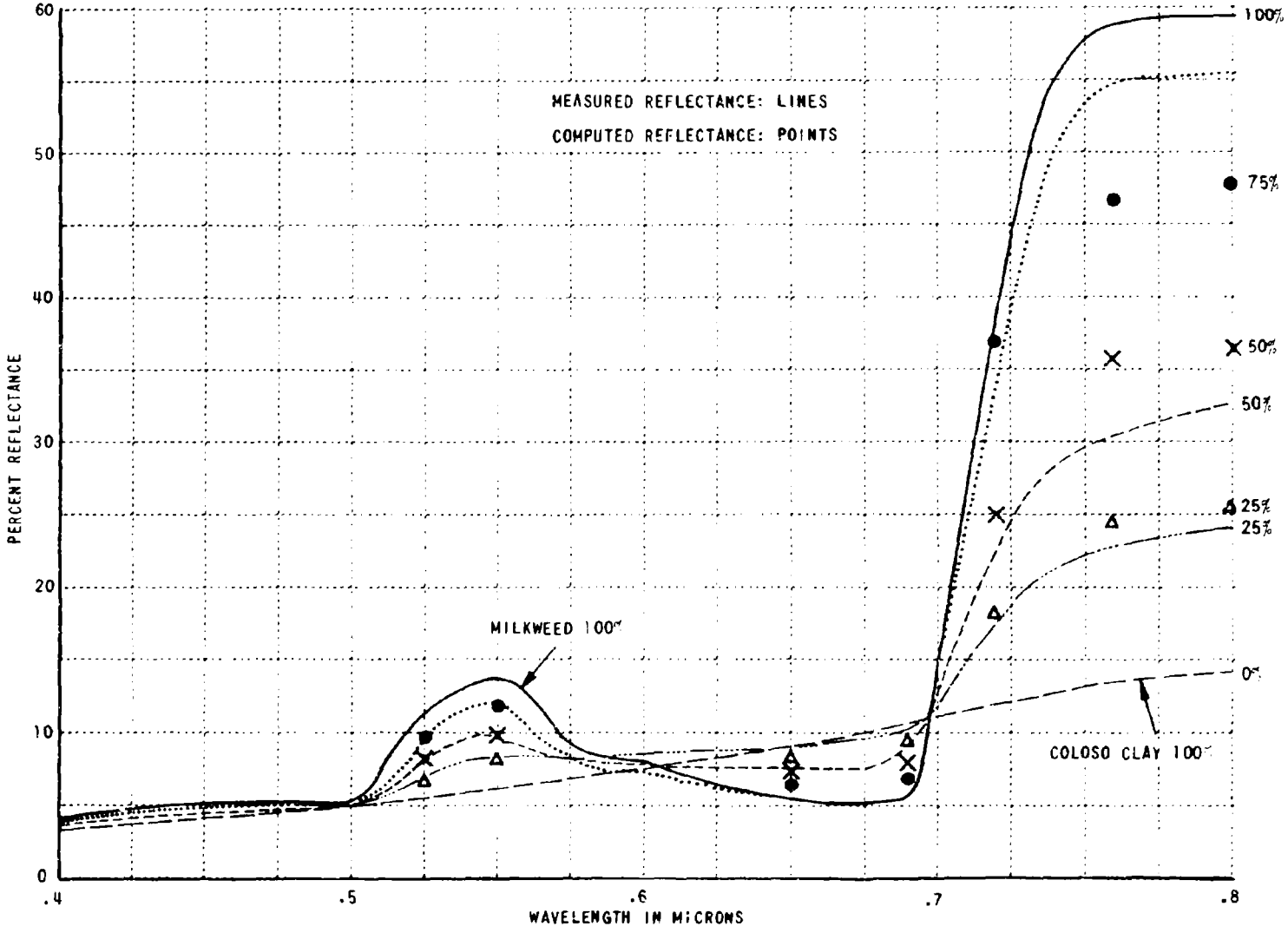

Figure 4 VEGETATION AND ALLUVIAL SOIL IN FIXED SAMPLE AREA

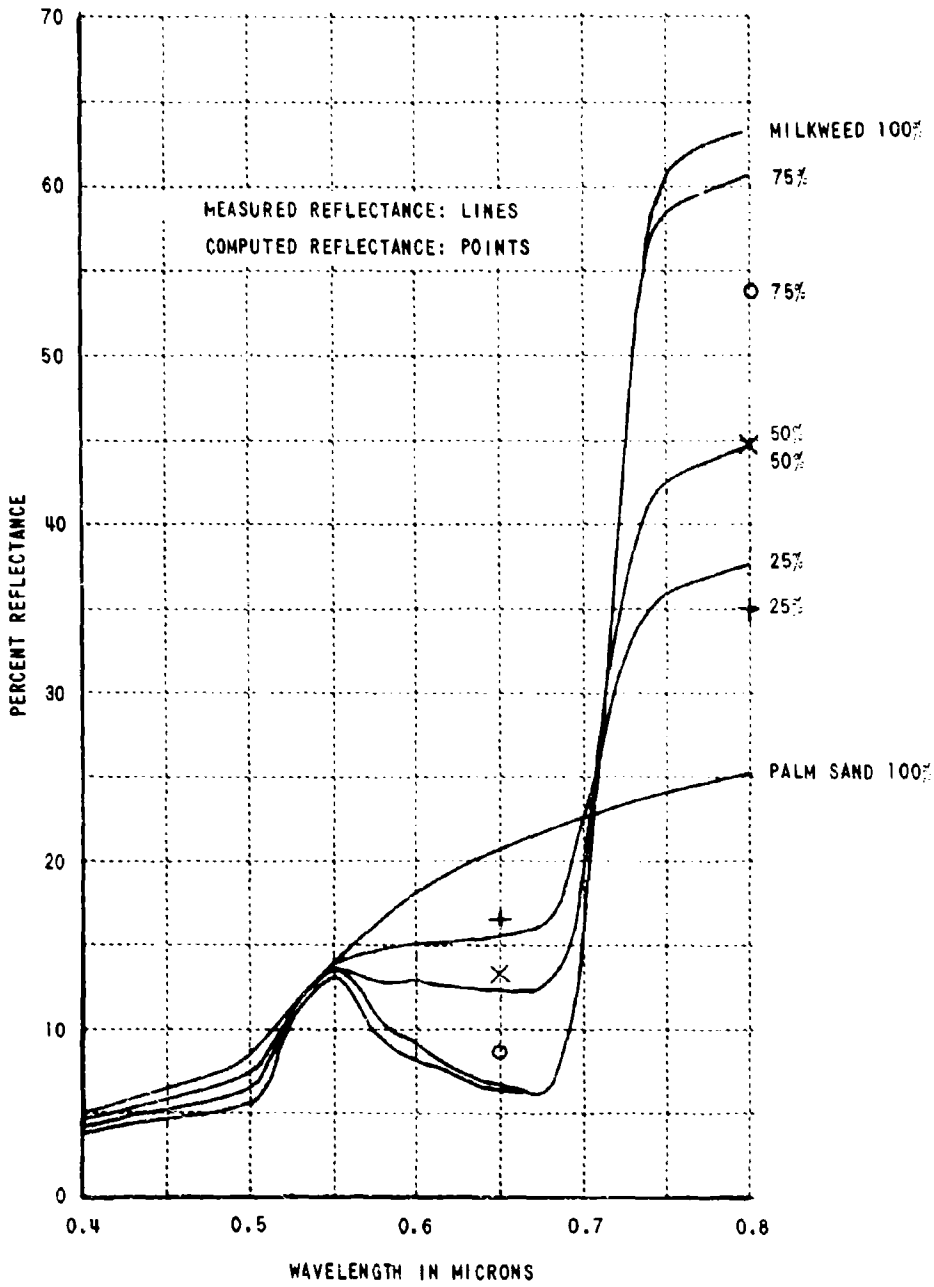

Figure 5 VEGETATION AND SAND IN FIXED SAMPLE AREA

curves are (100% solid line) identical within the precision of the spectrophotometer. Over the near infrared (0.7μ -0.8μ), the curve is on the order of 3-4% higher than the curve shown in Figure 4. This is attributed to a difference in the transmittances of the two leaf samples in this spectral region and therefore indicates the need to consider the transmittance of vegetation in determining the true reflectance of vegetation from spectral films.

Both Figures 4 and 5 illustrate the effect on spectral reflectance of having two different types of objects in the ground resolution element of the spectral camera system. In the case of the alluvial soil, a significant spectral difference occurs in the band near 0.55μ because the reflectance of the soil is approximately half that of vegetation. However, in the case of the beach sand, this reflectance value is nearly equal to that of the leaf in this spectral region (0.54μ) but significant differences occur below $.52\mu$ and beyond 0.55μ between the soil and vegetation curves. Such differences might be utilized to differentiate between the two soil types, provided vegetation type and distribution were the same, however the effects of soil moisture conditions must be considered. These effects are discussed in Section 4.2.4.

The differences between predicted values of reflectance and measured values are attributed primarily to having to remove the sample from the spectrometer for each measurement, in order to remove 1/4, 1/2, and 3/4 of the leaf sample. Thus slightly different areas of soil were exposed each time, and the surface structure change can easily cause the differences noted. Nevertheless, both curves indicate that the effect of two dissimilar objects in the aperture is to yield an area weighted average value of reflectance.

4.2.3 Vegetation Transmission

As indicated in the previous section, vegetation transmits, (Ref. 13) as well as reflects, energy in the near infrared. To illustrate this point, milkweed leaves were stacked over a backing of alluvial soil in layers of varying thickness and the reflectance values were measured. The resultant curves are shown in Figure 6.

Leaves generally absorb energy in the visible region of the spectrum (0.4-0.7μ) to carry out their photosynthesis process. In the .7μ - .9μ region less than 10% of the incident energy is absorbed so that reflected and transmitted energy is generally appreciable (i.e. 30-60%). The transmitted energy is then reflected according to the properties of the backing surface. Upon reaching the bottom surface of the leaf, some is transmitted through to be added to the first reflection and some is reflected back to the second surface for additional reflection, transmission and absorption. However, as the curves in Figure 6 show, a limit is reached rapidly. Since the aerial sensor looks down on vegetation it essentially looks at stacks of leaves. Therefore, if in real life the crowns of broad leaf trees and shrubs have at least the minimum number of stacked leaves to reach this limiting reflectance and the average number of holes in the crowns are the same in the ground resolution element of the camera system, the reflectance as derived from the image density or filtered film should be a constant.

Data such as the average number of leaves in a vertical profile of tree crowns and the average number and size of holes in the crowns is not normally obtained in a forest survey and was beyond the scope of this effort. Therefore, the assumptions regarding these properties of vegetation cannot be substantiated.

The only evidence that can be presented at this time which tends to substantiate these assumptions is given in Section 5, Signatures of Earth Objects and Background, where the majority of broad leaf vegetation is

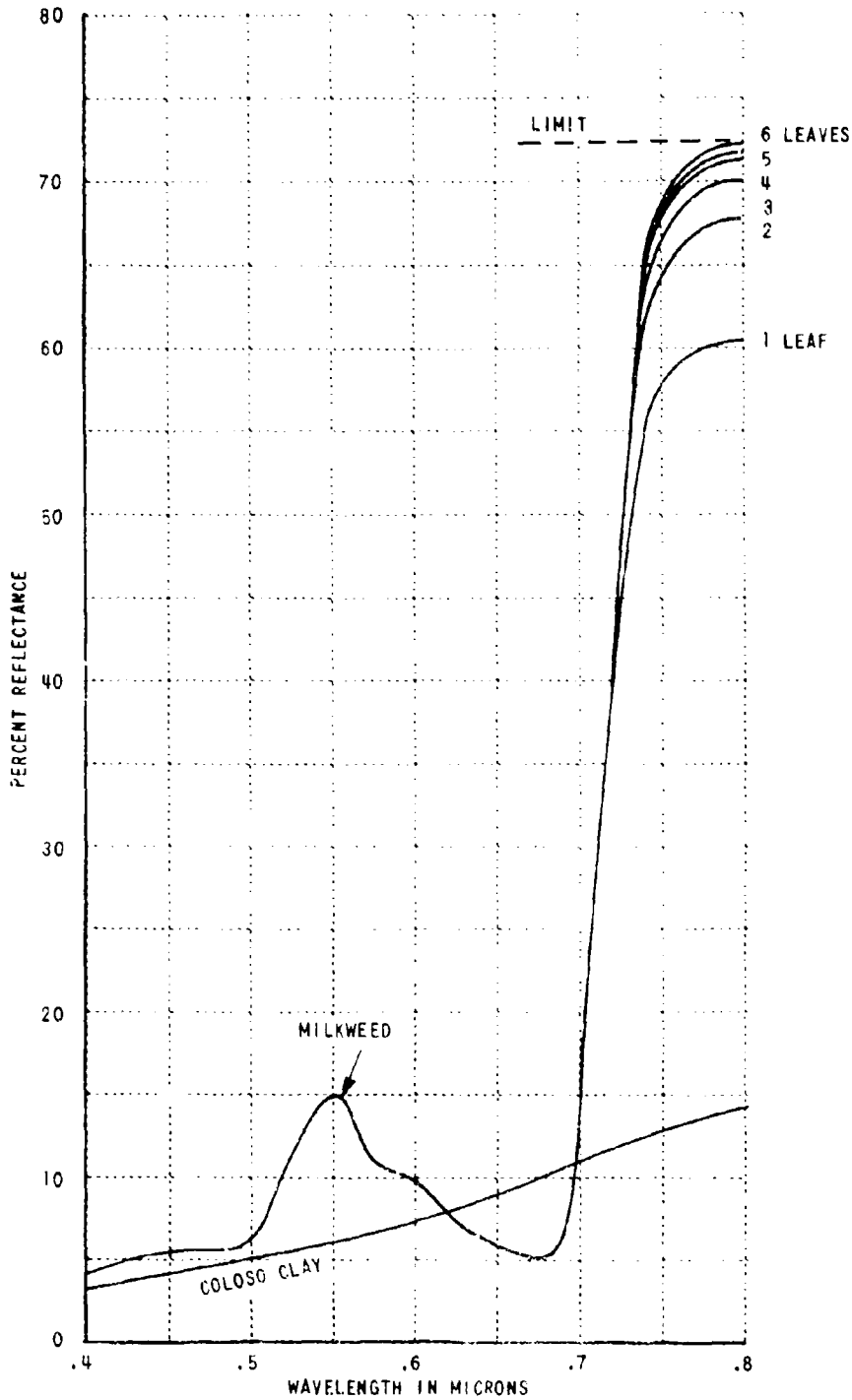

Figure 6 EFFECTIVE LEAF THICKNESS

eliminated from an aerial photographic scene by using the reflectance properties of the vegetation in a spectral band in the visible and one in the near infrared. This would not be possible, if the reflectance properties of these large areas of different types of vegetation were not the same in the two bands, as measured by the density of their images on the two films.

Inasmuch as the terrain analyst in comparing sites for facilities development generally encounters vegetation and must consider its potential as a construction material, the cost of removal, the type of equipment required and many other factors, additional research into how multi-band sensing can assist him is recommended.

4.2.4 Soil Moisture and Granularity

Judgments of soil moisture and granularity (surface texture) are commonly made by photo interpreters. Moisture is judged by tonal differences in soil images, whereas granularity is judged by the edge gradient of soil areas which have been subject to erosion and the number and patterns of surface drainage features present (Refs. 14, 15). Both moisture and granularity are terrain properties of major significance with respect to site selection and engineering evaluation because of their relationship to the bearing strength of soil and the usefulness of soil as a construction material.

Because of the general agreement of interpreters that soil moisture variations are more readily identified by their uniquely dark tones on near infrared photographs than on conventional visible light photographs it appears that multi band photographs might yield a means of obtaining a signature for soil moisture.

The spectral reflectance characteristics of soil samples collected during the field exercises in Puerto Rico were measured on a Beckman DK-2A spectrophotometer. The measurements were made on both wet and dry soil samples.

The results agreed well with published data (4), and confirmed that when moisture is added to a soil its reflectance is reduced. Appendix B contains tables of these data and the scientific literature contains more such data.

On this effort, however, limited experiments and analyses were conducted which have resulted in a new hypothesis for determining remotely differences in soil surface moisture content and structure, which may be related to subsurface moisture content and granularity.

To determine what happens to the reflectance properties of a soil when water is added a dry sample of sand was placed in the magnesium carbonate standard position in the Beckman DK-2A spectrophotometer. A second sample was placed in the sample position, both in bottle holders. Several measurements were made and the sample shifted in position to obtain a constant output of 100%, which indicated the samples were therefore identical even with respect to surface structure. Water was then added to the sample bottle and the lower curve shown in Figure 7 was obtained.

The fact that the largest difference occurs in the blue green rather than the near infrared indicates that absorption is not the major mechanism causing the change in reflectance, but instead a dispersion effect must be the cause.

It was also noted that the ratio of reflectance at 0.50 microns was appreciably lower than the ratio at 0.80 microns at which point a maximum occurred. Ratios were therefore computed for two other soils, gravelly clay and fine sand, and the resultant curves are shown on Figure 7, and as expected do follow the measured ratio curve.

Thus, if a terrain analyst judges two areas of the same soil have different image densities because of differences in surface moisture content, given the proper equipment, he can measure the spectral reflectance ratios from multi-band image densities and determine quantitatively whether or not

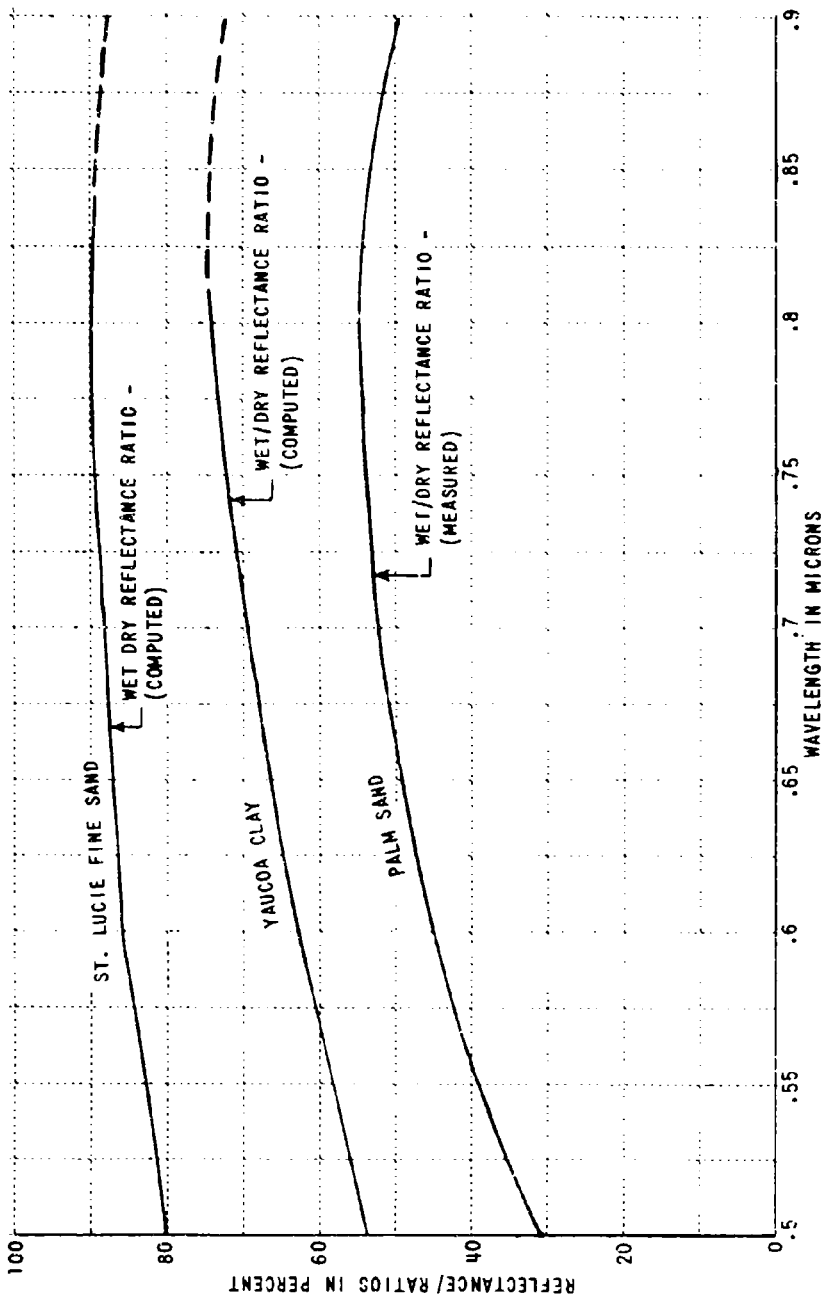

Figure 7 REFLECTANCE RATIOS FOR WET AND DRY SOILS

the ratios follow the shape of the reflectance ratio curve.

Since the observed density difference could also be caused by differences in surface structure, or differences in the amount of vegetation present it is necessary to determine how such differences behave spectrally in order to determine which is the cause of the differences in the image. In the case of vegetation, as can be seen from Figures 4 and 5 of Section 4.2.2, several interesting changes in the spectral reflectance ratios of two apparent soil areas of different densities on panchromatic film (0.40μ - 0.68μ) can occur. First, if the soil is a high reflectance soil such as the beach sand shown in Figure 5 the vegetation will cause a maximum to occur in the spectral ratios at 0.55 microns whereas a minimum will occur at about .65 microns. In the case of a low reflectance soil such as the alluvium shown in Figure 4 a maximum will still occur at .55 microns, however, it will be greater than 1.0 because the soil reflectance is lower than the vegetation reflectance in this band. The minimum will still occur at 0.68 microns regardless of soil type, because this is the major chlorophyl absorption band for vegetation, where reflectance is generally always lower than for any other object. Therefore, to determine whether or not vegetation is the cause of the density difference the interpreter observed between the two images he believes to be soil areas he can compute the ratios of reflectances in the .65 micron band and the .75 or 0.80 micron band for multi-band negatives and if the latter is greater than 1.0 and the former less than 1.0 he is sure vegetation is the cause. Recall that in the case of moisture differences the ratio in blue and red bands will be less than 1.

The granularity, or more realistically speaking, the surface structure of soil, also alters the apparent density or tone of a soil's image on aerial photographs. The coarser the surface structure, the more light traps are present, and the lower the apparent reflectance of the surface. This is illustrated in Figure 8 where the diffuse reflectance of graded aggregates from a gravelly clay sample was measured. A sample of silty clay

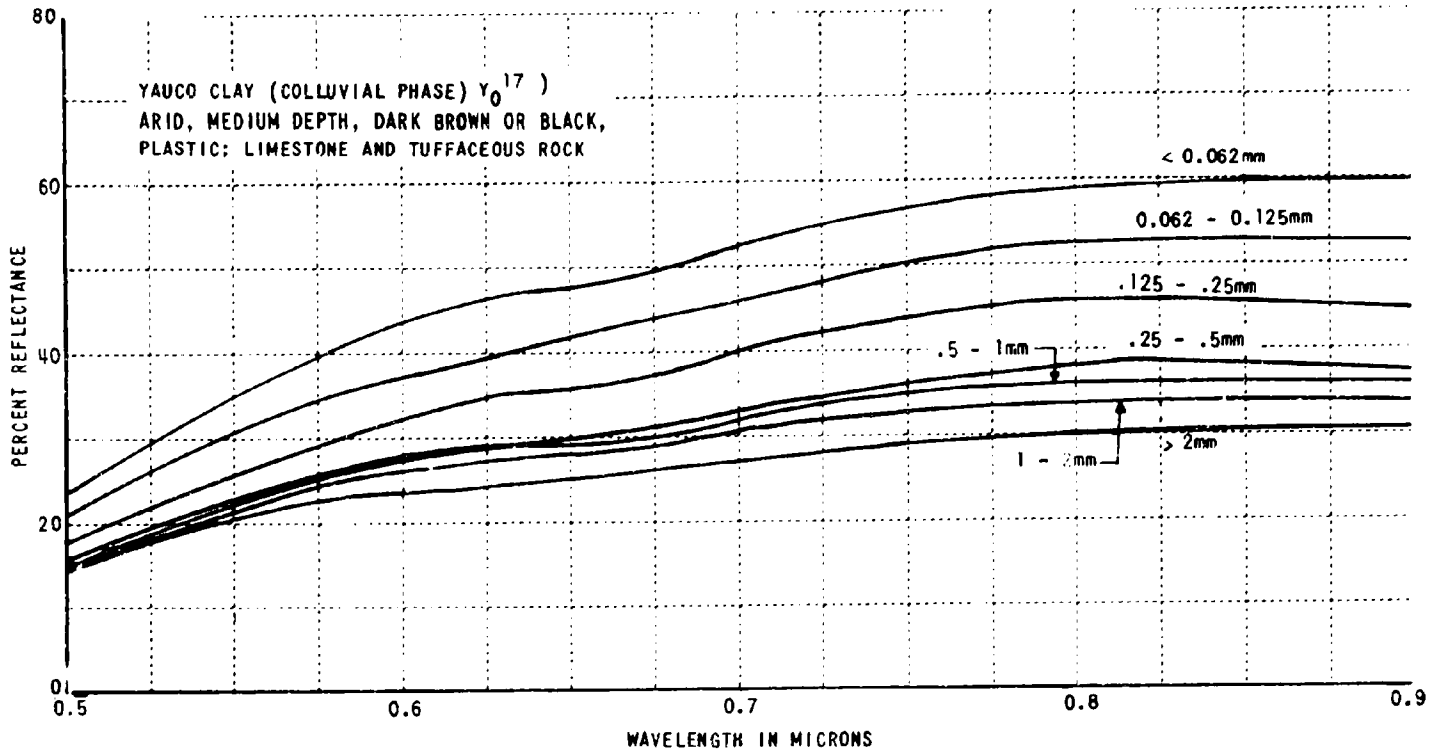

Figure 8 REFLECTANCE OF SIEVED SAMPLE OF GRAVELLY CLAY
(SALINAS, PUERTO RICO)

was also subjected to this same treatment with the same effect was noted. Therefore, it was assumed that the effects was independent of the soil type. To validate this assumption, the ratios of the spectral reflectance of each of the graded aggrates in sieves 1 ($< 2mm$), 2 ($1mm - 2mm$), 3 ($0.5mm - 1mm$), 4 ($0.25mm - 0.5mm$) and 5 ($0.125mm - 0.25mm$) to the spectral reflectance of the smallest graded aggregate in sieve 6 ($0.125mm - 0.062mm$) were computed for both soils. If the assumption of independence with respect to soil type is valid these ratios of reflectance should be equal for each soil type. The results are presented in table I below. In addition, if the ratios for the silty clay are plotted against the corresponding ratios for the gravelly clay soil they should fall along the one to one correlation line as shown in Figure 9. Considering the limited data sampled and the fact that even after sieving a soil sample there is a distribution of aggregate sizes within each graded sample, the correlation of ratios suggests that indeed the effect of soil structure on soil reflectance is independent of soil type. These results also suggest but do not prove that the density differences caused by structure is independent of wavelength for small differences, but wavelength dependent for large differences.

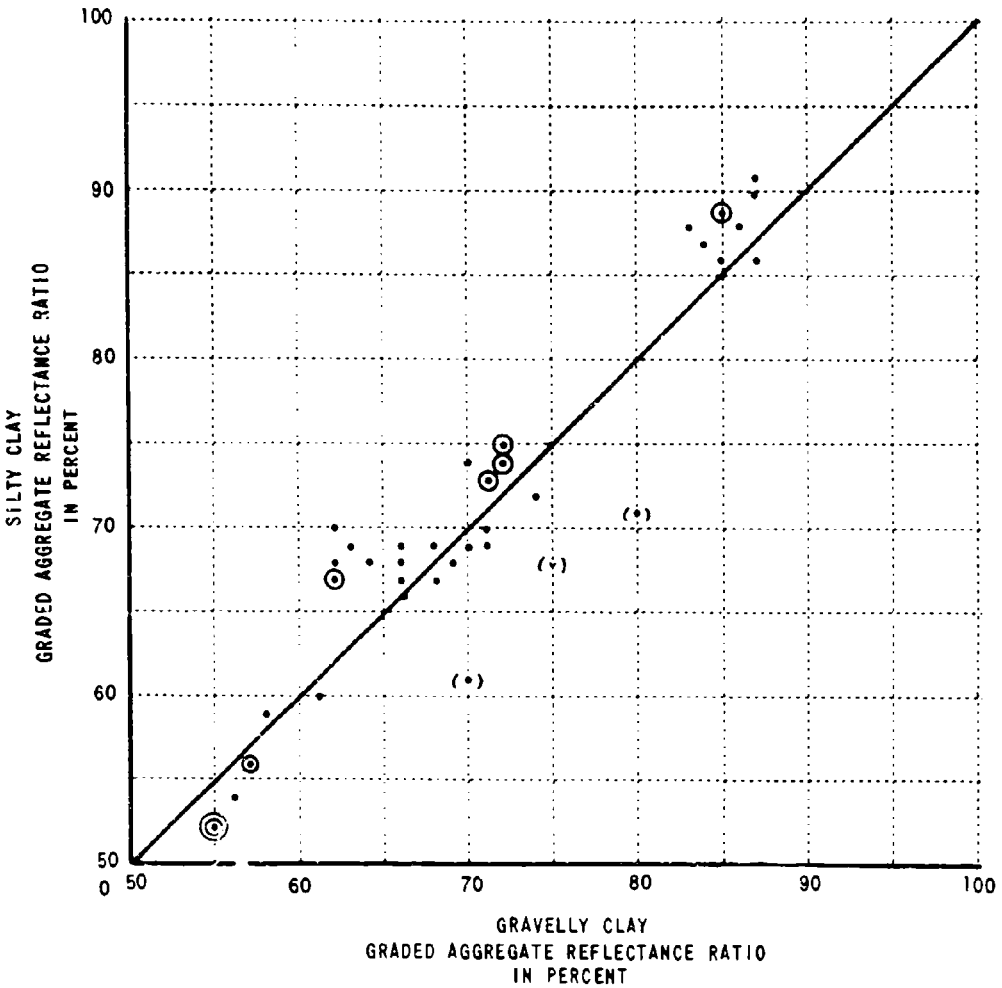

Figure 9 CORRELATION OF REFLECTANCE RATIOS FOR GRADED AGGREGATES OF TWO DIFFERENT SOIL TYPES

Table I Ratios of Spectral Reflectance for Graded Aggregates of Two Different Soil Types

	Silty Clay					Gravelly Clay				
Sieve Nos.	5/6	4/6	3/6	2/6	1/6	5/6	4/6	3/6	2/6	1/6
Wavelength	Spectral Ratio in Percent									
.50	0.86	0.75	0.71	0.68	0.61	0.85	0.75	0.80	0.75	0.70
.55	0.87	0.73	0.70	0.67	0.60	0.84	0.71	0.71	0.68	0.61
.60	0.91	0.72	0.69	0.66	0.59	0.87	0.74	0.71	0.66	0.58
.65	0.88	0.73	0.68	0.68	0.56	0.83	0.71	0.69	0.64	0.57
.70	0.86	0.75	0.69	0.69	0.56	0.87	0.72	0.70	0.63	0.57
.75	0.90	0.74	0.69	0.67	0.54	0.87	0.72	0.68	0.62	0.56
.80	0.88	0.74	0.69	0.67	0.52	0.86	0.72	0.66	0.62	0.55
.85	0.89	0.75	0.68	0.68	0.52	0.85	0.72	0.66	0.62	0.55
.90	0.89	0.74	0.67	0.70	0.52	0.85	0.70	0.66	0.62	0.55
Ratio of Sieve Sizes	2	4	8	16	32	2	4	8	16	32

Therefore to determine whether two soil images differ because of surface moisture or structure, one merely measures the spectral ratios of the two soil images in the blue region of the spectrum and the near infrared spectrum as described previously for moisture. If the latter is larger than the former, the cause is moisture, whereas structure will result in equal ratios or a larger ratio in the blue than in the near infrared. For differences caused by vegetation a red and near infrared band are used and the ratio will be less than one in the red and greater than one in the near infrared.

Once the cause of the tonal difference is determined, the absolute value of the ratios become significant. It appears from the data in Table I that for granularity, a ratio on the order of 0.85 to 0.90 indicates a factor of 2 difference in granularity, a ratio of 0.70 to 0.75 of factor of 4; a ratio of 0.65-0.70 a factor of 8; a ratio of 0.60-0.65 a factor of 16 and a ratio of 0.55 to 0.60 a factor of 32.

It appears that indeed multiband quantitative analyses can yield significant data for the terrain analyst with respect to soil moisture and surface structure (granularity). The key appears to lie in the understanding of the ratios of reflectance changes across the visible spectrum, not the absolute values. The results of this limited analysis are indeed encouraging and indicate additional research is warranted.

4.2.5 The 3-5 Micron Spectral Region

The 3-5 micron spectral region in the infrared can provide the Air Force terrain analyst with useful information relative to the thermal properties of natural earth objects and backgrounds. Maps based on data collected in the 3-5μ spectral band showing evidence of emissions in regions having hot springs or volcanic activity are presently a reality. However, because of a lack of knowledge of the emissivity properties of terrain features and the effects of the atmosphere, moisture content and geometric structure on the recorded imagery the full value of the information sensed is being limited.

The quantitative analysis approach used on the multiband photographic system if applied to the data from the 3-5 micron region offers a means of acquiring the knowledge necessary to utilize fully the information contained in this band. As with the multiband photographic system controls are required to relate image density to radiance. Appendix D describes in detail CAL's approach to establishing the required controls. Sufficient analysis of the data has been done to verify that the controls used during the field tests in Puerto Rico were adequate.

Two water trays (20 feet by 20 feet by 4 inches) were used as control targets (objects of known radiance) in the field. A 3°C temperature difference was maintained between them during data collection periods. The analysis indicates that a significantly larger difference is desirable to improve the precision of the derivation of the image density - object radiance relationship.

The fact that controls were established, under field conditions, which would allow a quantitative assessment of earth object radiance in this spectral region is a significant achievement toward the objective of full utilization of the information contained in the 3-5 micron spectral region.

4.2.6 Reflectance Standards

The terrain analyst is primarily interested in tonal differences between two otherwise similar images and the area extent of the differences. These differences represent such factors as the amount of timber requiring clearing, good timber for construction, area of shrub versus trees, distribution of surface moisture, distribution of rock outcrops, distribution of near surface rock, and many others. Many of these differences are expected to have spectral signatures but are either too subtle for the interpreter to detect or if detectable are used only for a qualitative judgment of their significance. Therefore, he must be aided by the use of a spectral densitometric analysis procedure which standardizes the properties of objects he recognizes, presents enhanced visual displays of the subtle densitometric differences, and allows a quantitative measurement of the observed differences. Quantitative spectral reflectance data can be derived from photographic imagery by an absolute method which requires an absolute measure of the spectral irradiance on an object, an absolute measure of the attenuation of the reflected energy, by the atmosphere, the camera system, the film processing system, and the densitometric analysis system. On the other hand, quantitative spectral reflectance data can also be derived from photographic imagery by a relative method, provided

the reflectance properties of some objects appearing in the photographic scene are known. The latter is the most practical method because, it eliminates the need for measurement of spectral irradiance, the need for an absolute measurement of atmospheric attenuation, sensor attenuations and processing attenuations, because the object whose reflectance is known is imaged simultaneously with the unknown objects of interest. Unfortunately, the reflectance properties of natural objects which occur in an aerial photographic scene are not known with any degree of precision. Therefore, present data collection efforts are forced to use man made objects such as painted panels of known reflectance as reflectance standards in deriving quantitative object reflectance from film image densities.

Vegetation, soil and water are the most common natural objects occuring on aerial photographic scenes of interest to the terrain analyst. Therefore, these are logical natural earth objects to use in deriving the reflectance of other earth objects of interest or variations of other images of soil vegetation and water from the standard images in the scene.

It is first necessary to prove that the spectral reflectance properties of a number of vegetation, soil and water body types, as measured from aerial film density and which the terrain analyst can recognize reliably from aerial photography are identical within the limits of precision set by the present state-of-the-art of remote sensing and sensitometric densitometric analysis systems.

Because of the broad scope and limited analysis of this effort conclusive proof of the assumption above could not be obtained, although additional evidence of its validity was obtained. In Section 4.2.3 it was shown that in the infrared region the reflectance of stacked leaves approaches a limiting value, suggesting that in using an aerial sensing system to measure reflectance many broad leaf trees will have identical reflectance in the near infrared. From Section 4.2.4, the effect of surface moisture on soil was shown to be independent of soil type as was the effect of surface structure on soil

reflectance. The effects of moisture and structure with respect to tree crown reflectance should also be investigated experimentally to establish whether these factors are also independent of vegetation type.

From reflectance data on soil and vegetation in the open literature, as well as data measured by CAL, there is additional evidence that these two terrain features may indeed be useful as standards. Reflectance data on leaf type from a variety of tree types, from different geographic areas, and measured by several different investigators over a span of twenty-two years were averaged and their one sigma derivations in spectral reflectance computed. Available soils data was treated similarly. The resultant curves are shown in Figure 10, and the raw data is presented in Tables II and III.

It should be noted that for the vegetation data of Table II single leaf samples rather than stacks were probably measured, accounting for the apparently equal reflectance between sand and vegetation in the near infra (0.70-0.90 microns). In Figure 10 in the case of reflectance measurements from spectral films it is expected that the reflectance of vegetation in this region of the spectrum will be significantly higher due to the transmission properties of vegetation as explained in section 4.2.3.

The fact that it was possible to select data from these diversified measurements of reflectance which yielded an average reflectance with deviation no larger than 30% of the average, suggests that with appropriate classifications of vegetation and soil, standard reflectance curves can be developed. Such a task, however, is beyond the scope of this effort, but is definitely warranted.

For the 3-5 micron region standards are required, having known emissivities and surface temperatures, in order to account for atmospheric attenuations and to relate image density to object radiance. Water bodies are likely candidates for emissivity standards, with associated temperature measurements made by the use of an airborne 8-14 micron radiometer or dropable devices.

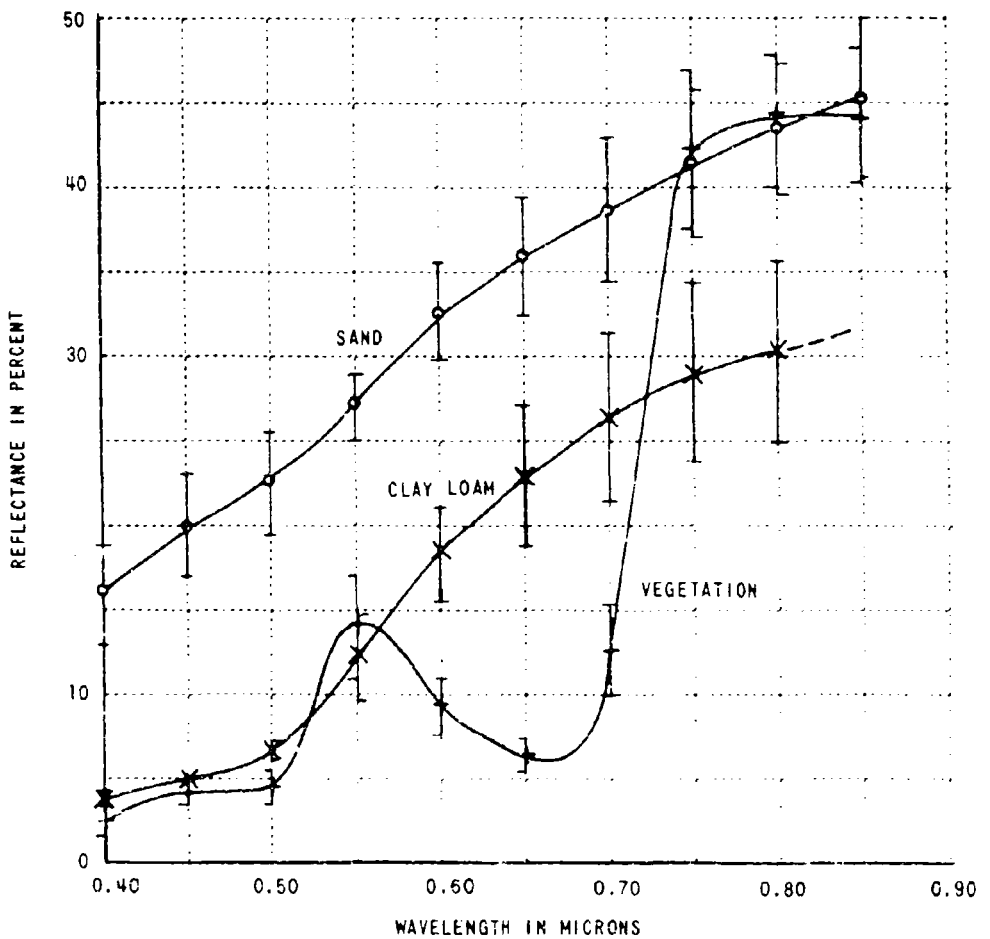

Figure 10 AVERAGE REFLECTANCE FOR POTENTIAL NATURAL STANDARDS

Table II

VEGETATION REFLECTANCE IN PERCENT

VEGETATION TYPE / SOURCE	DATE	WAVELENGTH IN MICRONS .40	.45	.50	.55	.60	.65	.70	.75	.80	.85
ILEX CORNUTA 1	1947	4	4	5	20	11	7	20	52	53	53
QUERCUS ALBA 1	1964	6	5	5	14	10	6	12	45	46	46
COTTONWOOD 1	-	5	5	6	10	7	6	13	40	40	40
COTTONWOOD 2	1960	5	6	7	14	10	7	13	/	/	/
PINE 2	1960	4	5	6	13	9	7	13	/	/	/
HARDWOOD 2	1960	4	5	5	15	10	7	14	/	/	/
BANANA 3	1965	3	/	4	13	7	5	13	42	43	44
MAHONIA 3	1965	3	3	3	13	8	5	13	44	46	46
ILEX 3	1965	3	4	5	9	7	5	14	38	40	40
COCONUT PALM 4	-	3	4	4	17	11	9	12	38	41	41
BEECH 4	-	3	3	3	16	11	7	10	35	42	42
WHITE OAK 4	-	3	3	3	18	12	8	15	45	45	45
BURR OAK 4	-	3	3	4	12	7	5	10	48	/	/
MAPLE 4	-	2	2	3	12	8	5	9	38	41	41
MINT 4	-	5	6	6	17	10	8	10	41	48	48
AVERAGE		3.73	4.14	4.60	14.20	9.20	6.47	12.73	42.17	44.0	44.09
ONE SIGMA		±1.10	±1.23	±1.30	±3.00	±1.74	±1.30	±2.66	±4.86	±3.98	±3.96

Table III

SOIL REFLECTANCE IN PERCENT

SOIL TYPE SOURCE LOCATION	WAVELENGTH IN MICRONS									
	.40	.45	.50	.55	.60	.65	.70	.75	.80	.85
ENIWETOK SAND 1 -	18	22	25	29	33	35	37	41	43	45
DAYTONA SAND 1 FLORIDA	15	20	24	29	33	37	39	41	43	43
DUNE SAND 2 TEXAS	14	18	20	25	37	41	45	47	49	51
RUBICON SAND 2 MICHIGAN	20	23	25	28	34	38	42	45	47	49
DORACO SAND ? PUERTO RICO	18	22	24	28	31	34	37	41	45	47
BEACH SAND 3 PUERTO RICO	12	15	18	24	29	31	33	35	36	37
AVERAGE ONE SIGMA	16.17 ±2.99	20.00 ±3.03	22.67 ±2.94	27.17 ±2.14	32.83 ±2.71	36.00 ±3.46	38.83 ±4.22	41.67 ±4.13	43.83 ±4.49	45.33 ±4.97
SANDY LOAM, RUSTON 2 GEORGIA	5	5	6	11	27	38	43	48	44	41
SANDY LOAM, ORANGEBURG 2 LOUISIANA	4	7	9	15	28	34	38	42	44	43
CLAY LOAM, NAALEHU 2 HAWAII	2	5	7	15	20	27	31	34	36	/
CLAY LOAM, NAALEHU 2 CALIFORNIA	3	5	6	9	14	17	20	22	24	26
CLAY LOAM, BLAKLEY 2 OREGON	3	5	7	12	20	24	26	28	28	/
CLAY LOAM, MOAULA 2 HAWAII	3	5	7	15	20	24	30	32	33	/
AVERAGE ONE SIGMA	2.75 ±0.50	5.00 ±0.00	6.75 ±0.50	12.75 ±2.87	18.50 ±3.00	23.00 ±4.24	26.75 ±4.99	29.00 ±5.29	30.25 ±5.32	

4.3 Sensor Limitations

As indicated in Section 3.0, the sensor system itself, if uncalibrated, can introduce sufficient error to eliminate all possibilities of obtaining a film record which can be analyzed quantitatively for the significant differences in terrain reflectance.

The Itek Model 002 Nine Lens Multi-band camera which was used on this effort was tested prior to use in the field to determine, as closely as possible, the precision which could be expected in ground object spectral reflectance determination from a densitometric analysis of its film records. The results of this test indicated that a precision on the order of ± 6% of the mean measured reflectance could be achieved. This was based upon the repeatability of the focal plane shutter across the film format. The details of the test are presented in Appendix C.

The MIAI infrared scanner used on this effort is designed to obtain high quality records for qualitative analysis. The major problem with respect to its use to obtain film records for a quantitative analysis relates to the circuitry utilized in signal pre-amplification. The modulation of the CRT spot which exposes the recording film is a function of the voltage difference between the instaneous signal received at the detector and a stored voltage level for the previous scan lines(Ref. 17). Thus the density produced is a function of the average scene radiance and should this change appreciably, as from water to land, the pre-amplifier will shift to maintain a pre-set voltage range to the CRT.

To account for this occurence, a constant stepped voltage generator was constructed to place a pre-amplifier voltage - density calibration wedge on the film record before and after each data run, and is described in detail in Appendix E.

The details of the entire procedure for sensing in the 3-5 micron region using the MIAI scanner are presented in Appendix D. Sensor technology is improving at a rapid rate, however, it should be guided by improvements in analysis technology. The results of this effort indicate a quantitative analysis approach to terrain evaluation is more than feasible. However, design criteria for sensors must change from obtaining a record which the interpreter will analyze qualitatively to obtaining a record from which object radiance can be easily related to image density.

5. SIGNATURES OF EARTH OBJECTS AND BACKGROUNDS

The concept of spectral signatures of earth objects and backgrounds is often narrowly considered to be the ability to measure the spectral reflectance properties of objects remotely and correlate them with in situ or laboratory measurements. Under this effort such comparisons were made with results ranging from good correlation to essentially no correlation. Such results were expected considering the effects of object surface structure and condition upon apparent reflectance as well as the difference in the basic geometry of the instruments used to measure the reflectance properties. The best of the comparisons was for an area of sand (Ref. 16) on a stabilized beach as shown in Figure 11.

The sample used for the laboratory measurements was acquired on 25 November 1968 and had a moisture content, by weight, of 6%. The change in reflectance, after oven drying, is consistent with the changes one would expect from loss of moisture as discussed in Section 4.2.4. The field photometer data were acquired on 26 November 1968 after showers had occurred and over an adjacent area of sand. The differences between the laboratory measures and the field measure are not consistent with a variation in moisture. They are however consistent with a possible surface structure; in situ measurements of soil reflectance were acquired over surfaces which appeared to be completely dry as a standard field procedure. Therefore, the in situ measures should match the dry sample laboratory measurement best. From the results of the granularity experiment described in Section 4.2.4 one would expect a slight difference in surface structure to result in spectral ratios between 0.90 and 1.00 with the ratio being a constant or decreasing with increased wavelength. The latter is generally the case for the in situ measurements of reflectance and the laboratory dry sample reflectance for the beach sand indicated in Figure 11.

The measurements made from the image density of sand on the Multi-band

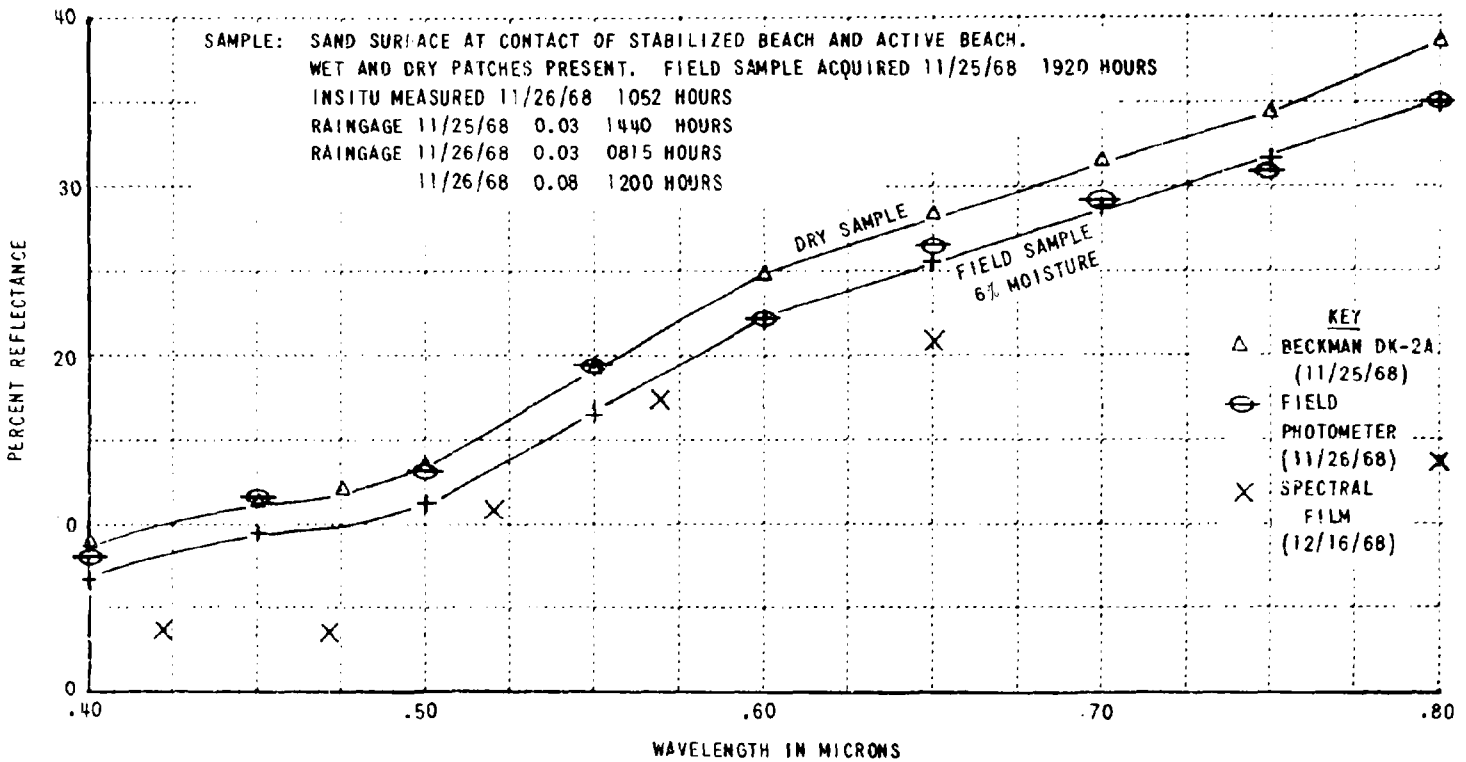

Figure 11 COMPARISON OF IN SITU LABORATORY AND AERIAL PHOTOGRAPHIC MEASUREMENTS OF BEACH REFLECTANCE

camera film were from the mission flown on 16 December 1968 after a period of considerable rain. These values are ratios of the apparent exposures of the known reflectance panel on the ground whose density was closest to an average exposure for the sand images times the known reflectance of the panel with no corrections for differences caused by format position of the images or variations in actual shutter speed across the format. Therefore, they are not expected to correlate well with in situ and laboratory measures. Nevertheless, the general shape of the curve is similar to the shape of the other curves expect for the low value at 0.80 microns. Figure 13 shows a second apparent reflectance curve for this same area of sand but measured from different films obtained from twice the flight altitude. The shapes of the two curves are much the same, indicating the camera system is consistent and thus suggesting that the differences in shape are real and attributable to the average reflectances of the micro surface features present on the soil surface (coconuts, puddles of water, brush, wood, etc.) within the ground resolution element of camera system. Indeed, these curves may well be more representative of the reflectance of the image considered as sand by the interpreter than either the laboratory or in situ measurements.

Three in situ measurements of vegetation are shown in Figure 12 together with a measurement from the spectral film densities for pasture grass and a laboratory measurement for milkweed. The in situ measures have a maximum in the visible spectrum (0.50μ), a minimum in the chlorophyl band (0.68μ) and a maximum in the near infrared (0.80μ) as do the laboratory measures. The curve derived from the spectral film lacks the minimum in the chlorophyl band probably due to the amount of soil in the ground resolution element of the camera system.

Let us assume that indeed spectral measurements made in the laboratory will differ from those made in situ and from those made from the measurement of image density. Furthermore, let us assume that the precision of the multi-band camera system is as good as a laboratory spectometer. We must then concern ourselves with how consistently the camera system will measure

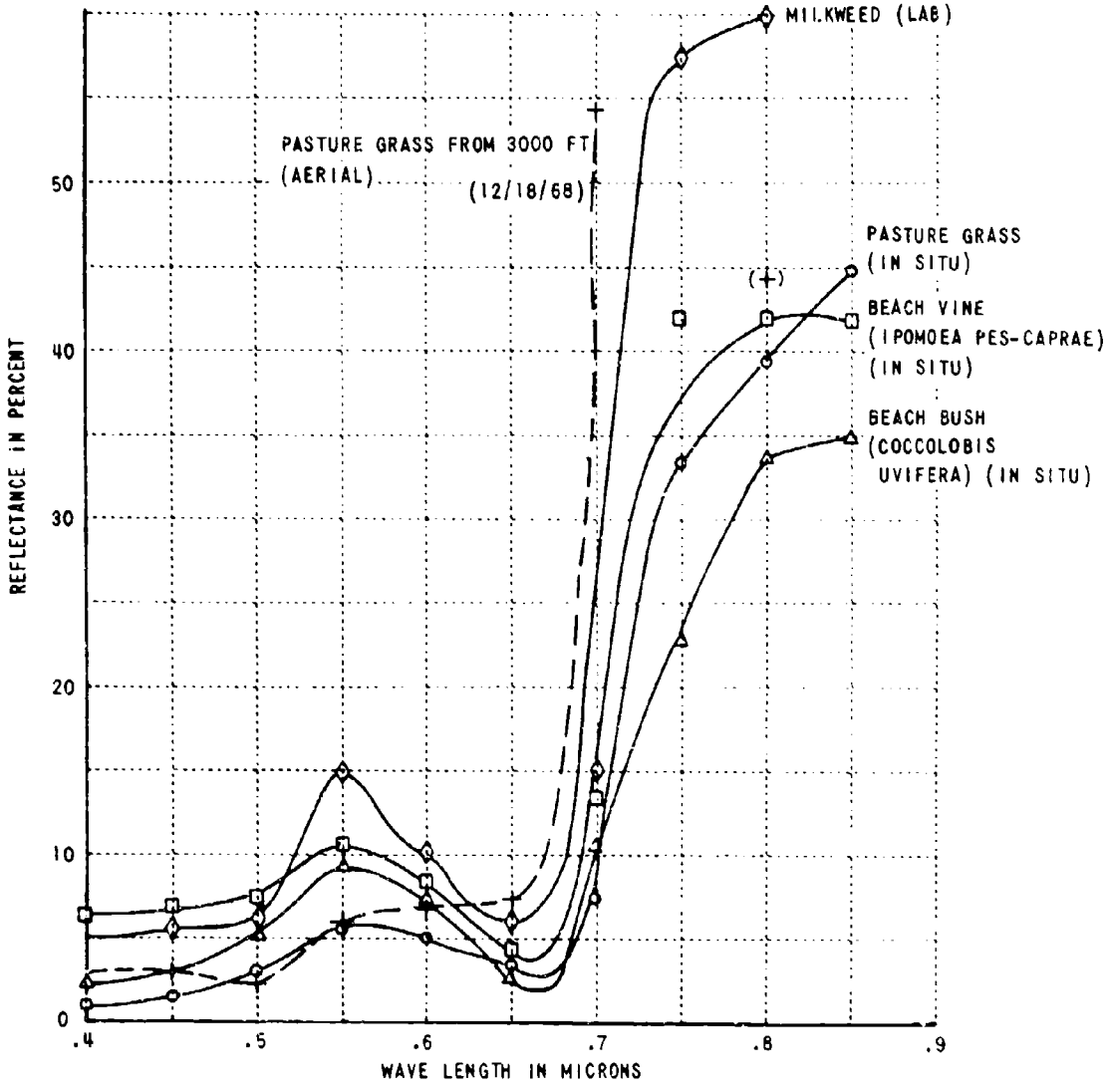

Figure 12 COMPARISON OF IN SITU, LABORATORY, AND AERIAL PHOTOGRAPH REFLECTANCE MEASUREMENTS FOR VEGETATION

ground object reflectance especially when the system is used at different altitudes.

Figures 13, 14, and 15 show reflectance measurements for an area of beach, an area of mangrove, and an area of pasture grass derived from spectral films taken at different altitudes. The good correlation of the shape of these curves from one altitude to another attests to the consistency of the multi-band camera system and the absolute levels to the affect of the atmosphere. Under a previous Air Force program (Refs. 8, 9) CAL showed that the greatest loss of image contrast occurs generally within the lowest 35,000 feet of the atmosphere. In addition, below 10,000 feet there is little selective absorption of different wavelengths of light by the atmosphere. The rate of attenuation of energy is very high in the first five to six thousand feet decreasing rapidly thereafter. Therefore a significant difference should occur between the data recorded at 3000' and 6000', whereas a smaller difference should be noted between the 6000' and 12000' (Figures 14 and 15) data across the visible spectrum, as is the case. Thus the assumptions made above regarding the precision of the aerial photographic method appears reasonable so that without attempting to correlate aerial measurements of reflectance to laboratory or in situ measurements of reflectance we can apply the broader concept of spectral signatures directly to the aerial film records. Specifically we can use image exposures (i.e. apparent reflectance properties) of objects recorded on two photographic scenes simultaneously to produce additional visual scenes, with spatially distributed ratios, sums, products or differences of exposures for all objects in the scene.

5.1 Bi Band Analysis for Terrain Signatures

As indicated previously in Section 2.0 CAL has developed a bi band spectral analysis technique which encodes water, soil and vegetation in specific density ranges on film. The process consists of reversing the 0.65μ band photograph, registering it with the 0.80μ band negative and contacting the pair onto copy film. This is essentially equivalent to dividing the image exposures

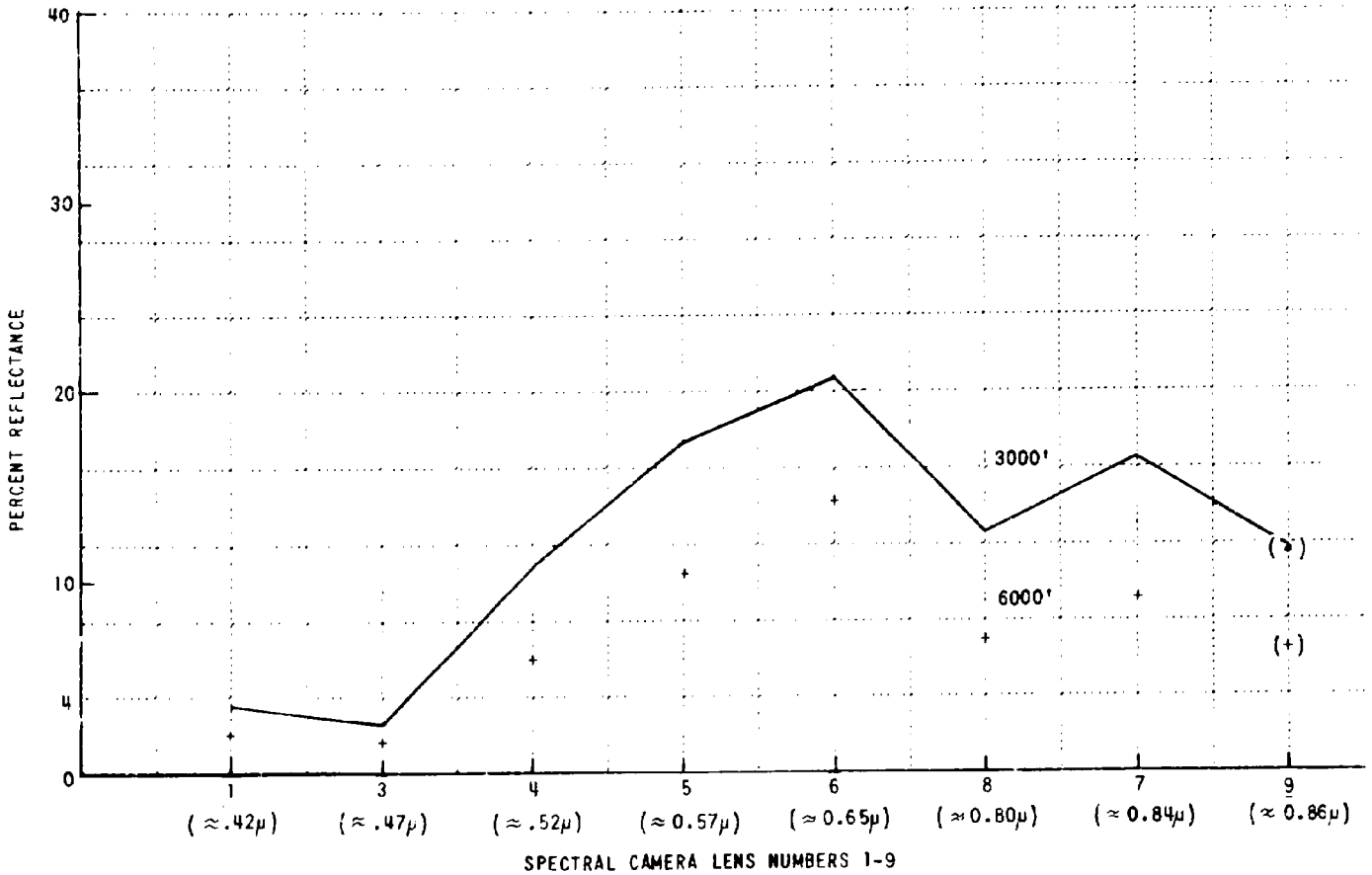

Figure 13 REFLECTANCE MEASUREMENTS OF BEACH SAND FROM FILTERED FILM

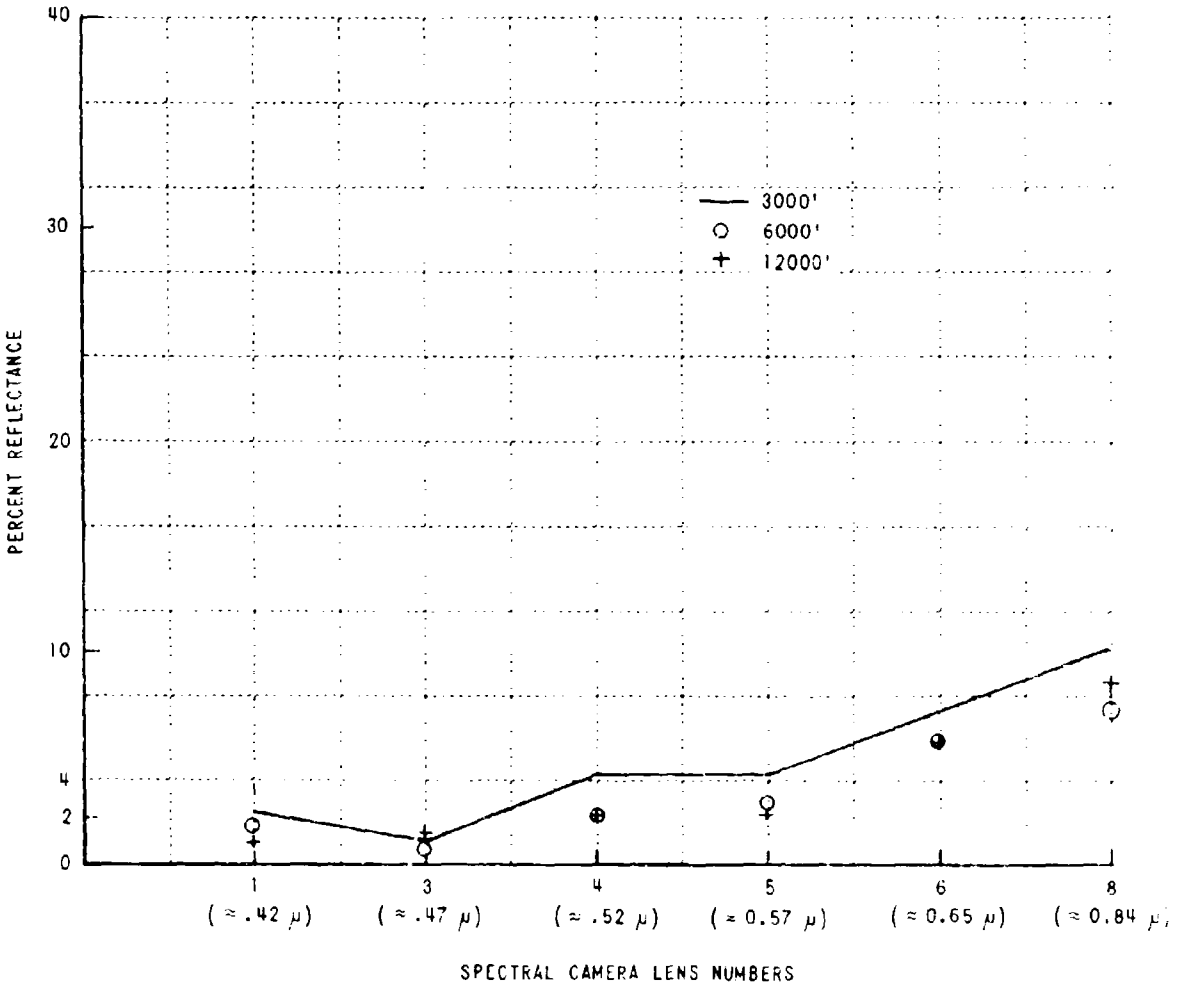

Figure 14 REFLECTANCE MEASUREMENTS OF MANGROVE FROM FILTERED FILM

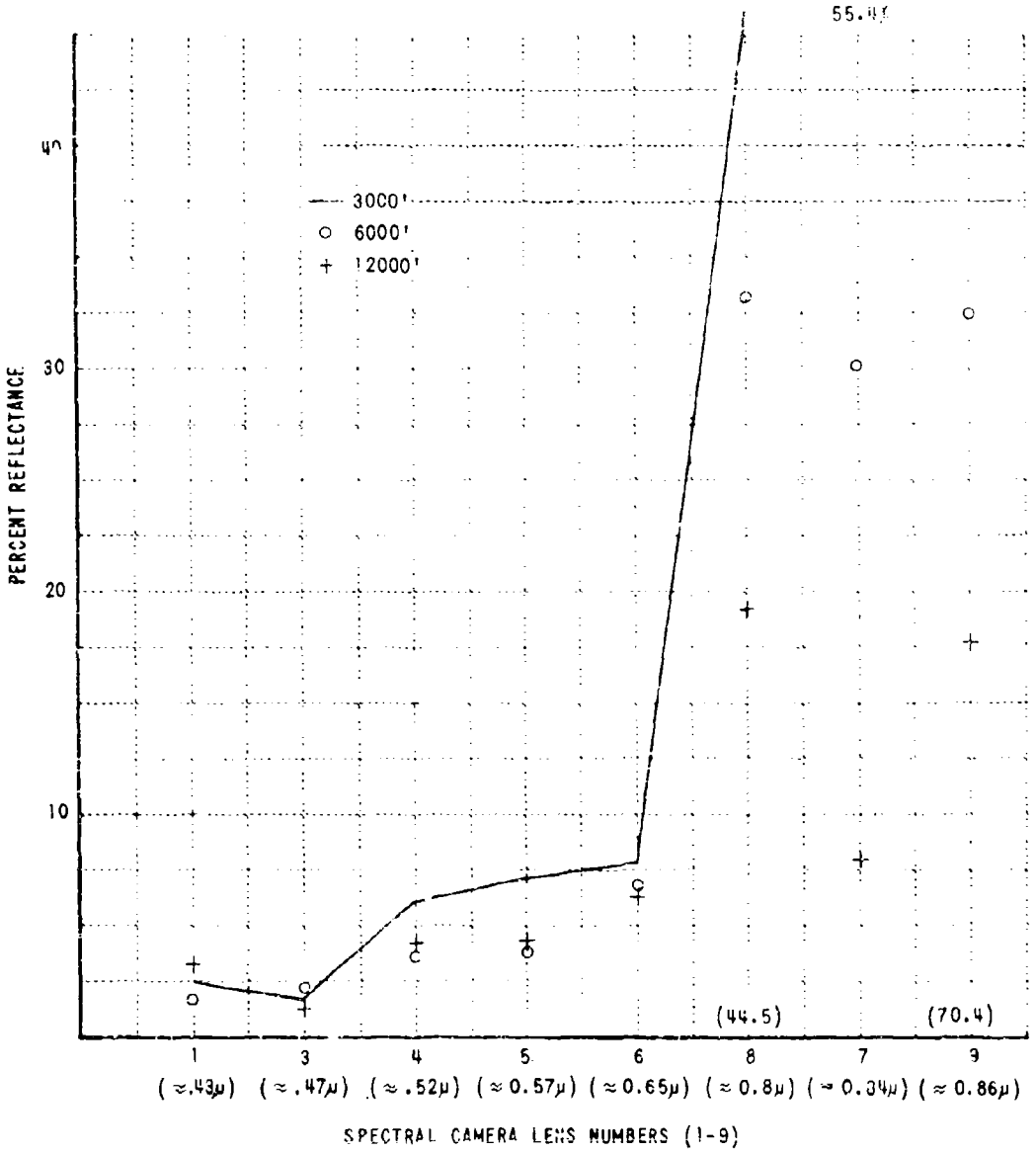

Figure 15 REFLECTANCE MEASUREMENTS OF PASTURE GRASS FROM FILTERED FILMS

in each band by the other, which of course the interpreter cannot do qualitatively, although he can interpret the product of the division. Figure 16 shows a beach test site (18°25'-65°46') in Puerto Rico photographed on conventional Plus-x film and a positive print of the scene in which the reflectances have been divided. The second step in the process is to digitize the scene on the copy film using a flying spot scanner or other suitable electro-optical device and have the computer print out a histogram of the distribution of the gray levels (reflectance ratios) in the scene as shown in figure 17. From this histogram and a visual interpretation of the copy scene, gray level ranges are selected which appear to represent water, soil, and vegetation, i.e. ranges I,II, and III on Figure 17. The computer then directs a flying spot scanner to print back on film the three density ranges as separate visual displays. The results of this step are shown in Figure 18. Comparison of these displays to the conventional Plus-X will reveal how good the selection of bands was in separating the basic environmental features. Features in shadows will have a different ratio than the same features in sunlight because of the different spectral irradiance distribution. However, it may be possible with additional research to determine a spectral preprocess technique to have the computer/flying spot scanner adjust these ratios to their proper values in sunlight.

The histogram of figure 17 is truly a gross spectral signature of a terrain environment in that the area contained within each gray level range is directly proportional to the area of soil, water and vegetation in the scene. The distribution of reflectance ratios (grey levels) will shift according to the relative areas of these features on the surface. If all ratios occur in the low reflectance ratio range the terrain environment is a body of water-land or ice, where as a peak in the low range and a substantial burn in the mid range could indicate a glacier at latitudes above the tree line or coastal contact in arid latitudes. A peak in the mid range indicates a desert, whereas a peak at the far end of the vegetation range indicates a lush forest. Considerable research is still necessary to develop this methodology into a refined spectral signature, however, even in its present state it is considered a major contribution

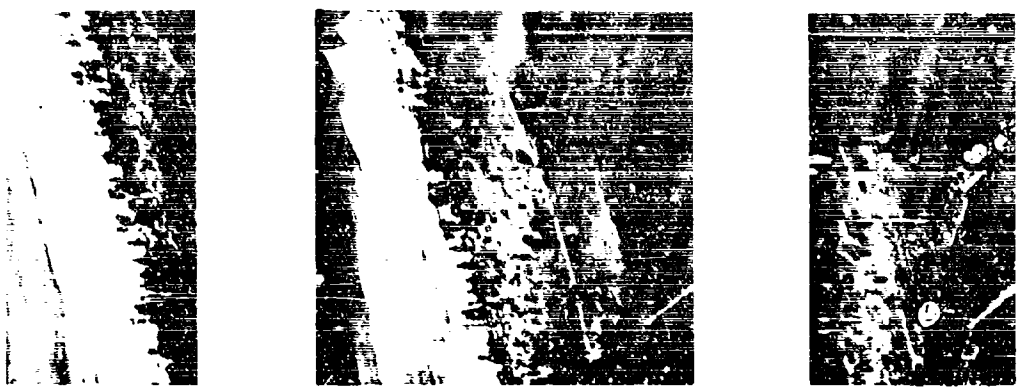

PLUS X OF SCENE

BI BAND SPECTRAL DISPLAY

Figure 16 CONVENTIONAL PLUS-X STEREO TRIPLET OF BEACH SITE AND BI BAND SPECTRAL DISPLAY

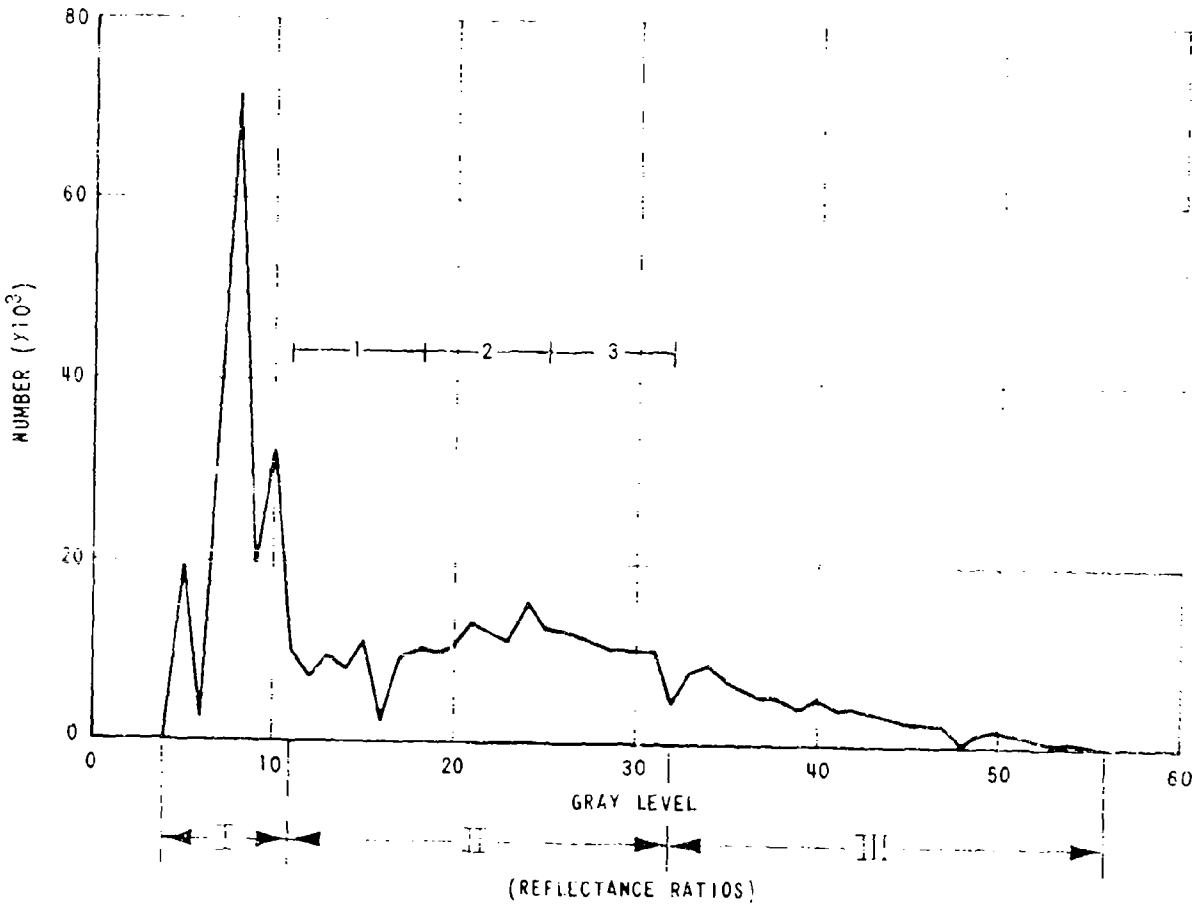

Figure 17 HISTOGRAM OF GRAY LEVELS (REFLECTANCE RATIOS) IN BI-BAND SPECTRAL DISPLAY

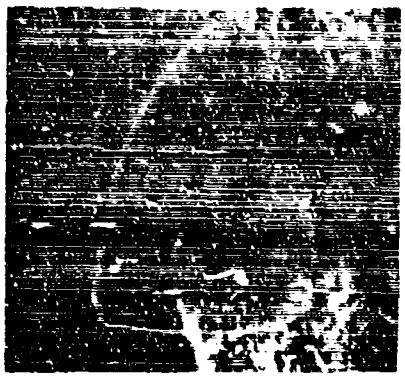

B1 BAND MASK (a)

WATER (b)

SOIL (c)

VEGETATION (d)

Figure 18 COMPUTER GENERATED SPECTRAL DISPLAYS OF EARTH OBJECTS

toward satisfying the Air Force's urgent need for developing spectral signatures of terrain.

One refinement to the methodology is to print out narrow grey levels within the gross ranges for water, soil and vegetation. The results of this step when applied to the soil range II shew on the histogram of Figure 17 (1,2, 3) are shown in Figure 19. This process provides additional information relative to area differences within the scene with respect to the gross classes of natural earth objects, water, soil and vegetation. In the water class, the differences will be related primarily to structural differences (sea state) in the surface because the two spectral bands used do not penetrate water to any appreciable extent. Should algae blooms or areas of turbidity (created by soil erosion) be present, these too will affect the grey level in the water range.

In the soil range Figure 19 the differences will be related to: a) the amounts of surface moisture present; b) small amounts of vegetation cover, and c) both tree shadows and areas of high surface moisture.

In the vegetation range, the differences will be related primarily to plant vigor, crown structure, and percentage of soil/vegetation in ground resolution element for grasses.

As pointed out in section 4.2.4 granularity differences in soils do affect the spectral reflectance properties in different bands differently. Therefore, applying the methodology discussed above to bands other than the .65μ and 0.80μ bands may indeed provide additional spectral signatures for other physical properties of terrain.

PLUS X

SOIL

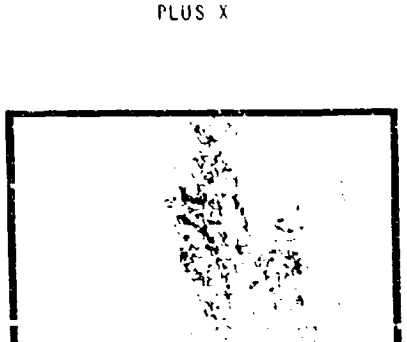

(a)

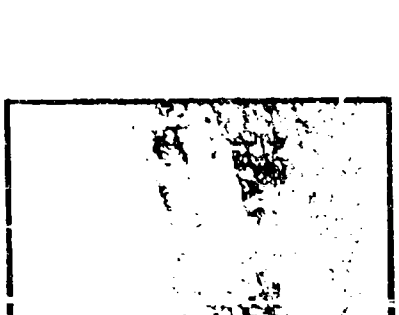

(b)

(c)

Figure 19 COMPUTER GENERATED SUBDIVISIONS OF THE SPECTRAL DISPLAY FOR SOIL

6. RESULTS AND CONCLUSIONS

As indicated in the Introduction and Summary, the primary objective of this effort was to support the Terrestrial Sciences Laboratory of the Air Force Cambridge Research Laboratories by acquiring field data (ground) from temperate humid, tropical environments (Puerto Rico). Even though poor weather conditions were encountered, the reduced data in the Appendices of this report attest to the successful accomplishment of this objective.

A limited analysis of the data was also called for with respect to correlating ground data and data extracted from the airborne remote sensor records for the purpose of defining terrain signatures.

The most important result of the entire effort is considered to be the successful development of methodology for determining terrain signatures from the application of a CAL developed bi-band photo-optical data processing method. In particular, the development of the methodology for utilizing bi-band spectral data to determine whether or not surface moisture or granularity is the cause of image tonal differences is considered significant.

It is concluded that this result represents a significant improvement in the state-of-the-art of analyzing remotely sensed multi-band spectral data by filling the gap between the purely qualitative interpretation methods and desirable automatic interpretation methods.

Other significant results pertinent to the ultimate objective of establishing terrain signatures for earth objects and backgrounds include:

- a correlation between measurements of total irradiance and spectral irradiance.
- laboratory assessment of the effects on reflectance caused by vegetation canopy structure and combinations of soil and vegetation within the ground resolution element of the remote sensor system

- laboratory assessment of the effect of surface moisture and structure on the apparent reflectance of soils.

Considering all of the results obtained on this effort we conclude that an electro-optical system for semi-automatic analysis of multi-band spectral data by bi-band techniques can be designed and fabricated today, which would greatly assist the Air Force engineer in his task of terrain analysis and site evaluation. Furthermore, such a system would have the inherent capability of expanding its own utility by providing the Air Force engineer with the equipment to test hypotheses relative to the limitless combination of multi-spectral data.

REFERENCES

1. E.B. Silvestro, Project Amvirt, ARPA Multiband Photographic and Infrared Reconnaissance Test, Vol. III of VI, Final Report, RADC-TR-67-306, July, 1967, CONFIDENTIAL.

2. T.J. Cronin, T.P. Rooney, R.S. Williams, Jr., C.J. Delineau, E.L. Pleasants, Ultraviolet Radiation and the Terrestrial Surface, AFCRL-68-0527, November 1968.

3. W.L. Wolfe, Handbook of Military Infrared Technology, U.S. Government Printing Office, 1965.

4. D. Laring, Target Backgrounds and Characteristics, Air Force Avionics Laboratory, WPAFB, July 1967.

5. P.L. Peacle, Project 8-31-03-014 Reflectance of Soil and Vegetation, Materials Branch, USAERDL, Fort Belvoir, Date unknown.

6. J.L. Walker, An Investigation of Spectrophotographic Techniques for Target Detection, RADC-TR-69-275, July 1969, CONFIDENTIAL.

7. Handbook of Geophysics, Revised Edition, USAF, ARDC, 1960.

8. M.J. Mazurowski, D.R. Sink, Attenuation of Photographic Contrast by the Atmosphere, Optical Society of America, Vol. 55, N. 1, 26-30, January 1965.

9. M.J. Mazurowski, E.B. Silvestro, J.P. Rinaldo, A Study of Photographic Contrast Attenuation by the Atmosphere, ASD-TDR-63-541, Air Force Avionics Laboratory, WPAFB, 20 June 1963.

10. J.E. Walker, Project AMPIRT, ARPA Multiband Photographic and Infrared Reconnaissance Test, Vol. I of VI, Final Report, RADC-TR-67-206, July 1967, CONFIDENTIAL.

11. K.S. Gibson, Spectophotometry, Circular 484, National Bureau of Standards, September, 1959.

12. F.E. Nicodemus, Directional Reflectance and Emissivity of an Opaque Surface, Applied Optics, Vol. 4, No. 7, July 1965.

13. D.M. Gates, H.J. Keegan, Spectral Properties of Plants, Applied Optics, Vol. 4, No. 1, January 1965.

14. Manual of Photographic Interpretation, American Society of Photogrammetry, 1960.

15. D.R. Leuder, Aerial Photographic Interpretation, McGraw Hill, 1959.

16. R.C. Roberts, Soil Survey of Puerto Rico, U.S. Department of Agriculture, January 1942.

17. D.F. Fisher, G. England, D.S. Fisher, Airborne Infrared Scanning System MIAI, University of Michigan, July 1965, CONFIDENTIAL.

18. O.G. Molinari, Grasslands and Grasses of Puerto Rico, Bulletin 102, University of Puerto Rico, Agricultural Experiment Station, August 1952.

19. F.J. Monkhouse, A Dictionary of Geography, Edward Arnold Ltd. 1966.

20. R.P. Briggs, Provisional Geologic Map of Puerto Rico and Adjacent Islands, U.S. Geological Survey, 1964.

21. Thornthwaite, C. Warren, The Climates of North America According to a New Classification, Geographic Review, Vol. 21, 1931.

22. E.V. Giusti, M.A. Lopez, Climate and Stream Flow of Puerto Rico, Caribbean Journal of Science, Vol. 7, Sept-Dec. 1967.

23. USA Standard, Nomenclature and Definitions for Illumination Engineering Z7-6, Illumination Engineering Society.

Appendix A

SPECTRAL IRRADIANCE DATA

Spectral irradiance at ground level was measured in the field using a CAL designed and fabricated, filtered photometer system. Figure A-1 shows the face of the data panel which was photographed using a motor driven, 250 exposure, Nikon 35 millimeter camera. In addition to the 10 irradiance meters, the panel includes wind speed and direction meters and a clock. Cycle rates consistent with the multiband camera rates were used during flight tests. Irradiance was also measured when insitu measurements of reflectance of ground objects were made with the CAL spectral reflectance photometer.

Approximately 1500 -35mm frames of irradiance data were recorded during the field test, under conditions ranging from clear sky to heavy overcast.

To reduce the raw data, all photo frames were read under a microscope and the 10 irradiance readings, the clock reading and the wind speed and direction readings were tabulated on data sheets. To convert the meter readings to energy values the calibration curve shown in Figure A-2 was used. The curve was derived from the slide rule converter supplied with each meter by the manufacturer. In reducing the raw data to determine the irradiance conditions encountered throughout the test, it was noted that erratic results were obtained after 8 December 1968, from some of the meters. However, by comparing the readings in each band prior to 8 December 1968 with the readings after 8 December 1968, for all meters at the same levels of total irradiance, correction curves, such as the one shown in Figure A-3, were obtained for those spectral bands which appeared to give erratic results. The cause of this problem was traced to moisture entering the detector cell.

From the raw data for ten different days between 23 November 1968 and 14 December 1968, the meter readings for each spectral band, during a period when the total irradiance was relatively constant, were converted to energy values and averaged. The ratio of the values of irradiance, used by Keegan and Gates (Reference 13) for direct sunlight to the maximum values measured by CAL instrumentation were computed as shown in Table A-1. These ratios were then used to normalize the CAL measured spectral irradiance data, at different levels of total irradiance, to the curve used by Keegan and Gates. The resultant irradiance curves are shown in Figure 2, Section 4.1 of the text.

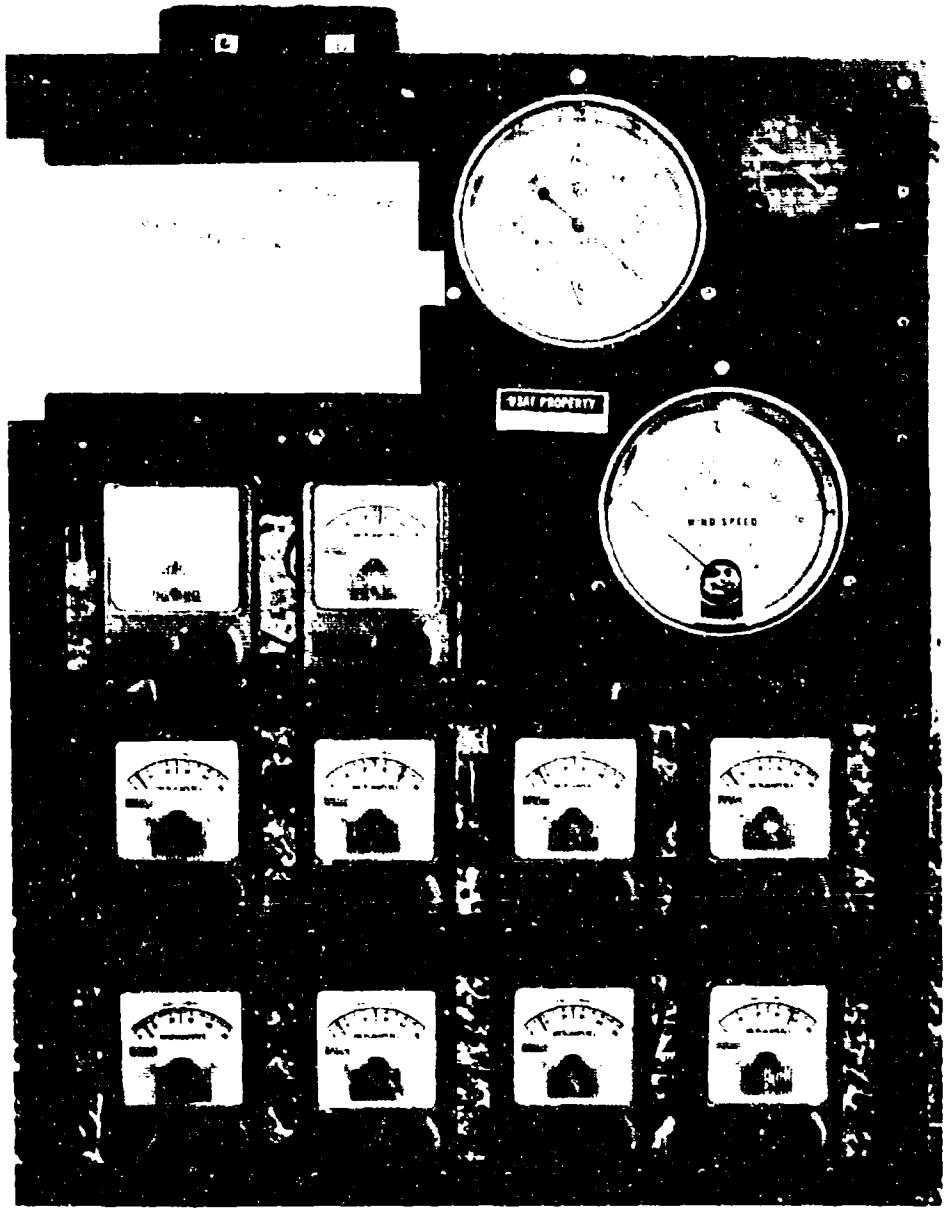

Figure A-1 CAL DEVELOPED SPECTRAL IRRADIANCE PANEL

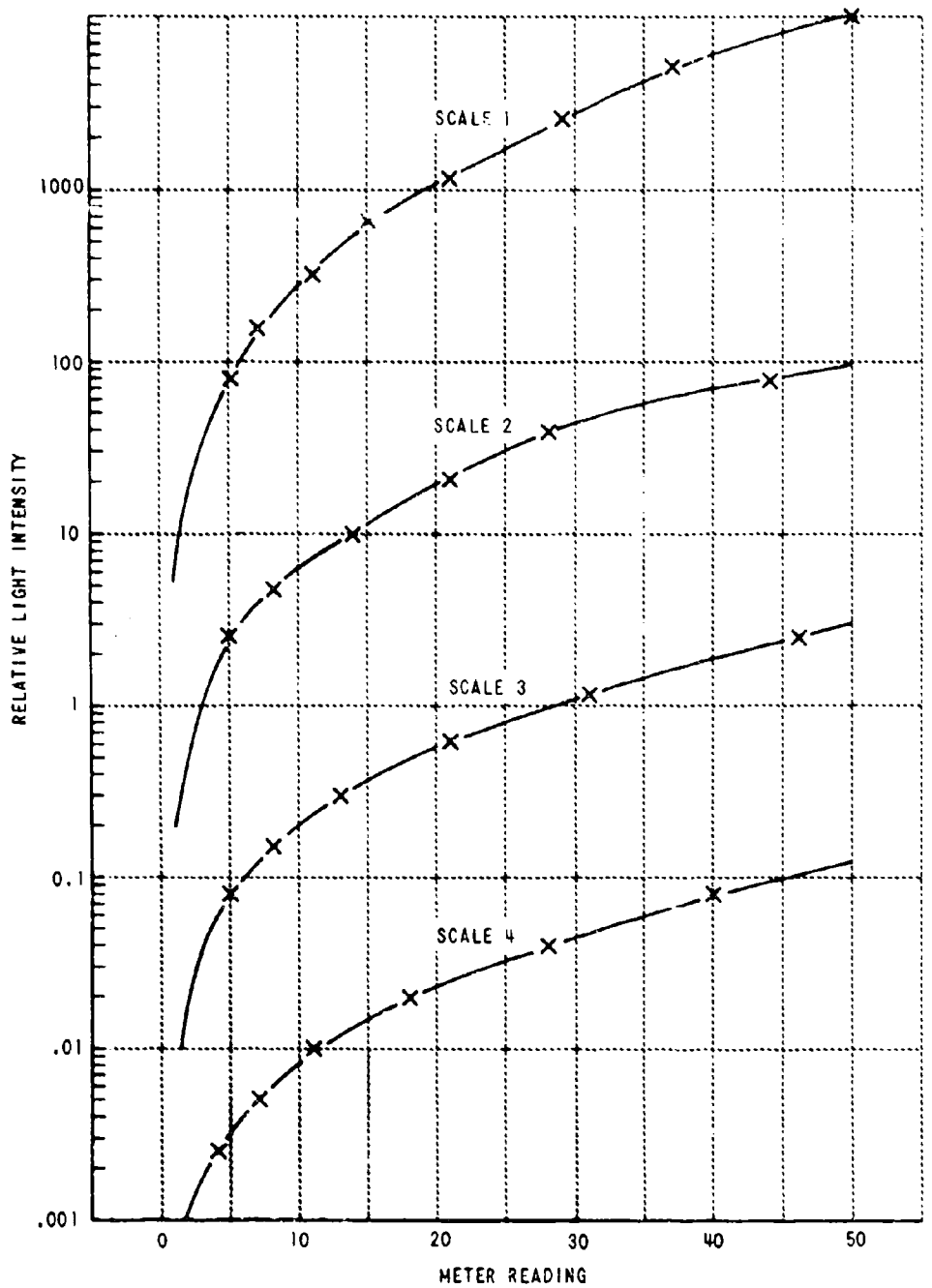

Figure A-2 CONVERSION SCALE

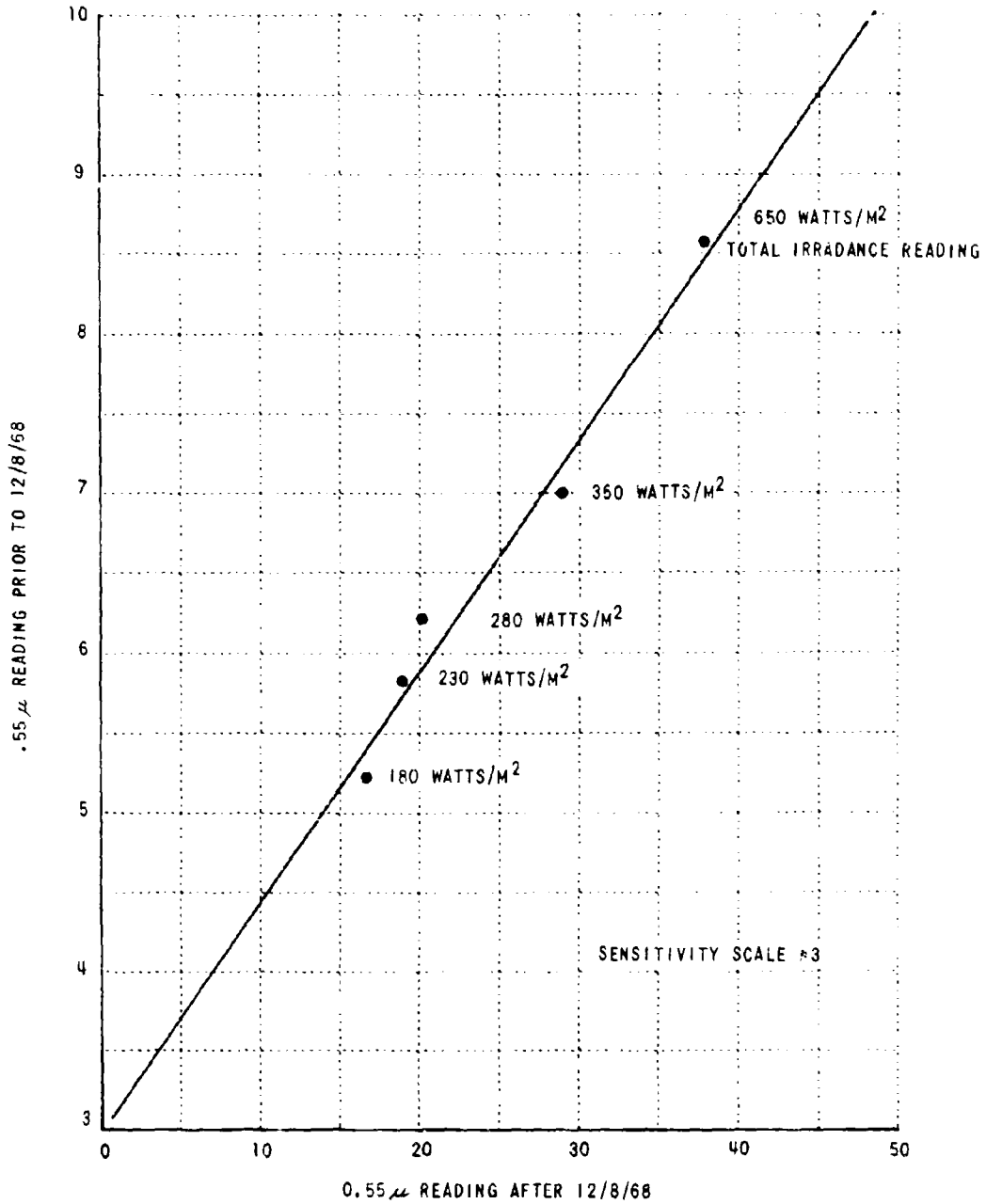

Figure A-3 CORRECTION FOR 0.55 μ READINGS

Table A-1

IRRADIANCE CONDITIONS THROUGHOUT TEST
PERIOD 11/23/68 - 12/14/68, PUERTO RICO

	SPECTRAL BANDS									
	.40μ	.45μ	.50μ	.55μ	.60μ	.65μ	.70μ	.75μ	.80μ	
MAX	6.5	0.20	0.80	1.20	8.0	1.60	1.90	2.80	3.00	CAL MAX. MEASURES
STD.	2	5.5	5.5	6.5	7.6	8.6	9.0	9.1	9.2	KEFCAN AND GATES STANDARD
CORR.	0.31	17.5	6.6	5.7	0.95	5.1	4.7	3.5	3.1	RATIO
1-15 (AVG)	5.0	0.16	0.065	0.90	6.5	1.4	1.7	2.5	2.8	10 SAMPLES 650 (Watts/m²) ♦
NORM.	1.0	2.8	4.5	5.1	6.3	7.6	8.0	8.2	8.7	
1-14 (AVG)	2.7	0.14	0.05	0.80	5.8	1.1	1.5	2.0	2.5	9 SAMPLES 500 (Watts/m²) ○
NORM.	0.8	2.4	3.3	4.6	5.5	5.8	6.1	6.6	7.7	
1-12 (AVG)	3.8	0.10	0.04	0.65	5.1	0.82	1.0	1.5	1.4	8 SAMPLES 550 (Watts/m²) △
NORM.	1.2	1.8	2.6	3.7	4.8	4.4	4.7	4.3	4.5	
1-10 (AVG)	4.8	0.08	0.025	0.45	4.2	0.60,	0.62	0.8	1.0	11 SAMPLES 280 (Watts/m²) □
NORM.	1.5	1.4	1.5	2.6	4.0	5.2	2.0	2.6	3.1	
1-8 (AVG)	2.8	0.06	0.015	0.22	2.0	0.30	0.34	0.44	0.5	6 SAMPLES 180 (Watts/m²) ✕
NORM.	0.9	1.1	09	1.5	1.9	1.6	1.6	1.5	1.5	
1-6 (AVG)	2.5	0.04	0.01	0.12	1.0	0.16	0.11	0.20	0.22	1 SAMPLE 120 (Watts/m²) ◊
NORM.	0.8	0.7	0.7	0.7	1.0	0.9	0.7	0.7	0.7	

Table A-2

RATIOS OF IRRANDIANCE CHANGES

	SPECTRAL BANDS									
TOTAL	.40μ	.45μ	.50μ	.55μ	.60μ	.65μ	.70μ	.75μ	.80μ	
0.77	0.80	0.86	0.77	0.90	0.89	0.76	0.76	0.80	0.89	650 - 120
0.54	1.20	0.64	0.60	0.73	0.77	0.58	0.59	0.62	0.49	(Watts/m^2)
0.43	1.50	0.50	0.35	0.51	0.61	0.42	0.35	0.32	0.36	+
0.28	0.90	0.39	0.21	0.25	0.31	0.21	0.20	0.18	0.17	
0.18	0.80	0.25	0.16	0.11	0.16	0.12	0.09	0.09	0.08	
0.70	1.5	0.75	0.79	0.80	0.87	0.76	0.77	0.65	0.56	
0.56	1.9	0.58	0.45	0.57	0.73	0.55	0.48	0.40	0.40	500 - 120
0.56	1.1	0.46	0.27	0.28	0.35	0.28	0.26	0.25	0.20	(Watts/m^2)
0.21	1.0	0.29	0.21	0.15	0.20	0.15	0.12	0.10	0.11	o
0.80	1.5	0.77	0.58	0.70	0.82	0.73	0.62	0.60	0.72	
0.51	0.75	0.61	0.35	0.35	0.40	0.36	0.34	0.35	0.35	550 - 120
0.34	0.62	0.39	0.27	0.19	0.21	0.20	0.15	0.16	0.16	(Watts/m^2)
										Δ
0.62	0.60	0.79	0.60	0.50	0.48	0.50	0.35	0.38	0.48	280 - 120
0.45	0.55	0.50	0.47	0.27	0.25	0.28	0.24	0.27	0.25	(Watts/m^2)
										□
0.67	0.89	0.64	0.78	0.54	0.55	0.56	0.44	0.47	0.47	180 - 120
										(Watts/m^2)
										◊

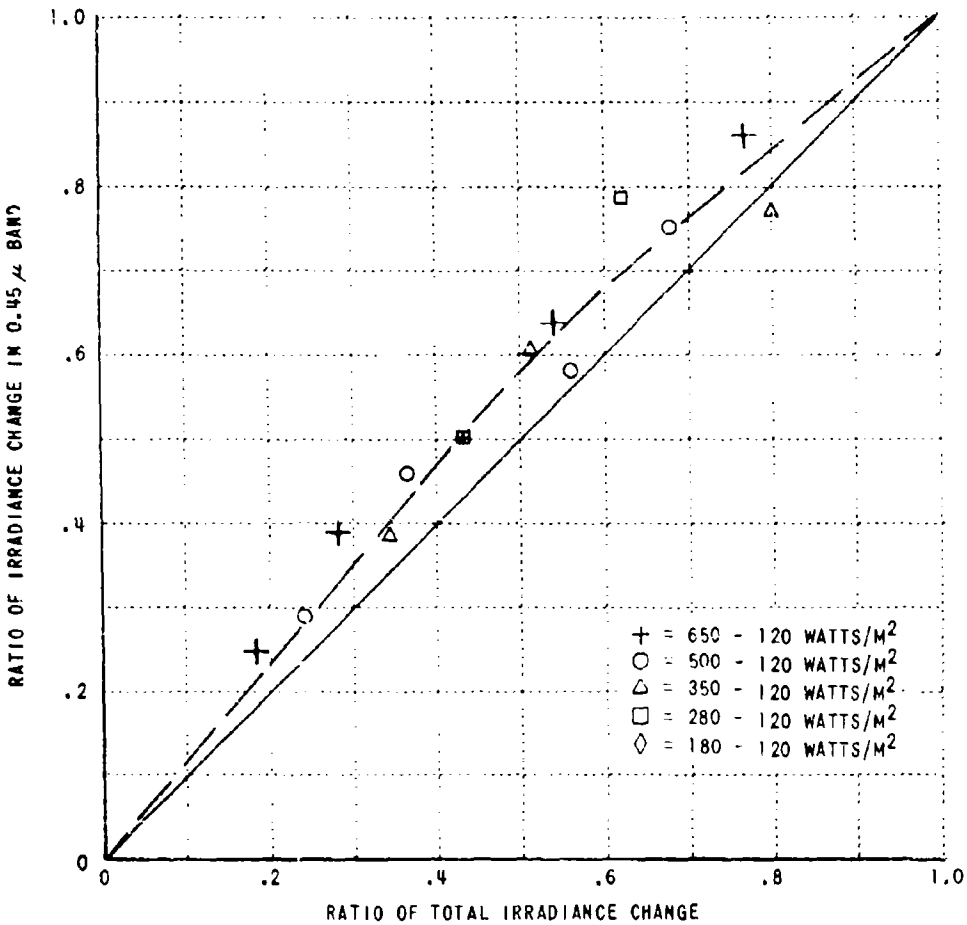

Figure A-4 RELATIONSHIP OF CHANGE IN IRRADIANCE IN 0.45 μ BAND TO CHANGE IN TOTAL IRRADIANCE

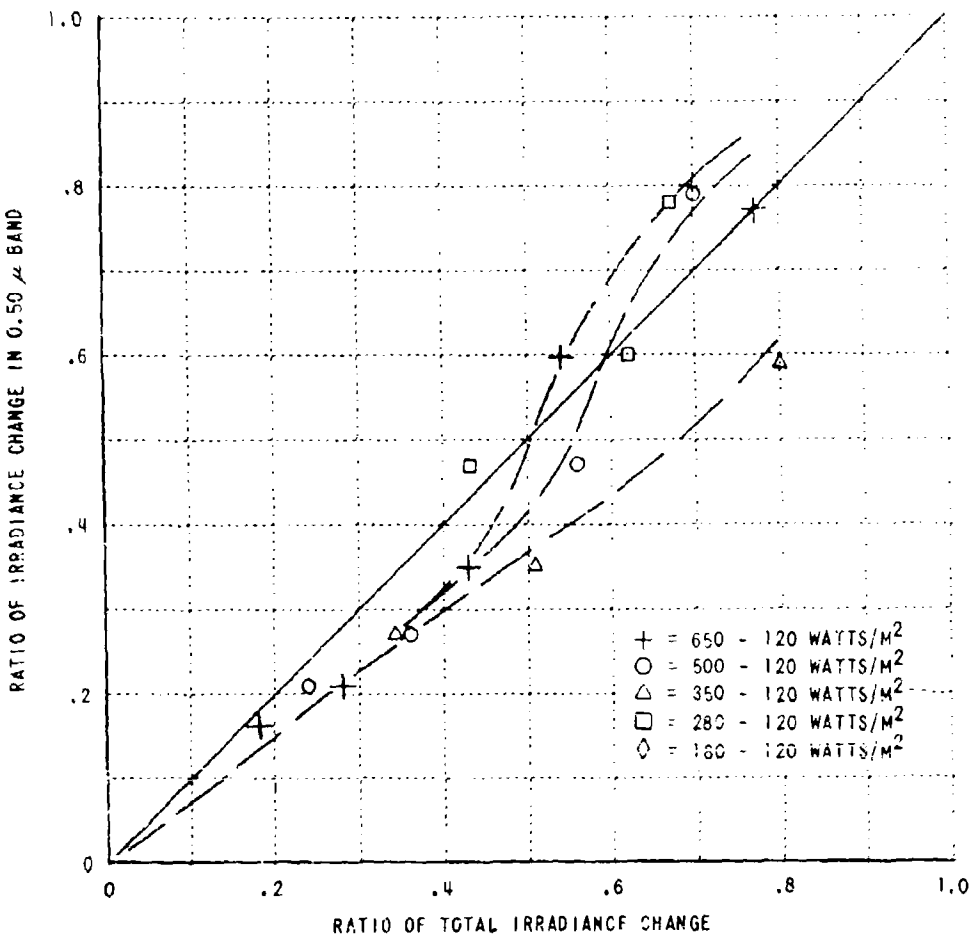

Figure A-5 RELATIONSHIP OF CHANGE IN IRRADIANCE IN 0.50 μ BAND TO CHANGE IN TOTAL IRRADIANCE

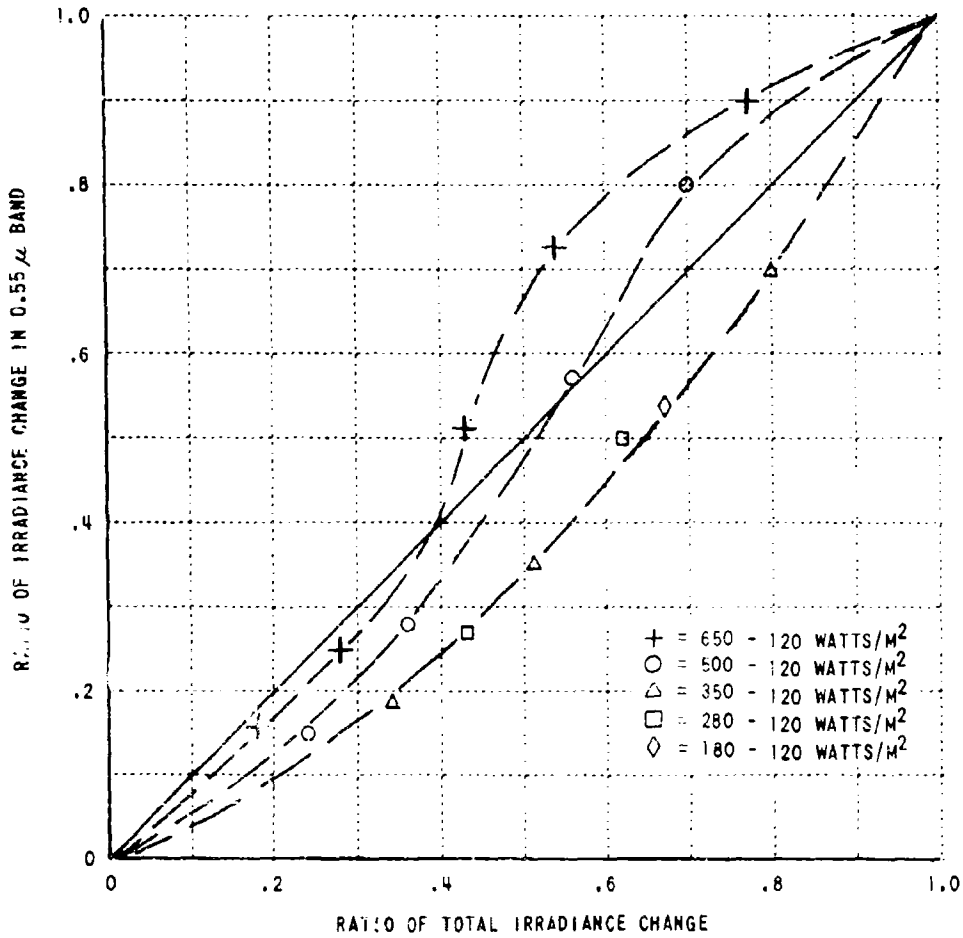

Figure A-6 RELATIONSHIP OF CHANGE IN IRRADIANCE IN 0.55 μ BAND TO CHANGE IN TOTAL IRRADIANCE

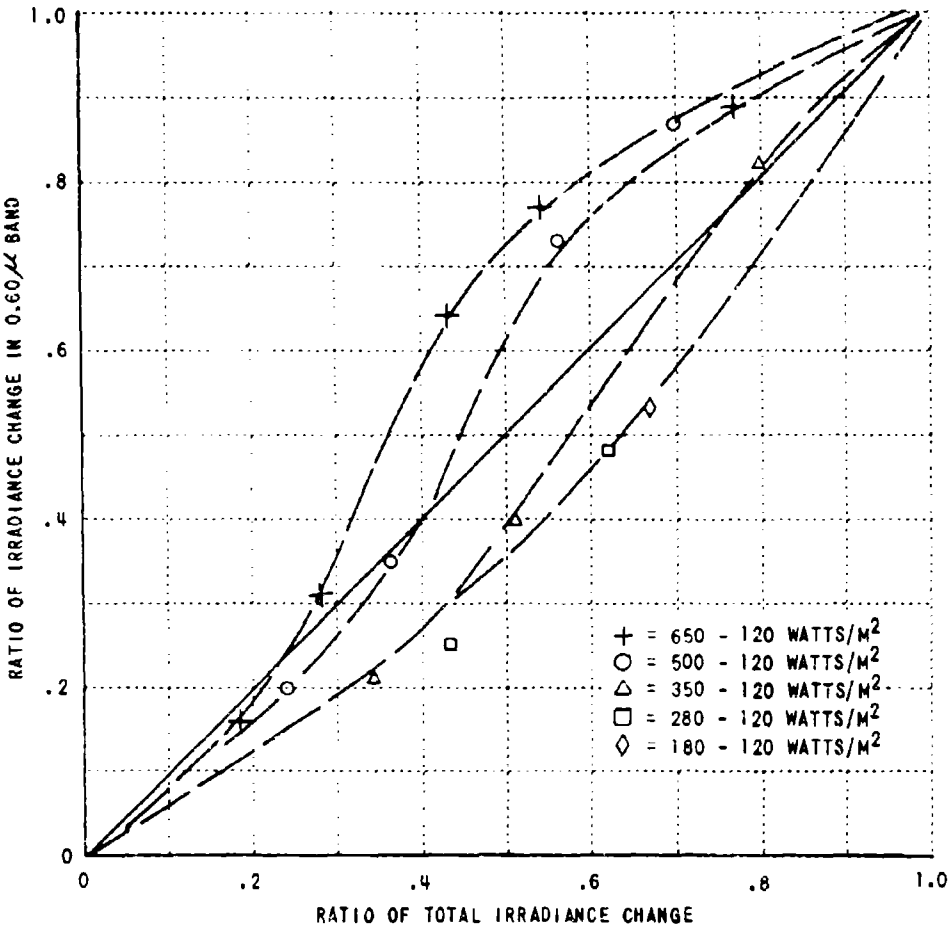

Figure A-7 RELATIONSHIP OF CHANGE IN IRRADIANCE IN 0.60μ BAND TO CHANGE IN TOTAL IRRADIANCE

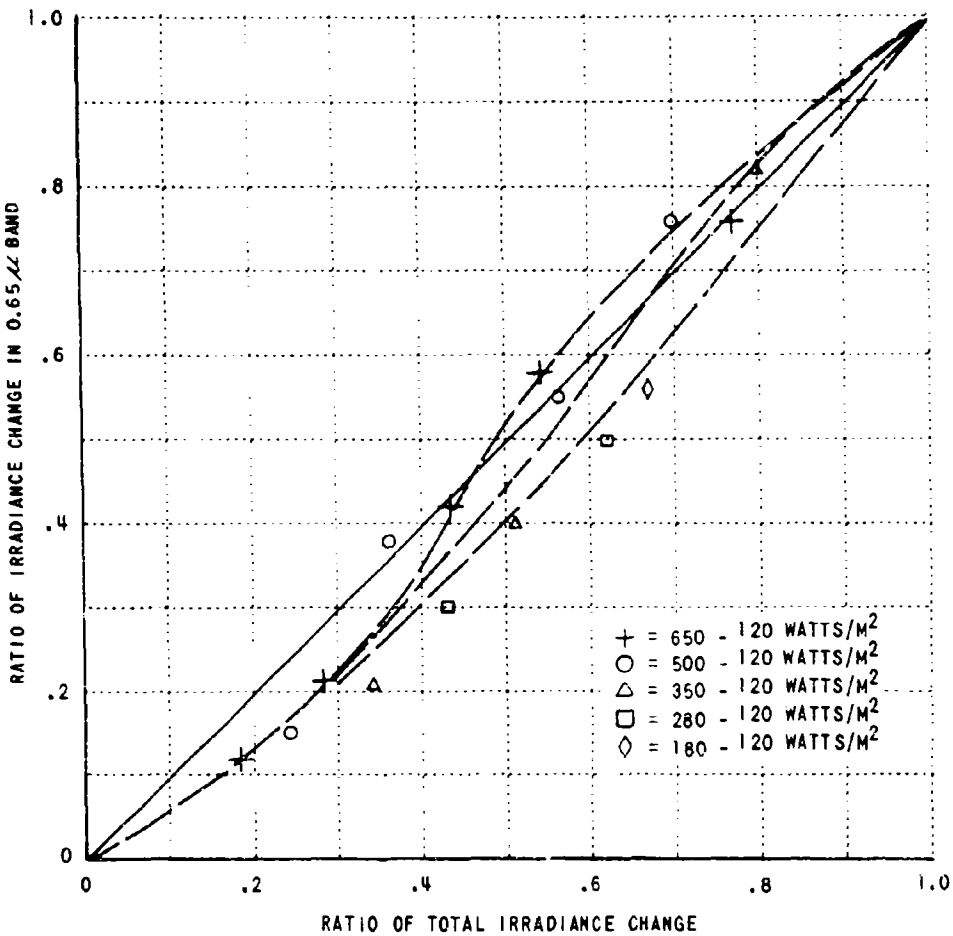

Figure A-8 RELATIONSHIP OF CHANGE IN IRRADIANCE IN 0.65μ BAND TO CHANGE IN TOTAL IRRADIANCE

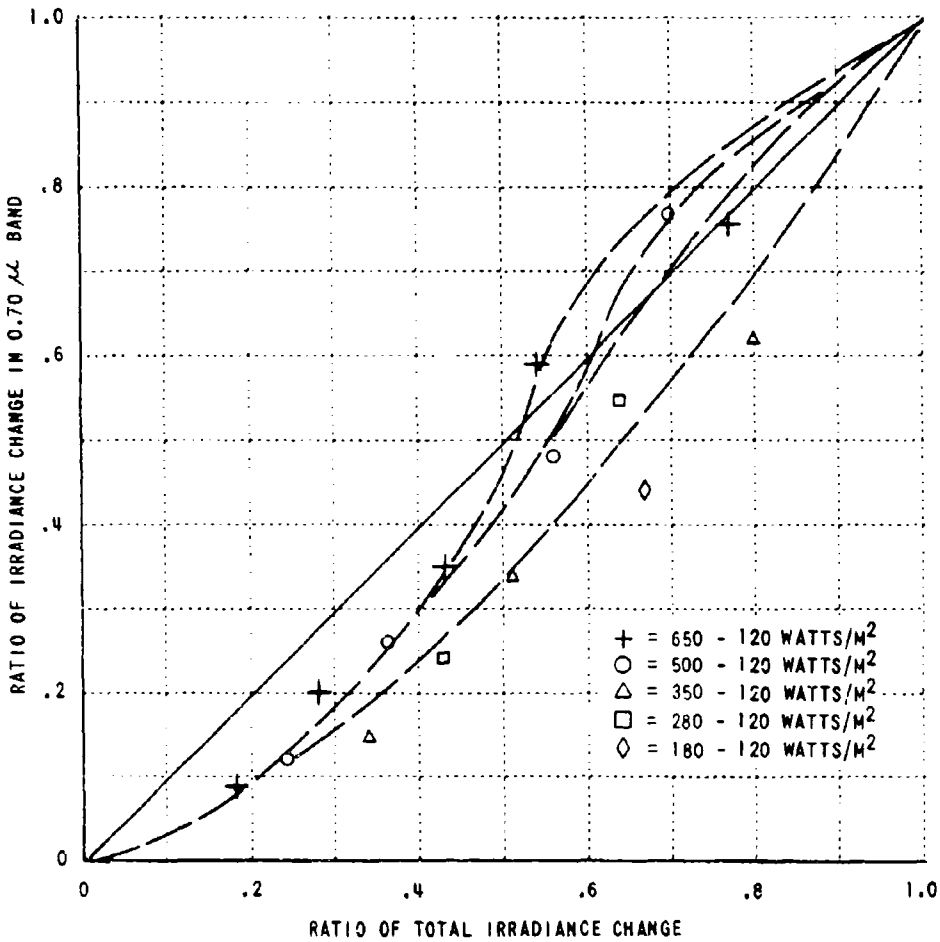

Figure A-9 RELATIONSHIP OF CHANGE IN IRRADIANCE IN 0.70μ BAND TO CHANGE IN TOTAL IRRADIANCE

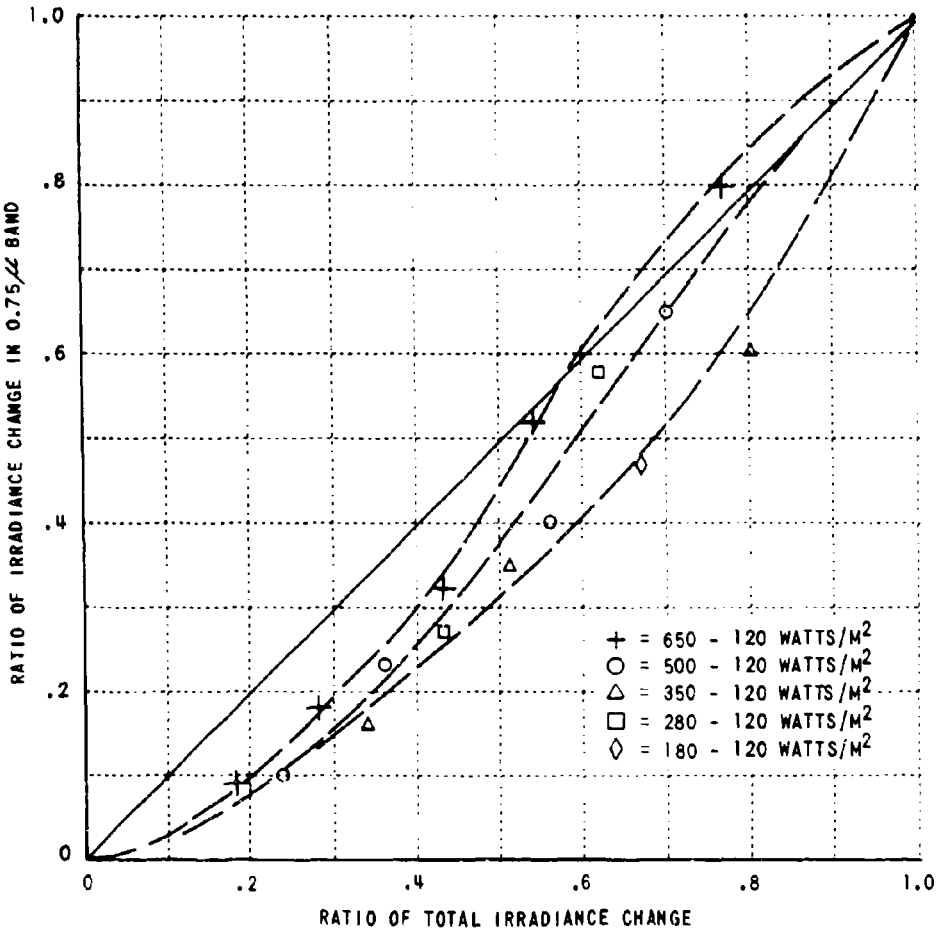

Figure A-10 RELATIONSHIP OF CHANGE IN IRRADIANCE IN 0.75 μ BAND TO CHANGE IN TOTAL IRRADIANCE

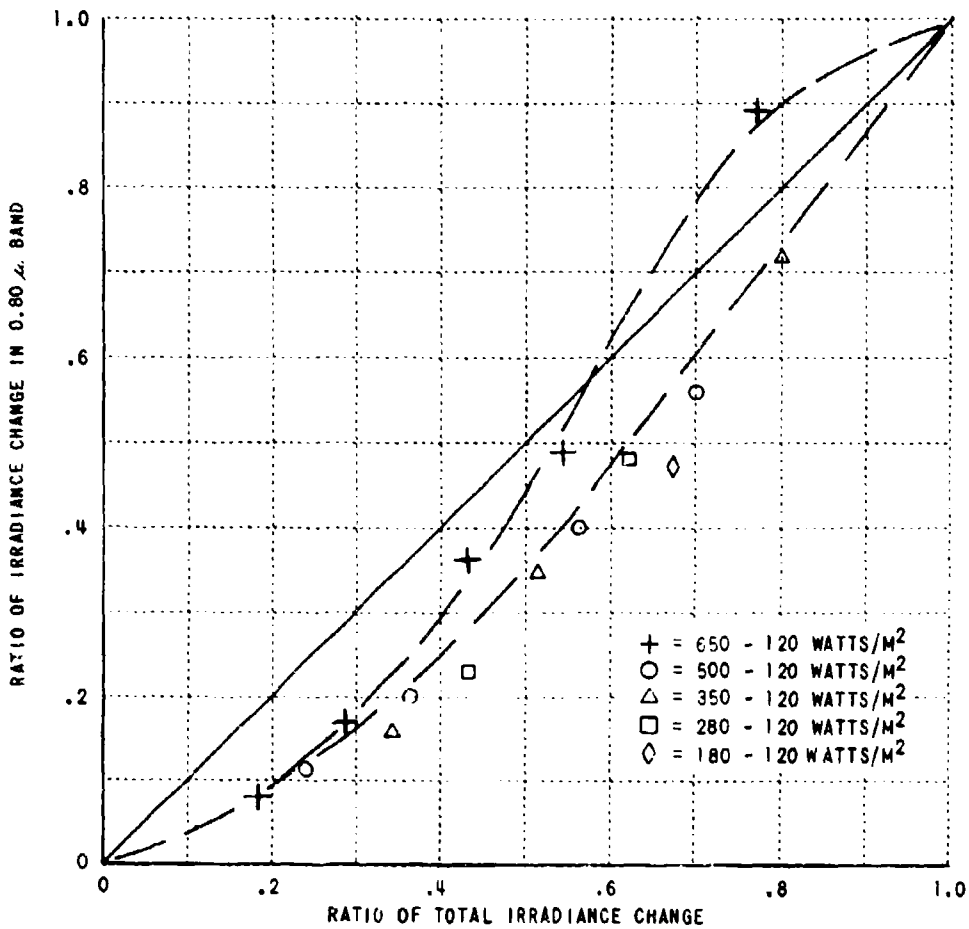

Figure A-11 RELATIONSHIP OF CHANGE IN IRRADIANCE IN 0.80 μ BAND TO CHANGE IN TOTAL IRRADIANCE

Because relatively few data are available on changes in spectral irradiance compared to simultaneous changes in total irradiance, the data of Table A-1 were further reduced to ratios of changes as shown in Table A-2 and the results plotted as a correlation graph in Figure 3 of Section 4.1 of the text. Figures A-4 through A-11 are curves for each band across the visible and near infra red spectrum. Several interesting effects are noted from these plots.

First, in the case of blue light (0.45μ band) the majority of points lie above the one to one correlation line indicating the percentage change in irradiance is practically always larger in the spectral band than the percentage change indicated by the total irradiance measurement.

Second for the 0.50μ though 0.80μ bands the spectral change is generally larger than the total on bright, direct sunlight or scattered cloud days until the irradiance drops to approximately one half the peak values at which point the change is generally smaller for the spectral irradiance than for the total.

Third, for over-cast days the spectral changes are generally smaller than the changes in the total irradiance.

Finally, the changes in the 0.65μ band appears to most closely correspond to the changes in the total irradiance.

Appendix B

SPECTRAL REFLECTANCE

TABLE OF CONTENTS

TABLES

TABLES (Cont.)

SPECIFIC MAP REFERENCES

Specific map references or reports containing related map references are indicated below:

1. Geology — Provisional Geologic Map of Puerto Rico and Adjacent Islands, R.P. Briggs
United States Geological Survey
Map I-392, 1964.

2. Soils — Soil Survey of Puerto Rico, R.C. Roberts
United States Department of Agriculture
January 1942 (Out of Print).

Soil Map Eastern Sheet
Soil Map East Central Sheet
Soil Map West Central Sheet
Soil Map West Sheet
Soil Index

3. Topography

Punta Picua Site — Rio Grande Quadiangle
Puerto Rico
7.5 Minute Series
United States Department of the Interior
Geological Survey

El Yunque Site — El Yunque Quadiangle
Puerto Rico
7.5 Minute Series
United States Department of the Interior
Geological Survey

Salinas Site — Coamo Quadiangle
Puerto Rico
7.5 Minute Series
United States Department of the Interior
Geological Survey

Salinas Quadiangle
Puerto Rico
7.5 Minute Series
United States Department of the Interior
Geological Survey

Cabo Rajo — Cabo Rajo Quadiangle
Puerto Rico
7.5 Minute Series
United States Department of the Interior
Geological Survey

Las Mesas	Rosario Quadiangle Puerto Rico 7.5 Minute Series United States Department of the Interior Geological Survey
Dos Bocas	Utuado Quadiangle Puerto Rico 7.5 Minute Series United States Department of the Interior Geological Survey
Utuado	(See Dos Bocas above)
Palmas Altas	Barchoneta Quadiangle Puerto Rico 7.5 Minute Series United States Department of the Interior Geological Survey
Dorado	Vega Alta Quadiangle Puerto Rico 7.5 Minute Series United States Department of the Interior Geological Survey

4. Geology

Coamo Quadiangle Salinas Site	Glover, Lynn, 3d, 1961a, Preliminary Report on the geology of the Coamo Quadiangle, Puerto Rico: U.S. Geol. Survey, Misc., Geol. Int. Map I-335
Salinas Quadiangle Salinas Site	Glover, Lynn 3rd, 1961b, Geologic map of the Salinas Quadiangle, Puerto Rico U.S. Geol. Survey Misc. Geol. Int., Map I-337
Mayaquez	Maltson, P.H. 1960, Geology of the Mayaguez area, Puerto Rico, Geol. Soc. America Bull., V.71, Mo. 3, p. 319-362
Utuado	Weaver, J.D., 1958, Utuado Pluton, Puerto Rico. Geological Soc. America Bull., V.69, No. 9, p. 1125-1142

5. Climatology — Smedley, Climate of the States, Puerto Rico and the Virgin Islands. U.S. Department of Commerce, Weather Bureau No. 60-53.

1. INTRODUCTION

During the course of this effort a considerable amount of spectral reflectance and other data related to earth objects has been collected. Some has been used in the limited analysis. It is the purpose of this appendix to compile the remainder of the raw data. To make it as useful as possible, it has been organized on the basis of the latitude and longitude of the location on the Island of Puerto Rico from where the data were acquired. The relative locations are shown on the map of Puerto Rico in Figure B-1.

The data includes: 1) Total diffuse reflectance measurements using a Beckman DK-2A spectrophotometer; 2) In situ reflectance using a CAL designed filter photometer; 3) Reflectance data from spectral film density; 4) Soil granularity data; and 5) Soil moisture data.

Soil samples were collected primarily from the top two inches of the surface of soil areas. They were placed in air tight plastic bags and returned to the laboratory. Small amounts (about 100 grams) of the samples were placed in 2" x 2" x 1/2" plastic spectrometer sample holders for reflectance measurement. These measurements are referred to as "Bag" measurement indicating the moisture content was at the in situ state of the day obtained. Water was then added to the sample holder and time allowed for the soil to saturate. Measurements in this state are referred to as "Sat." measurements. A few samples were first dried in an oven at 105° to obtain "Dry" measures of reflectance, then saturated and redried in steps to determine the change in reflectance with change in moisture content. For these cases, the actual moisture content by weight was measured and is shown with the tabulated reflectance data. Frequent references (16) are made to the soil survey of the island of Puerto Rico conducted by R.C. Roberts from 1928 through 1936, in which are found descriptions of the soils whose reflectance properties were measured on this project.

Also reference (18) are made to the grassland survey of Puerto Rico conducted by Ovidio Garcia-Molinari for descriptions of some types of vegetation whose reflectance properties were measured on this project.

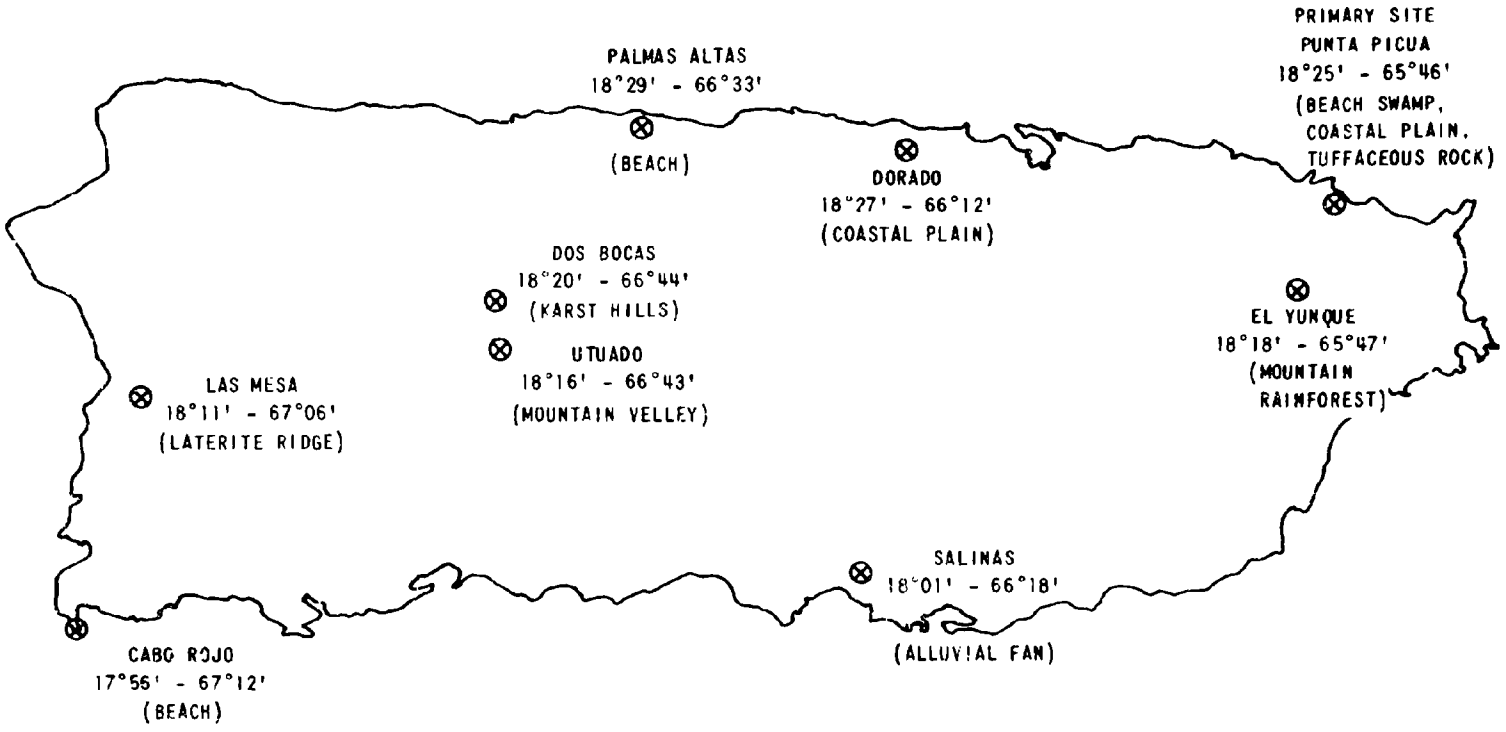

Figure B-1 SITES

2. PUNTA PICUA 18°25'N - 65°46'W

Because of its complexity of backgrounds and soils, this site was the major site from where samples were obtained. Figure B-2 shows the basic land forms of the site; 1) the Atlantic Ocean shoreline; 2) the beach; 3) the mangrove, 4) the coastal plain and 5) the Tuffaceous sandstone hills. A ground control target array was emplaced at LOCATION 1 and data were recorded at this location as well as at positions designated by other arabic numerals, both on Figure B-2 and indicated in tables.

2.1 Beach

The laboratory measurements of sand reflectance were obtained using a Beckman DK-2A spectrophotometer. The sand on this beach is described by Roberts (16) as either Palm Sand (Pb, pg. 344) or Catano Sand (cd, pg, 343). Roberts indicates the former contains one quarter inch rod like shells, where as the latter does not; the former is yellow whereas the latter is gray. All sand samples from this location had rod like shells and were yellow in color and have therefore been classed as Palm Sand, although a difference in reflectance was noted between sand samples from the active beach (2) and the middle of the stabilized beach (4), i.e. the beach surface covered with vegetation.

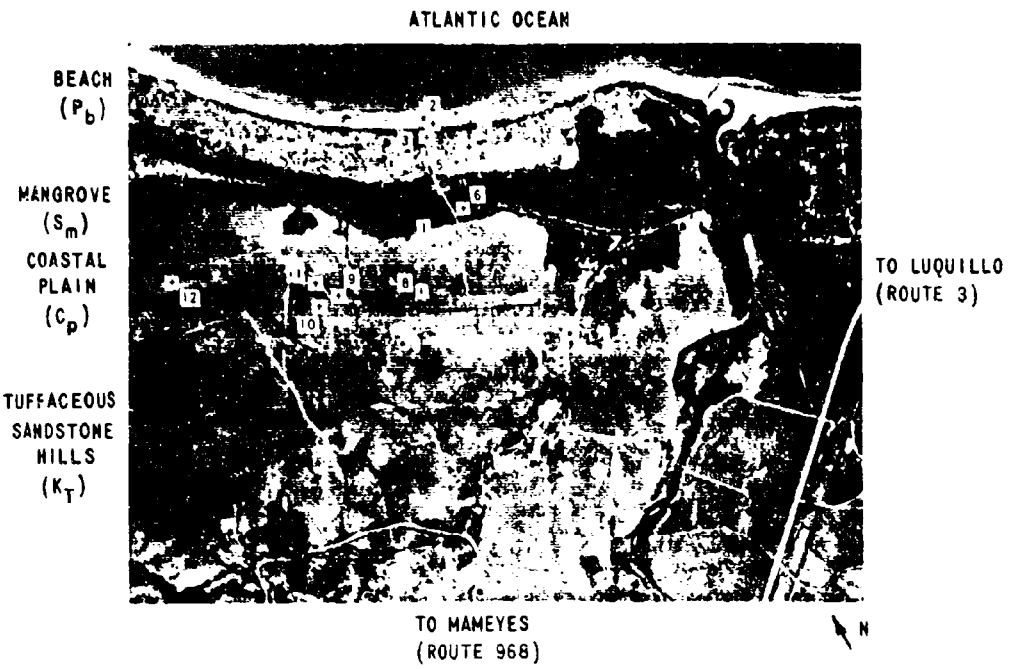

Figure B-2 PUNTA PICUA SITE

TABLE B-1 LABORATORY REFLECTANCE OF PALM SAND AT PUNTA PICUA (Pb)

	(6/17/68)		(11/23/68)		(11/25/68)		(11/26/68)	
λ	SAT.	DRY	BAG SAMPLE	DRY	BAG SAMPLE	DRY	BAG SAMPLE	DRY
.4	4	12	7	9	7	9	4	9
.45	6	15	9	12	9	12	5	11
.5	7	18	11	14	11	14	6	12
.55	14	21	16	19	16	20	8	15
.6	18	26	21	25	22	25	11	19
.65	20	29	24	28	25	29	13	21
.7	21	33	27	31	29	32	17	26
.75	22	35	30	34	31	35	21	31
.8	23	36	34	37	34	38	26	35
.85	24	37	-	-	-	-	-	-
.9	25	38	-	-	-	-	-	-
LOCATION	2		3		3		4	

	(11/25/68)		(11/23/68)		(6/17/68)	
λ	BAG	DRY	SAT.	DRY	SAT.	DRY
.4	4	8	-	-	-	-
.45	6	11	-	-	-	-
.5	7	12	8	13	8	17
.55	12	18	13	20	11	21
.6	18	24	19	26	15	25
.65	20	27	22	30	17	27
.7	23	30	25	33	18	29
.75	26	33	28	35	19	30
.8	28	35	29	38	20	32
.85	-	-	30	39	21	33
.9	-	-	30	40	21	34
LOCATION	2		3		2	

In addition to laboratory measures of reflectance, in situ measures were obtained at the locations indicated above using a CAL designed filter photometer.

TABLE B-2 IN SITU REFLECTANCE OF PALM SAND AT PUNTA PICUA (Pb)

λ	(12/1/68)	(12/1/68)	(11/26/68)	(11/26/68)	(11/23/68)
.40	12	-	-	-	11
.45	11	9	4	9	13
.50	10	7	4	10	13
.55	18	9	8	16	18
.60	23	11	12	22	17
.65	30	16	19	27	27
.70	29	19	16	31	28
.75	31	24	20	34	31
.80	32	26	31	35	34
.85	34	28	28	36	-
LOCATION	2	4	4	3	3

The measurements of the reflectance properties of the palm sand from the arieal, spectral films were presented in the text in Section 5 and therefore are not repeated here.

The distribution of grain sizes for this sand was obtained using a standard sieving procedure, and is as follows:

PALM SAND GRAIN SIZE DISTRIBUTION

Sieve Size	%
> 2mm	< 1
1-2mm	< 1
0.5-1mm	1
0.25-0.5mm	61
0.125-0.25mm	35
0.062.0.125mm	2
< 0.062mm	< 1

The moisture content by weight varied from a maximum of 32% for saturation to a low of 1% for the sample obtained from location 2 on 11/23/68 in the evening.

SAMPLE LOCATION	% MOISTURE BY WEIGHT
2 LABORATORY-SATURATION	32-26
2 (11/23/68) PM	1
3 (11/25/68) PM	6
2 (11/25/68) PM	1
4 (11/26/68) PM	11

Laboratory measurements of leaf reflectance from vegetation cover over this beach were impractical in that neither the geometry nor the plant vigor could be retained. In situ measures were recorded. Some appear in the text and the remainder are presented below.

TABLE B-3 IN SITU REFLECTANCE OF VEGETATION AT PUNTA PICUA BEACH

λ	11/23/68	11/26/68	11/26/68	11/26/68	11/26/68	11/26/68
.40	2	-	5	-	5	6
.45	4	3	-	2	-	2
.50	4	3	4	5	-	7
.55	7	10	7	9	9	10
.60	5	9	5	8	3	5
.65	4	12	4	7	3	15
.70	10	16	11	17	4	26
.75	28	31	34	47	21	38
.80	35	45	50	45	29	48
.85	44	36	43	53	24	62

LOCATION	4 Coccolobis Uvifera Woody Plant	5 Sporobolus Tufted Grass	5 Remirea Martima Sedge	5 Low Grass	4 Coccolobis Uvifera Woody Plant	2 Ipomoea Pes-Caprae-bay hops vine

Rain occurred frequently throughout the test period in the form of short showers. The following data were recorded from the rain gage at location 1.

Date	Time	Rain Depth	Accumulation
11/23/68		Set up 0"	
11/25/68	1440	0.03"	
11/26/68	0815	0.03"	0.06"
11/26/68	0827	0.045"	0.105"
11/26/68	1000	0.060"	0.160"
11/27/68	0930	1.400"	1.560"
11/27/68	1130	1.000"	2.560"
11/30/68	-	4.33"	6.890"
12/1/68	-	0.09"	6.98"
12/2/68	0830	0	6.98"
12/2/68	1030	0.25"	7.23"
12/2/68	1100	0.05"	7.28"
12/3/68	0200	0.04"	7.32"
12/4/68	1000	0.11"	7.43"
12/5/68	0800	0	7.43"
12/9/68	1100	0.01"	7.44"
12/10/68	0930	0.04"	7.48"

An excellent reference (20) to rainfall and soil moisture conditions across the island of Puerto Rico for 1955-1956 is available in the scientific literature.

2.2 MANGROVE

A partially drained mangrove swamp occurs between the beach and the coastal plain. Because of the drainage ditches which have been emplaced to drain the swamp, few large areas of the highly interwoven complex of root systems so typical of mangrove swamps remain. However, at location 6, Figure B-2 such a situation was present.

Two samples of the soil (muck) were acquired and their reflectance properties measured in the laboratory.

TABLE B-4 LABORATORY REFLECTANCE OF SALADAR MUCK (Sm) IN MANGROVE

	(11/23/68)		(12/3/68)	
λ	SAT.	DRY	SAT.	DRY
.4	2	5	3	6
.45	2	6	3	7
.5	3	7	3	8
.55	3	8	4	9
.6	4	9	5	10
.65	4	10	6	12
.7	6	12	8	14
.75	8	15	9	15
.8	10	17	11	18

No insitu measurements of the soil reflectance could be obtained because of the extremely low light level under the mangrove canopy. An in situ measurement was obtained for a fresh cut, high density sample of leaves from the mangrove trees per se, and is tabulated below.

TABLE B-5 INSITU REFLECTANCE OF MANGROVE LEAVES

WAVELENGTH	(12/5/68)	WAVELENGTH	(12/5/68)
.4	2	.65	3
.45	(8)	.70	10
.5	3	.75	62
.55	7	.8	62
.6	5	.85	60
LOCATION	1		

Although there appeared to be three rather distinct levels of mangrove trees which may have related to the three species of mangroves known to be present in Puerto Rico, (i.e. Black Mangrove, Avicennia nitida; white mangrove, Laguncuhria racemasa; and Mangrove, Phizophora mangle,) this was not established in the field.

The spectral reflectance values for mangrove were also derived from the spectral films and are presented in Section 5 of the text.

Roberts describes this soil as[16] Coastal Swamp, poorly drained, black, mostly organic materials, Saladar Much (S_m). A detailed description can be found on page 356 of Robert's survey.

2.3 Coastal Plain

From the mangrove to the contact with the slope of the tuffaceous sandstone a coastal plain. The soil in this plain is classed by Roberts as Coloso Silty Clay (cp), a poorly drained, brown, plastic, tuffaceous material. A complete description occurs in his survey on page 330. The area is presently being used as a pasture and is covered with pasture grass or in areas still subjected to flooding, tussock grass.

Although few areas of bare soil are present in this area, soil samples were collected and reflectance values derived in the laboratory.

TABLE B-6 LABORATORY REFLECTANCE OF COLOSO SILTY CLAY (cp)

	(6/17/68)		(12/1/68)		('2/1/68)	
λ	SAT.	DRY	BAG	DRY	BAG	DRY
0.4	3	8	4	13	4	9
.45	4	11	5	14	5	11
.5	5	12	6	15	5	12
.55	7	14	7	16	6	13
.6	8	16	8	18	7	14
.65	9	18	9	20	8	16
.7	11	20	10	22	9	18
.75	13	22	11	24	10	20
.8	15	25	13	26	11	23
.85	17	27	-	-	-	-
.9	19	29	-	-	-	-
LOCATION	7		1		1*	

*Site 30' from 1, but had been hosed down for 30 minutes prior to taking sample.

In situ measurements of soil reflectance were obtained on a surface exposed as a result of cattle moving across the coastal plain. Its geometry was altered each day by hoof prints and surface moisture. Nevertheless the data are presented below.

TABLE B-7 IN SITU REFLECTANCE OF COLOSO SILTY CLAY (ep)

λ	(12/1/68)	(12/4/68)	(12/9/68)
.4	2	3	7
.45	2	4	5
.5	2	4	4
.55	5	5	7
.6	2	7	9
.65	6	10	9
.7	6	8	11
.75	10	9	17
.8	15	12	18
.85	17	12	-
LOCATION	8	8	8
RAINFALL (ACCUMULATED READING)	6.98"	7.43"	7.43"

It should be noted that although the above tabulated data do not correlate well with each other there is a definite trend associated with the rainfall data presented earlier in this appendix.

No areas of bare soil, of sufficient size for deriving meaningful measurements of reflectance from the spectral films, were imaged from the minimum flight altitude of 3000 feet.

The identification of specific grasses within the general class called Pasture grass was not possible, primarily because of the heavy grazing which occurred. Although the time of year was correct for distinguishing between Carib grass and Para grass the effects of heavy grazing precluded such identifications.

Again, only in situ reflectance measurements and measurements from spectral film density were feasible considered geometry and plant vigor. The reflectance values derived from the spectral films are presented in the text, along with some of the in situ data. The remaining in situ data are presented below.

TABLE B-8 IN SITU REFLECTANCE OF PASTURE GRASS ON COLOSO SILTY CLAY (cp)

λ	(12/1/68)	(12/4/68)	(12/9/68)	(11/25/68)*	(12/5/68)*
.4	1	3	3	-	2
.45	4	3	4	3	4
.5	4	3	4	3	5
.55	9	6	8	5	12
.6	7	8	7	6	10
.65	6	8	9	4	10
.7	14	10	10	37	33
.75	34	33	45	48	53
.8	48	43	48	43	70
.85	58	48	33	46	90
LOCATION	8	8	8	1	1

*Protected from grazing.

TABLE B-9 IN SITU REFLECTANCE OF TUSSOCK GRASS ON COLOSO SILTY CLAY (cp)

λ	(12/1/68)	(12/4/68)	(12/9/68)
.4	4	2	2
.45	3	5	2
.5	7	5	3
.55	8	6	6
.6	9	6	4
.65	11	7	5
.7	14	10	10
.75	32	21	21
.8	37	23	32
.85	41	22	34
LOCATION	8	8	8

The variability in in situ measurements of vegetation is expected to be large. The primary reason for this is that unless the vegetation is a low surface grass, such as at Location 8, it is extremely difficult to: a) define the surface being measured and b) to insure that the relative distance between the photometer and the surface being measured is maintained a constant, throughout the measurement period. Nevertheless, the data above in several cases shows the vegetation trend, ie. a peak, in the 0.55 μ green band a minimum in the 0.65 μ band (chlorphyl band) and a maximum in the 0.70 μ -0.85 μ bands (near infrared).

2.4 Tuffaceous sandstone Hill and Contact With Coastal Plain

Location 9 is on the contact between the coastal plain described above and an area of tuffaceous sandstone hills. One, highly disturbed area of soil was found in which the soil appeared more brown in color than the samples of Coloso Silty Clay taken from Location 8.

TABLE B-10 COMPARISON OF REFLECTANCE OF SOIL ON LANDFORM CONTRACT, TO COASTAL PLAIN SOIL AND (cp) TUFFACEOUS SANDSTONE OUTCROP (k_T)

λ	CONTACT	COASTAL PLAIN	OUTCROP
.4	3	3	6
.45	4	4	7
.5	4	4	7
.55	5	5	6
.6	6	7	12
.65	7	10	19
.7	9	8	14
.75	11	9	19
.8	13	12	20
.85	14	12	17
LOCATION	9	8	11

An in situ measurement of the surface reflectance was recorded (9) and is compared to an in situ measurement (8) for Coloso Silty Clay and an outcrop of tuffaceous sandstone (11) all obtained on the same day. The higher overall reflectivity of the tuffaceous sandstone outcrop is obvious from the data as is the large increase in the red region of the spectrum 0.60 - 0.65μ. However, the difference between the two soils is lost in the precision of the measurement, even though the eye could detect a subtle difference in the field.

Other in situ measures of pasture grass on the slope of the tuffaceous sandstone hill (10) and over a highly weathered tuffaceous sandstone bolder are presented below in Table B-11.

TABLE B-11 IN SITU REFLECTANCE OF TUFFACEOUS SANDSTONE HILL AREA

λ	Tuffaceous Sandstone Bolder (12/4/68)	(12/9/68)	Pasture Grass (12/4/68)	(12/9/68)	Bamboo 12/4/68
.4	4	4	2	3	4
.45	4	4	3	4	4
.5	4	4	4	3	5
.55	6	6	6	7	13
.6	7	6	5	7	14
.65	7	11	7	3	10
.7	9	7	10	-	21
.75	15	8	33	-	40
.8	14	11	35	-	51
.85	19	16	40	-	53
LOCATION	10	10	10	10	9

Palmas Altas Clay Area (Pm)

To the west of the test site at location 12 is a small area quite apparent from its lighter tone on the conventional aerial photograph. The area is mapped by Roberts, to be Palmas Altas Clay (Pm) very similar to Coloso Silty Clay but more poorly drained, black and more saline. A full description is given on Page 348 of his survey.

In situ measurements were made of the soils reflectance properties for comparison to the in situ measurements of the Coloso Silty Clay and in situ vegetation measures were also recorded. The data are tabulated in Table B-12.

TABLE B-12 COMPARISON OF IN SITU REFLECTANCE OF TUSSOCK GRASS ON TWO DIFFERENT SOILS

λ	Palmas Altas Clay	Coloso Silty Clay	Tussock Grass Palmas Altas	Tussock Grass Coloso Silty Clay
.4	3	7	-	2
.45	10	5	6	2
.5	9	4	4	3
.55	12	7	9	6
.6	13	9	11	4
.65	17	9	8	3
.7	16	11	13	10
.75	17	17	56	21
.8	17	18	50	32
.85	22	-	56	34
LOCATION	12	8	12	8

As expected because of its light tone on panchromatic film the Palmas Altas Soil and vegetation were generally better reflectors across the visible spectrum than the Coloso Silty Clay and Vegetation. In the .65μ band which indicates vegetation vigor the tussock grass over the Palmas Altas Clay showed a reflectance of almost a factor of 3 higher than tussock grass over the Coloso Clay. This is probably due to the salinity of the soil retarding the grass growth. In the near infra red it still maintained the typically high reflectance for vegetation. Generally, the near infra red reflectance for plants drops when growth is retarded, however, this is not always true.

Other measurements, such as surface temperature and moisture contents of soils were made at this site, strictly for a quantitative analyses of the spectral films and are therefore of no general value and are not included in this report.

3. EL YUNQUE RAIN FOREST SITE 18°18' - 65°47'W

This site is located close to the highest elevation on the island of Puerto Rico. As pointed, out by Briscoe (22) the vegetation at this elevation is much smaller than is normally expected in a mature rain forest, probably due to the almost continuous cloud cover present. Others refer to this forest as a cloud forest rather than a rain forest, and apply the term rain forest to the lower elevation Tabonuco forest which indeed has tree heights and diameters more consistent with rain forests of Southeast Asia.

The topography of areas such as El Yunque make the development of a ground transportation system extremely costly. The continuous poor weather conditions preclude the establishment of an effective air lift support system, where it may be imperative to emplace a support facility in such an environment. Because of the continuous poor weather, it is difficult to obtain remote sensor data over such an area. Finally, even if such data are acquired the canopies provide natural camouflage of the soils below, which are of primary interest to the terrain analyst.

If on the other hand, relationships could be established between tree-reflectance and soil environment below, remote sensor spectral data could conceivably be useful in terrain evaluation studies. Therefore an attempt was made to collect both aerial and ground data from this site. However, only one aircraft mission over the area was possible because of the cloud conditions, and ground reflectance measurements were precluded because of the low illumination level resulting from the cloud condition and dense canopy. Nevertheless, the control panels were in place at location 1 as shown in Figure B-3 so that reflectance data can be derived from the spectral films.

Because of camera exposure problems (shutter banding) a preprocessing procedure beyond the scope of the present effort is required to correct differences caused by banding for a quantitative analysis of this film. Furthermore, the soils data available in the literature (16), on the site area,

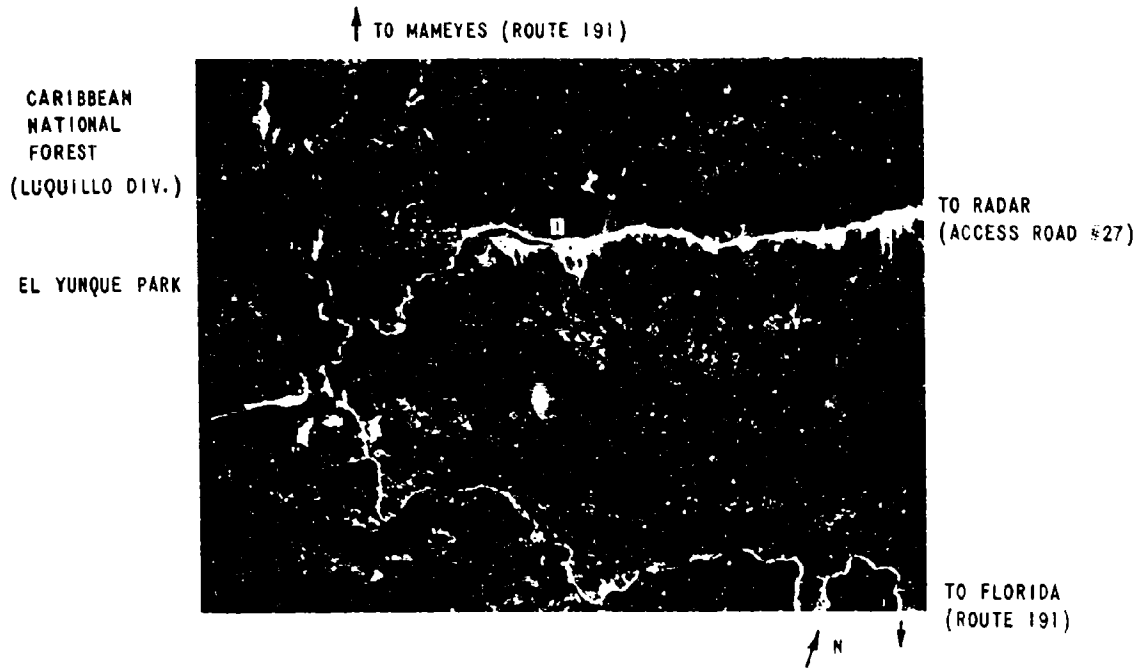

Figure B-3 EL YUNQUE RAINFOREST SITE

is too general to be useful in establishing any correlation between soils and vegetation.

In situ reflectance measurements for Bamboo and clearing grass in the vicinity of the control panels (1) were taken and are presented below.

TABLE B-13 IN SITU REFLECTANCE OF VEGETATION AT EL YUNQUE

(11/30/68)

λ	Bamboo	Grass
.40	3	6
.45	3	6
.50	4	4
.55	11	
.60	10	9
.65	7	4
.70	13	14
1 LOCATION	1	1

4. SALINAS SITE 18°01'N - 66°18'W

The site is on the south shore (Carribean side) of the island. It is a savannah environment with the typical acacia trees and guinea grass the predominant vegetation of the area. Both sedimentary (limestone, sandstone, and shales) and volcanic (tuffaceous) rocks are present in the area. The soils are predominantly clays, however, some contain appreciable amounts of sand and stone fragments. The site is shown in Figure B-4.

Laboratory Reflectance

A soil sample was acquired from locations 1 and 2, shown on Figure B-4. According to Roberts, these soils are: Amelia Clay (Aw) and Yauco Clay, Colluvial Phase (Yo) and are described on pages 263 and 259 respectively in Reference 16. In addition, two samples of soil were obtained from a road cut in an area described as Descalabrado silty clay (De - page 240) just to the north west of the area shown in Figure B-4. The reflectance data for these samples are presented below.

TABLE B-14 REFLECTANCE OF SOIL AT SALINAS

	Aw	Aw	Yo	Yo	De"A"	De"B"
	S	DRG	BAG	DRG	DRY	DRY
.40	1	5	10	13	5	5
.45	2	7	13	16	6	7
.50	3	8	15	19	7	8
.55	4	11	22	26	11	12
.60	6	14	27	31	14	17
.65	7	16	31	33	17	20
.70	9	19	32	36	19	24
.75	11	21	35	39	23	26
.80	12	23	38	42	26	30
.85	14	25	-	-	-	-
.90	22	28	-	-	-	-

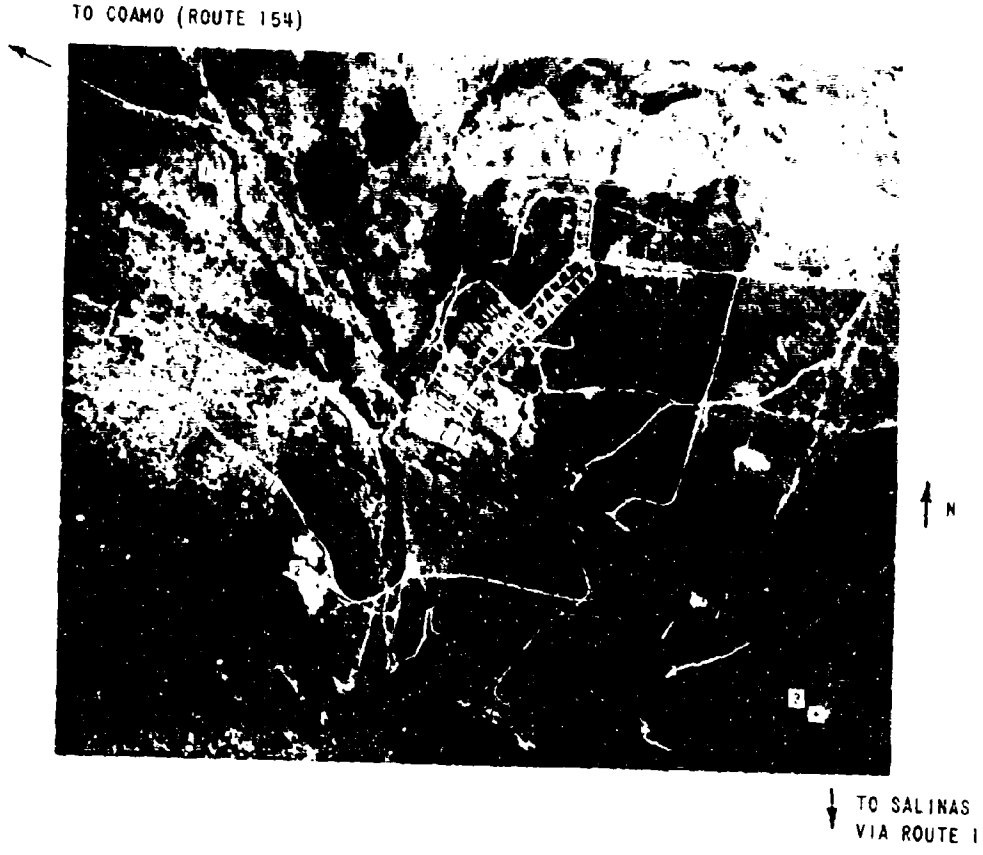

Figure B-4 SALINAS SITE

The sample of Yauco Clay (Yo) was thoroughly sieved to the distribution indicated below and the reflectance of each sample of different grain sizes measured as indicated in the text.

TABLE B-15 GRAIN SIZE DISTRIBUTION BY WEIGHT

Grain Size	> 2mm	1-2mm	0.5-1mm	0.25-0.5mm	0.125-0.25mm	0.062-.125mm	< 0.062mm
YAUCO CLAY	37	18	17	12	9	5	2
AMELIA CLAY	56	18	12	7	4	2	2

Although classed as a clay by Roberts, he notes the presence of limestone rock fragments in the Yauco Clay, colluvial phase, and granular materials in the Amelia Clay.

In situ measures of reflectance were also made at location 2 and to the west of the area covered by Figure B-1.

TABLE B-16 IN SITU REFLECTANCE OF SOILS IN SALINAS

λ	(11/28/68)	(11/28/68)	(11/28/68)	(12/8/68)
.40	5	1	1	6
.45	10	1	1	12
.50	6	1	2	13
.55	9	2	4	19
.60	11	5	5	23
.65	12	12	8	--
.70	23	7	13	33
.75	27	7	16	35
.80	24	11	16	43
.85	?	13	21	36
SOIL TYPE	(Oe)	(Oe"A")	(Oe"B")	(Yo)

Good agreement is shown between the in situ reflectance (Table B-16) and laboratory (Table B-14) measurements of reflectance for the Yauco(Yo) while the Descalabrado Silty Clay (De"A" and "B"s show the effects of surface moisture.

Three additional in situ reflectance measures were taken at location 3 as shown on Figure B-4. One was over coarse gravel (cobbles) in the dry river bed and the others were on an erosion slope adjacent to the river. The former is designated as R_V by Roberts and is described on page 278 of his report.

TABLE B-17 IN SITU REFLECTANCE OF ALLUVIAL SOILS AT SALINAS

	Coama Silty Clay Loam (Cos)		River Wash (Rv)
	Erosion Surface		
	Granular	Chips Clay Cracks	Cobbles
λ			
.4	6	9	-
.45	12	11	8
.50	14	12	11
.55	17	21	15
.60	20	22	13
.65	19	25	12
.70	27	32	16
.75	25	29	16
.80	40	38	21
.85	32	32	20
LOCATION	3	3	3

Most of this area is either grassland or planted to crops. One in situ measure of the grass at location I was obtained.

TABLE B-18 IN SITU REFLECTANCE OF GRASS ON AMELIA CLAY

λ	11/28/68
.40	3
.45	12
.50	11
.55	11
.60	12
.65	22
.70	16
.75	37
.80	31
.85	30
LOCATION	I

5. CABO RAJO 17°58'N - 67°03'W

On the extreme south west tip of the island of Puerto Rico is a limestone promontory on which a light house is located, Cabo Rajo. This area was not selected as a site for detailed study, but was visited during a site inspection trip in June of 1968. A sand sample was obtained from the beach at location 1 as shown on figure B-5. The sample was saturated with water and dried in a series of five steps, with reflectance measurements made at each step. The results are tabulated below. Roberts classifies this sand as Jaucas Sand and it is described on page 345 of his report. The white coral fragments of this sand explain its unusually high reflectance relative to other sands of the island. Another sample was sieved to obtain the distribution of grain sizes shown below.

TABLE B-19 REFLECTANCE OF JAUCAS SAND

Wavelength μ	Moisture Content:	.36	.31	.5	.1	Dry
.4		.24	.25	.26	.29	0.33
.45		.26	.31	.35	.36	.40
.50		.31	.36	.38	.41	.45
.55		.38	.43	.46	.48	.51
.60		.41	.47	.50	.52	.55
.65		.43	.49	.52	.54	.57
.70		.45	.51	.55	.57	.60
.75		.47	.53	.57	.59	.62
.80		.49	.55	.59	.61	.63
.85		.50	.56	.61	.63	.65
.90		.51	.58	.62	.64	.66

TABLE B-20 GRAIN SIZE DISTRIBUTION OF JAUCAS SAND

Grain Size	>2mm	1-2mm	.5-1.0mm	.25-.5mm	.125-.25mm	0.062-0.125mm	<0.062
By Weight	0.1	0.1	0.5	1.0	88.8	9.5	

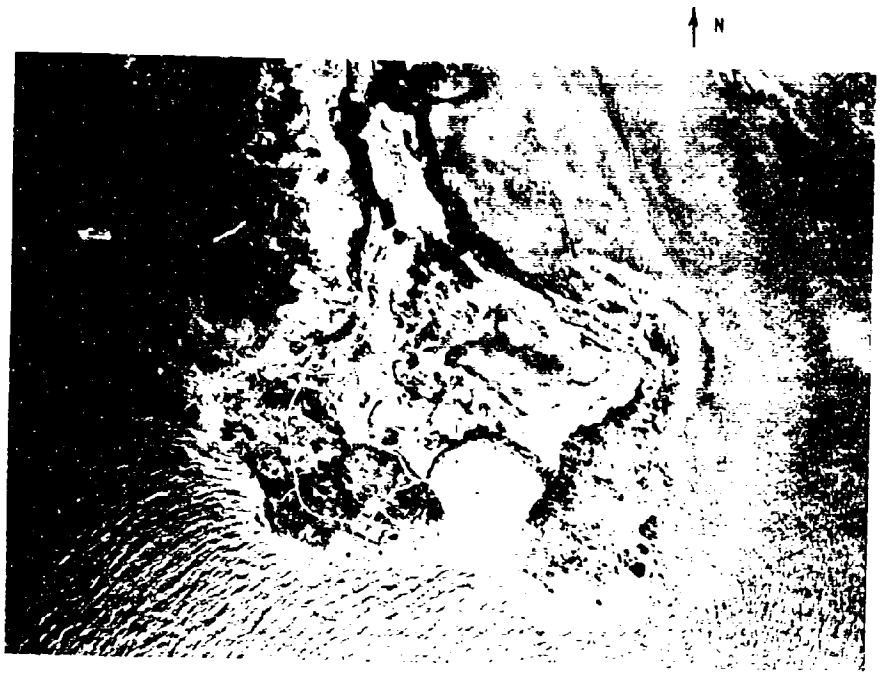

Figure B-5 CABO ROJO

6. LAS MESAS 18°11'N - 67°06'W

In the west central part of the island is a unique latosolic soil, namely the Nipa Clay (Nc), by Roberts[16]. A large area of the soil occupies the crown of a hill known as Las Mesas south east of Mayagüez, Puerto Rico on Route 349, as shown in Figure B-6. Roberts also indicates a large area of the soil being present near the coast south west of Mayagüez. Associated with this soil is a silty clay, Rosario (Rs) by Roberts, which even he indicates to be very similar to a shallow phase Nipa Clay. There is some question therefore between soil scientist as to the validity of the separate classifications for these soils.

Three samples of surface soils were obtained from different locations on Las Mesas, as shown on Figure B-6, 1, 2, 3. The laboratory reflectance measurements for these samples are tabulated below.

TABLE B-21 LABORATORY REFLECTANCE OF NIPA CLAY AT LAS MESAS

λ	(6/28/68)	(6/28/68)	(6/18/68)	(6/18/68)	(6/18/68)	(6/18/68)	(11/28/68)	(11/28/68)	(12/11/68)
.380	2	3	2	1	4	6	1	7	4
.400	2	4	3	3	5	7	3	8	5
.420	3	5	4	6	7	8	5	9	5
.440	4	6	5	7	8	10	7	11	7
.460	7	11	9	12	13	15	13	17	10
.480	8	11	11	13	16	18	16	20	12
.500	11	14	15	17	18	20	17	23	14
.520	13	16	17	20	21	23	20	25	16
.540	15	20	19	21	22	25	22	28	18
.560	16	22	21	23	24	27	-	-	-
.580	18	25	22	25	26	30	-	-	-

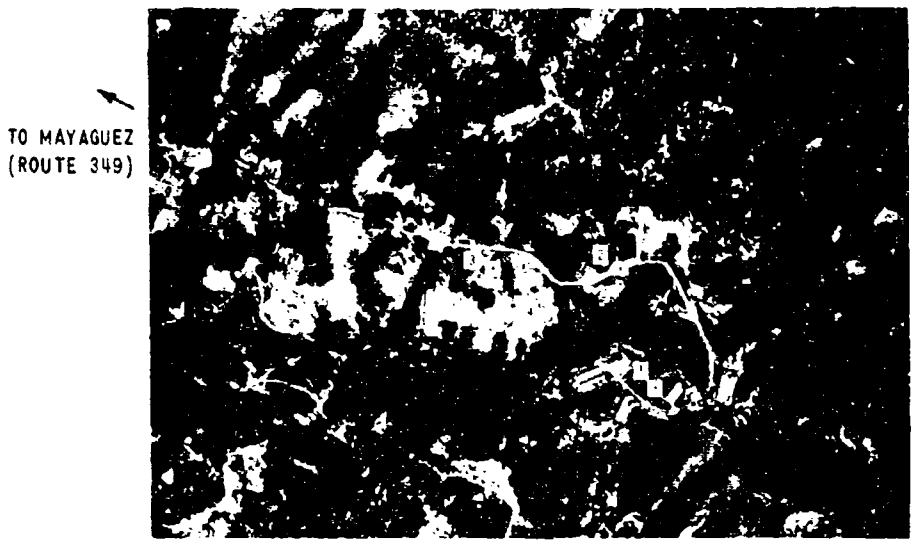

Figure B-6 LAS MESAS SITE

In addition to the reflectance measures above, the 6/18/68 Sample 2 was sieved and the following distribution of grain size obtained.

TABLE B-22 GRAIN SIZE DISTRIBUTION OF NIPA CLAY

Sieve Size	> 2mm	1-2mm	.5-1mm	.25-.5mm	.125-.25mm	.062-.125mm	< 0.062mm
% Weight	0.1	.4	4	25	34	22	15

This distribution agrees within 14% with the findings of Roberts. Seventy one percent of his sample taken for 0-5 inch depth fell between 2 and 0.05 millimeters as compared to eighty five percent for this sample.

At a road cut, location I1, a shallow (0-5 inch) yellow soil was noted. Because of its sharp contrast in color to the red Nipa and Rosairo soils of the area it was indeed a curiosity; so a sample was obtained. The results of the laboratory measurements of Reflectance are tabulated below.

TABLE B-23 REFLECTANCE OF "YELLOW" SOIL

λ	Sat	-8Gm H_2O	-15Gm H_2O	-19Gm H_2O	DRY
.40	8	6	4	7	14
.45	14	10	8	13	20
.50	18	13	11	17	25
.55	33	28	24	31	42
.60	41	37	34	39	49
.65	42	37	34	39	49
.70	45	40	37	43	52
.75	49	45	41	46	56
.80	53	49	46	51	60
.85	58	53	50	55	64
.90	62	57	54	60	68

It should be noted that with this soil as well as other soils containing mostly fines, that surface cracks develop in the sample surface upon drying. These cracks act as light traps lowering the apparent reflectance of the sample below that measured for the saturated state. This is another case which points out the importance of the surface structure to the understanding of the reflectance measured for a surface.

In addition to the laboratory measures of reflectance, in situ measures of soil reflectance were also recorded, and are tabulated below.

TABLE B-24 IN SITU REFLECTANCE OF LATOSOLIC SOIL

λ	(6/18/68)	(11/29/68)	(12/14/68)	(12/14/68)	(12/14/68)
.40	5	4	2	2	4
.45	6	5	2	3	-
.50	6	-	4	5	2
.55	8	11	4	7	6
.60	11	8	10	16	7
.65	13	12	10	19	9
.70	18	13	14	25	12
.75	20	16	15	31	12
.80	19	20	22	33	14
.85	-	30	24	30	22
LOCATION	3	1	1	1*	1**

* Light surface highly weathered outcrop

** Dark surface highly weathered outcrop

At location 4 on figure B-6 an outcrop of serpentine (k_s) occurred. According to Briggs[20] and others, this unconformity of rock forming mineral underlies the entire ridge known as Las Mesas and is the parent material of the Nipa Clay (Nc) which caps the ridge top. A sample was obtained and reflectance measures run in the laboratory. The results are tabulated below:

TABLE B-25 REFLECTANCE OF SERPENTINE (ks)

λ	Fresh Face Samples				Iron Stain Samples		Yellow Inclusions	
.40	-	-	-	-	-	-	-	-
.45	-	-	-	-	-	-	-	-
.50	14	15	18	19	7	9	16	20
.55	16	17	18	20	10	12	26	28
.60	17	19	18	20	15	16	33	32
.65	16	18	17	19	16	17	32	30
.70	16	18	17	18	17	17	30	27
.75	16	18	16	18	18	19	30	27
.80	16	18	16	18	18	19	31	28
.85	16	17	16	17	18	18	31	28
.90	15	16	15	16	17	17	30	26
SAMPLES	"A"	"B"	"C"	"D"	"E"	"F"	"G"	"H"

It is interesting to note that the spectral reflectance curves of the yellow inclusions in the serpentine rock samples bear a general resemblence to the curves of the "yellow" soil reflectance measures given previously. This suggests that perhaps a large inclusion produced the unusual limited area of "yellow" soil at this site.

In situ reflectance measurements were obtained for vegetation at this site and are tabulated below. The grasses, at location 1 of figure B-6, the area for which right of entry permits were available, were planted for lawn cover not pasture. No blooms were present, nor were there any other clues to make an identification. Molinari[18] gives an excellent discussion of commonly occuring grasses of the serpentine hills of Puerto Rico on pages 102-112 of his text on grasslands, however, he does not cover ornamental grasses. Reflectance readings were taken primarily to determine whether or not major difference from the grasses of other areas were apparent. A cursory comparison failed to show any such differences.

TABLE B-26 IN SITU REFLECTANCE OF VEGETATION LAS MESAS

λ	Grass Tall	Grass Tall	Grass Short	Grass Short	Bamboo	Coconut Palm
.40	1	1	4	1	3	2
.45	4	2	6	4	6	3
.50	6	4	7	2	8	-
.55	8	9	11	11	16	7
.60	5	5	11	8	17	8
.65	6	5	4	5	12	6
.70	8	13	11	11	19	12
.75	29	52	47	62	46	72
.80	43	52	30	62	75	74
DATE	11/29	12/14	11/29	12/14	12/14	12/14

7. DOS BOCAS 18°20'N - 66°44'W

This site is in the west-central part of the island in the Rio Abajo forest. The topography is typical of tropical karst, commonly referred to as haystack hills. There are very few areas of deep soil. Those which are present are restricted to the bottom of depressions and in general are of such limited extent they are used only for crops or for pasture.

One soil sample was collected for location 1 on figure B-7. Robert's classifies this soil as Lares Clay, red subsoil phase and gives a description on page 271 of his report. The laboratory reflectance measurements for this soil are shown below.

TABLE B-27 LABORATORY REFLECTANCE OF LARES CLAY DOS BOCAS

λ	w/o cracks	w/cracks
.50	7	4
.55	11	7
.60	16	11
.65	19	13
.70	22	15
.75	25	18
.80	26	18
.85	26	17
.90	25	17
LOCATION	1	1

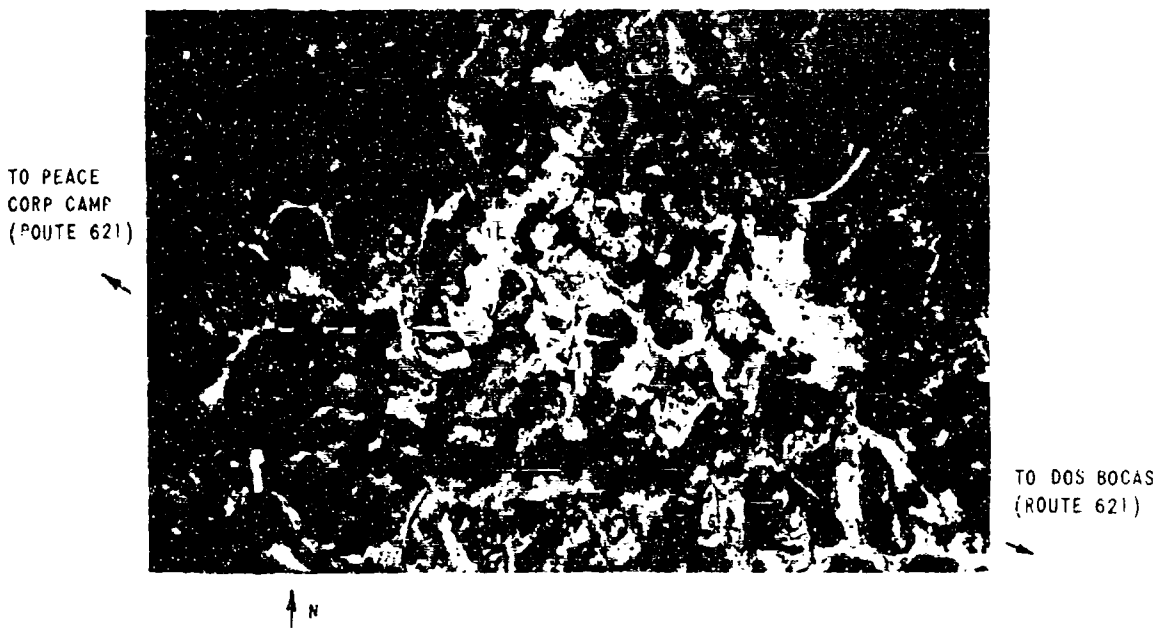

Figure B-7 DOS BOCAS SITE

Sample of the pink and white limestone of the area were obtained along with a sample of diorite. Laboratory reflectance measures were also taken using these rock samples.

TABLE B-28 LABORATORY REFLECTANCE OF LARES LIMESTONE (T_1-PINK)

λ	Fresh		Fresh	Fresh	Weathered	Weathered	Weathered
.50	51	45	50	55	51	50	51
.55	50	51	45	50	58	50	48
.60	61	62	55	60	60	61	59
.65	66	68	61	64	64	64	64
.70	69	71	65	67	68	68	68
.75	72	73	68	70	68	69	70
.80	73	74	68	69	68	69	68
.85	73	74	68	69	68	69	70
.90	73	74	68	69	68	69	70
Sample	[illegible]		[illegible]	[illegible]	[illegible]	[illegible]	[illegible]

TABLE B-29 LABORATORY REFLECTANCE OF LARES LIMESTONE (T_1-WHITE)/DIORITE

λ					
.50	53	54	44	45	8
.55	60	60		42	9
.60	68	67	55	57	8
.65	71	72	57	57	8
.70	75	76	63	62	7
.75	77	77	68	66	7
.80	81	81	71	69	8
.85	82	80	73	71	8
.90	83	82	73	73	7
SAMPLES	[illegible]	[illegible]	[illegible]	[illegible]	Diorite

Low illumination levels on both trips to this site precluded the collection of any in situ reflectance data.

8. UTUADO 18°16'N - 66°43'

This site is also in the west-central highlands, a few miles south of Dos Bocas in a Plutonic Rock (Tk_p) area. There are alluvial deposits of sand, (Qa) a by product of the weathering process of the granities at the lower elevations which are used for construction purposes. One such deposit is located at position 1 on figure B-8. Roberts classifies this soil as Estacion Sandy Loam (E) and describes it on pages 519-520 of his report. Briggs (20) describes the deposits as alluvial materials (Qa). A sample of this sandy loam was obtained from location 2 shown on figure B-8. Also to the northwest along route 111 in the granite area, a land slide was observed exposing a medium-stiff red massive clay which appear related to areas of Jayuya silty clay loam. Samples were also obtained at this location. Reflectance measurements were run in the laboratory.

TABLE B-39 REFLECTANCE OF SAMPLES (Qa) AT UTUADO

λ	SAND-ESTACION (E)				SAND-JAYUYA (Jy)			
.4	4	6	8	10	8	24	24	29
.45	5	7	11	12	14	31	31	36
.5	6	7	13	13	18	34	34	39
.55	8	9	17	17	25	43	44	49
.6	10	11	21	21	31	48	49	55
.65	13	14	24	25	34	52	54	58
.7	16	16	25	27	38	55	57	61
.75	18	18	29	31	40	58	60	64
.8	20	20	32	34	40	57	59	63
SAMPLE	BAG "A"	BAG "B"	DRY "A"	DRY "B"	BAG "A"	BAG "B"	BAG "A"	BAG "B"

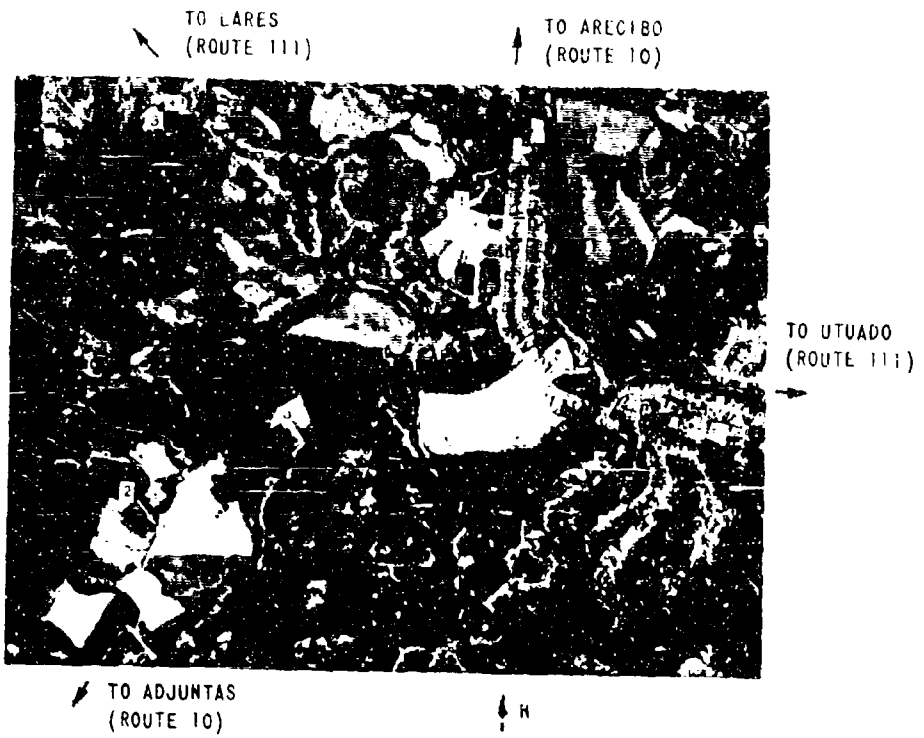

Figure B-8 UTUADO SITE

TABLE B-31 REFLECTANCE OF LATOSOLIC SOIL AT UTUADO

λ				
[illegible]	1[illegible]	1[illegible]	12	[illegible]
[illegible]	1[illegible]	13	1[illegible]	1[illegible]
[illegible]	18	[illegible]	2[illegible]	2[illegible]
.6[illegible]	22	26	28	29
.7	[illegible]	30	32	31
.75	27	33	[illegible]	[illegible]
.8	28	34	[illegible]	[illegible]
.85	28	31	[illegible]	34
[illegible]	[illegible]	[illegible]	[illegible]	34
SAMPLES	[illegible]	[illegible]	[illegible]	[illegible]

Three in situ measures of sand reflectance were obtained before rain curtailed data collection in the field.

TABLE B-32 IN SITU REFLECTANCE OF SAND (Qa) AT UTUADO

λ	DRY	WET	WET
.4	–	4	2
.45	16	6	8
.5	15	–	8
.55	19	11	11
.6	27	14	11
.65	30	19	16
.7	32	20	19
.75	47	26	25
.8	46	21	26
.85	55	23	3[illegible]
SAMPLES	[illegible]	[illegible]	[illegible]

9. PALMAS ALTAS 18°29'N - 66°33'W
DORADO 18°27'N - 66°12'W

During the inspection of sites in June of 1968, two other samples of soil were acquired. One, a sample of magnetite sand (Pb-black) from a beach at Palmas Altas and the other a fine sand (Su-white) from Dorado. Briggs (20) refers to this sand as beach and dune deposits (Qb) noting conspicuous occurrences of magnetite may be present. Roberts (16) notes the deposit as Palm sand, (Pb) and notes the high percentage of magnetite and the change to a dark color for this deposit.

With respect to the fine white sand, Briggs classifies it as blanket deposits (QT_B) with the road from Dorado west to Parcelas Brena completely within this grouping. Roberts reports a variety of White fine sands along this route. Based upon the location from which we acquired our surface sample of soil it would be identified as Saint Sucre Fine Sand (Su). The results of laboratory reflectance measurements are tabulated below.

TABLE B-33 LABORATORY REFLECTANCE OF DORADO SAND (Su)

λ	SAT 27%	16%	9%	7%	DRY
.4	4	5	7	8	18
.45	6	7	9	10	20
.5	7	8	10	12	22
.55	8	10	12	16	25
.6	10	12	15	17	27
.65	12	14	17	19	30
.7	14	17	19	22	32
.75	16	19	22	25	35
.8	19	22	24	28	38

TABLE 5-33 LABORATORY REFLECTANCE OF PALMAS ALTAS SAND (PR)

λ	2.5%	15%	DRY
.4	2	3	7
.45	3	4	9
.5	4	5	10
.55	5	6	12
.6	6	7	14
.65	6	7	14
.7	6	7	14
.75	6	7	14
.8	6	7	14

10. Climatology

The climate of an environment plays a major role in establishing the terrain features which will occur in a specific environment. Roberts (16) provides a brief but meaningful chapter on the climate of Puerto Rico, including specific relationships between vegetation occurrence and climate, animal adaption and climate, soil color and climate and race distribution and climate.

Such relationships are very important to the geologist, geographer, soil engineer, forester and many others in establishing the reasons for specific terrain feature occurrences. To the image interpreter of remote sensor data these relationships are also important, because with prior knowledge of the climate of an environment he is psychologically conditioned for the recognition of images related to the climatology. Without prior knowledge, recognition of specific terrain features unique to particular climates conditions establishes the climatology of the area under analysis. Unfortunately, research to establish refined, quantitative relationships between climatology and terrain features has not been given backing commensurate with its importance with respect to remote sensing.

Thornthwaite (21) attempted to quantify climate in terms of a climate index involving the ratio of mean monthly precipitation to mean monthly evaporation. Quisti and Lopez (22) attempted to correlate annual stream flow to annual rainfall with this climates index for several rivers in Puerto Rico. Although the results did not show perfect correlation they were encouraging. More of this type of quantitative climatic research is necessary in order to derive the remote sensing techniques which will allow an interpreter to evaluate the climatology differences between areas from remote sensor data.

Appendix C

HRK, MODEL 002 MULTIBAND CAMERA CALIBRATION

1.0 INTRODUCTION AND SUMMARY

To collect the spectral aerial photography from which to derive, quantitatively, the spectral reflectance of ground objects from image densities, an aerial camera is required that reliably records image density from frame to frame and across the format of a single frame. Under previous programs, CAL showed that several aerial cameras with focal plane shutters could not be used to collect spectral data because of very large, non repeatable errors in the shutters speed.

The Itek Multiband Camera, Model 002, which was to be used to collect the required spectral films, has a focal plane shutter, with a slit for each of the nine lens positions in the camera. Therefore it was necessary to evaluate the performance of this shutter. This was accomplished on 25 July 1968 at AFCRL by personnel from the Terrestrial Science Laboratory (CRJT) and from CAL. Data were acquired to evaluate the uniformity of the shutter speed across the 70-mm format, the repeatability of the shutter on consecutive exposures and the transmission characteristics of the lens/filter components. This appendix documents the results of the CAL analysis of the test data.

As expected, systematic differences in shutter speed occuring across the format were present. However, these differences are repeatable with a one sigma deviation of ±6% or less of the mean. Although sufficient data were not obtained to prove that the errors for the 1/60 and 1/120 of a second speeds would be the same order of magnitude as for the 1/30 of a second speed, the data which was obtained suggests this was true.

Two camera problems were also noted during this analysis. First, light leaks occur on the first frames of a sequence and on all single frames exposed manually. Second, parallel lines (light) appear on the infrared film used in the channel for frames 7, 8, and 9, which are believed to be related to the pressure of the vacuum back or rollers.

On a previous program CAL derived the reflectance of ground objects from spectral film densities with a precision of ± 6-7% of the mean value of reflectance. The repeatability of the shutter speed for the aerial cameras used was on the order of ±5%. Therefore it is concluded that the Itek Model 002 Multiband camera, with its ±6% or less shutter variation can be used to collect meaningful spectral data, but that the resultant measurements of ground object reflectance will be less precise than measurements made by CAL on previous programs.

The details of the tests performed are discussed in the following sections.

1.1 BENCH TESTS

The test procedure for determining the shutter speed of a focal plane shutter with respect to position across the film plane is to photograph a rapidly cycling calibrated light source. The position of the slit in the focal plane shutter will be recorded on the film each time the light flashes.

The separation of two adjacent slit images multiplied by the cycling rate of the light source is the average linear speed of the slit for the selected format position. The shutter speed (i.e., the time interval over which the film is exposed in normal camera use) is the width of the slit divided by its linear speed.

The test procedure for determining the relative loss in transmission across the format is to photograph a uniform light source located close to the front of the lens. A line across the format, perpendicular to the direction of motion of the shutter, is at a constant shutter speed, (i.e., all points along such a line are exposed for the same time) therefore the difference in densities are a function of the transmission properties of the lens and filter only.

1.2 TEST PROCEDURE

The Itek 9-lens camera was set up on a bench in a laboratory at AFCRL. Windows were partially covered to reduce the ambient light level in the laboratory. A strobe light (Strob-a-tac) was placed on the bench at the side of the camera and aimed at a 30" x 40" white composition board placed in front of the camera about one foot from the lenses.

Starting at a shutter speed of 1/30 of a second and an f/number of f/2.4, a series of five exposures were taken. The composition board was removed and a uniform light source was placed in contact with the lenses and a series of three exposures taken. The f/number was changed to f/8 and a second series of exposures were taken with the composition board in place. This process was repeated for an f/number of f/22 and shutter speeds of 1/60 and 1/120 of a second. For the 1/120 of a second exposures, the cycling of the strobe was increased from 1200 cpm to 2400 cpm.

The three rolls of 70-mm film from the camera were processed by CRJT personnel in a Morse B5A rewind type processor. Kodak D-19 chemicals and an appropriate processing time were used to obtain a film gamma of 2.0. The films were then brought to CAL for analysis.

Each frame used to determine shutter speeds was scanned on CAL's model 1140 Mann microdensitometer using a slit aperture (1 mm x 20 microns). Because the focal plane shutter is on the order of 1/4" away from the film plane, the edges of the slit images were not sharp. Therefore, the criterion of locating the slit edge at the half-peak power point of the density trace was used to establish the points for measuring slit widths and cycles. Frames which were grossly overexposed were not used because the edges were broadened by the over-exposure. Four consecutive frames were used to determine the repeatability of each shutter in 5 to 6 positions across the format. One frame and eight lenses were used to check the deviations between lenses at several positions in the format. Standard deviations were determined for all results.

1.3 DATA ANALYSIS AND RESULTS

1.3.1 Density for Shutter Variations

The quantitative analysis to be used on this AIGRL Project (TERRAVAL) begins with the measurement of the densities of the images of interest on all nine filtered films of the Itek camera. A model 1140 Mann microdensitometer with a measurement accuracy of ±0.02 in density of ±5% in transmission will be used. Without the calibration tests which have been performed one would have to assume that the exposures for the 9-1 lenses were equal for any indicated shutter speed and for any position across the format. As Table C-1 shows, the average shutter speed for the nine lenses had deviations as large as ±20%. Such a deviation would introduce a density error of 0.08 times the gamma to which the film is processed. For Project TERRAVAL, we anticipate processing to a gamma of +2.0 which would result in a density error of ±0.16. Errors in terrain reflectances derived from such data would be of questionable utility. Therefore, to reduce this error each lens/shutter system requires calibration.

Table C-1

AVERAGE SHUTTER SPEED ACROSS FORMAT

Format Position*	Indicated Shutter Speeds 1/30 (0.0333 sec)	1/60 (0.016 sec)	1/120 (0.00833)
0.3	0.0300 ±18%	--	--
0.6	0.0324 ±9%	--	--
0.8	--	0.0168 ±17.2%	0.00890 ±6%
0.9	0.332 ±12%	--	--
1.2	--	0.0161 ±12%	0.00859 ±8%
1.3	0.332 ±10%	0.0167 ±19%	--
1.6	0.332 ±10%	--	0.00844 ±9%
1.8	--	0.0165 ±12%	--
1.9	0.331 ±15%	--	0.00844 ±6%
2.0	--	0.0174 ±22%	--

*Distance in inches from leading edge of frame.

Table C-2 shows the mean shutter speed for each lens position, derived from four consecutive exposures for five to six positions in the 70-mm film format. These data are shown again in the histogram of Figure 1. In 38 of the 46 (87%) measurements made, the deviation is ±6% or less. Five of the eight remaining measurements were obtained from the extreme edges of the film format where large errors are likely because lens transmission falls off drastically making it difficult to measure slit widths and cycle distances accurately from the microdensitometer traces of the test films. Because the majority of the deviations are ±6% or less and because the large deviations occur in at the edge of the format, it is concluded that the repeatability of the Itek 9-lens camera shutter at 1/30 indicated speed is ±6% or better over most of the 70-mm format.

The question now arises as to whether or not the repeatability is valid for the 1/60 and 1/120 indicated speeds. As Table C-1 shows, there appears to be a slightly larger variation in shutter speeds at 1/60 of a second and slightly less variation at the 1/120 speed. The majority of the test films for the 1/60 and 1/120 shutter speeds were underexposed and therefore a complete analysis, as given the 1/30 shutter speed, was not possible. Lens No. 2 however, did have reasonable exposures at all shutter speeds. This was because the lens was not filtered and the film in that position was Plus-X Aerecon which has a dynamic range adequate to accommodate the factor of 4.0 difference in exposure between the 1/30 of a second and 1/120 of a second. Table C-3 compares the shutter speed results for Lens No. 2. Because the one sigma deviations for the 1/60 and 1/120 results are ±6% or less, it is concluded that the repeatability of the shutter is ±6% or better at the three indicated shutter speeds of 1/30, 1/60 and 1/120 of a second. In terms of an image density error, for film developed to a unit gamma the ±6% deviation in repeatability means a ±0.025 density variation which is very close to the precision of the microdensitometer, in 0.020 in density.

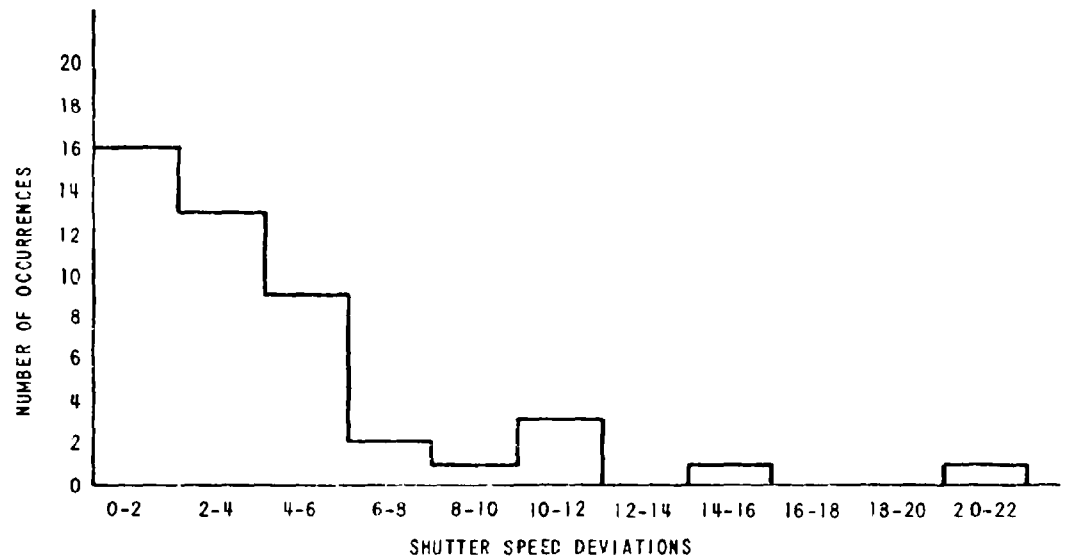

Figure C-1 HISTOGRAM OF THE ONE SIGMA DEVIATION OF SHUTTER SPEED MEASUREMENTS AT 1/30 OF A SECOND

Table C-2

SHUTTER SPEED (IN SECONDS) REPEATABILITY FOR FOUR CONSECUTIVE EXPOSURES

Format* Position	LENS POSITIONS								
	1	2	3	4	5	6	7	8	9
0.3	0266 ±6%	0287 ±10%	--	0315 ±16%	0318 ±12%	--	0325 ±3.6%	0312 ±1%	0278 ±22%
0.6	0303 ±2%	0298 ±5.4%	0327 ±2%	0334 ±6%	0326 ±5%	0329 ±4%	0329 ±3%	0330 ±4%	0331 ±3%
0.9	0320 ±5%	0325 ±3.7%	0326 ±2%	0335 ±3%	0328 ±5%	0333 ±1%	0327 ±2%	0345 ±8%	0334 ±2%
1.3	0335 ±4%	0315 ±2.9%	0335 ±4%	0328 ±2%	0322 ±7%	0329 ±6%	0334 ±6%	0343 ±2%	--
1.6	0328 ±12%	0317 ±4%	0327 ±2%	0315 ±14%	0330 ±2%	0340 ±1%	0341 ±2%	0342 ±3%	0338 ±6%
1.9	--	--	0329 ±0%	--	0313 ±1%	0333 ±3%	--	--	0344 ±4%

*Distance in inches from edge of frame.

Table C-3

COMPARISON OF LENS NO. 2 SHUTTER SPEEDS (IN SECONDS)
MEASUREMENTS - 1/30, 1/60, AND 1/120

Format* Position	Indicated Shutter Speeds 1/30 (0.0333 sec)	1/60 (0.0167 sec)	1/120 (0.00833)
0.3	0.0287 ±10%	--	--
0.6	0.0298 ±5%	0.0185 ±6%	0.00925 ±6%
0.9	0.0325 ±4%	--	0.00953 ±4%
1.1	--	0.0192 ±5%	-
1.3	0.0315 ±3%	--	--
1.6	0.0317 ±4%	--	0.00910 ±1%
1.9	--	0.0196 ±4%	0.00888 ±3%

*Distance in inches from edge of format for film developed to a unit gamma, the ±6% deviations in repeatability means a ±0.025 density variation, which is very close to the precision of the microdensitometer, i.e., ±0.020.

1.4 CAMERA OPERATIONAL PROBLEMS

Figure C-2 shows the first set of simultaneous frames taken during the bench test, at a shutter speed of 1/30 of a second and an f/number of 2.4. The very white images of frames 1, 3, 5, 6, 7, 8, and 9 are the results of one or more light leaks in the camera. This pattern occurred in 40 out of 80 frames taken. The 40 frames on which the pattern occurred were either exposed one at a time (uniform light source photos) or were the first frame in the series of five frames for shutter tests. This suggests that the light leak occurs only on the start cycle and not on the recycle. It was recommended that this light leak be found and repairs made in that short passes were expected to be used during the tests in Puerto Rico which could result in the loss of valuable data from the light leak.

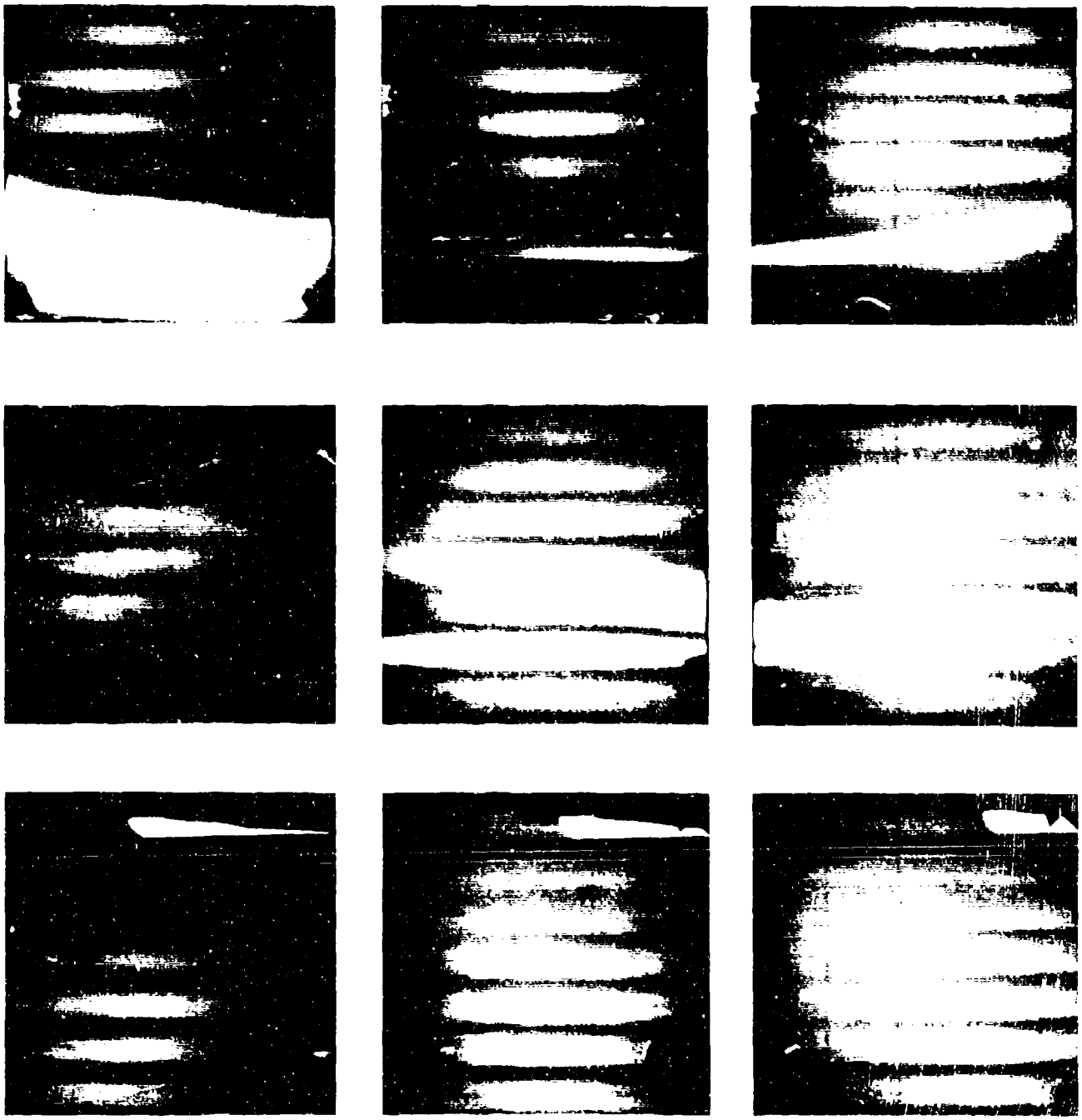

Figure C-2 LIGHT LEAKS IN MODEL 002 MULTIBAND CAMERA

It was also noted that the frame counter for frames 7, 8 and 9 failed to operate and the counter for frames 1, 2 and 3 did not function properly. The correct marking of frames is essential in that ground panels for identification are not feasible at the scales to be flown in Puerto Rico. Therefore, it was also recommended that these counters be repaired and spares be carried to Puerto Rico for field repairs, if necessary.

Finally, four parallel lines in the direction of flight were noted on the infrared film. These lines were light in tone, but were not scratches. It appears that these lines are pressure marks either related to the vacuum back or the transport roller. In either case they would have a significant effect upon the measurement density for images in these locations. It was therefore recommended that maintenance be undertaken to eliminate these lines.

Because of the requirements for the use of this camera on other projects prior to its use in Puerto Rico these repairs could not be made. However, being aware of the light leak, the AFCRL flight crew turned the cameras on early to avoid loss of data over the target area. Since the quantitative analysis of the films has been of limited extent, no difficulty has been encountered because of the counter problem or the lines on the infra red film.

II. CONCLUSIONS AND RECOMMENDATIONS

The Itek, Model 002, 9-lens camera can be used to take filtered aerial photographs with which to conduct a meaningful quantitiative analysis to derive ground object reflectance although the precision will be less than could be scheduled. It is recommended that only images with between the lens shutters located 0.2 inches or farther past the leading edge of the film format be used for densitometric analysis to reduce the large errors which may be introduced by the shutter in the first 0.2 inches of travel.

Appendix D

TERRAIN SENSING IN THE THREE TO FIVE MICRON SPECTRAL BAND

1. INTRODUCTION

AFCRL has an infrared sensor (MIAI) which records data for determining the relative radiances of terrain features in the 3 to 5 micron region of the spectrum, from image densities on film. To perform a densitometric, quantitative analysis of terrain feature radiance in this band, a control procedure similar to that used for the visible and near infrared portions of the spectrum is required. This appendix describes a control procedure that can be used to derive quantitative data on the radiance of ground object in the 3-5 micron band. The control procedure consists of utilizing ground control targets, a signal generating device in the aircraft and a technique to relate image density to radiance at the detector. Because of difficulties encountered in the field inadequate sensor data was obtained to validate properly the procedure, by a quantitative analysis of natural earth object radiance. However, the limited data reduction performed suggested that the procedure is valid.

Had adequate data been collected additional methodology is provided for obtaining measurements of ground object emissivities and surface temperature from the film image densities.

2. THE PROBLEMS

The basic process of obtaining quantitative values of object radiance from measurements of the density of imagery obtained using a remote detection device is similar whether the device operates in the visible, near infrared or far infrared portion of the spectrum. The remote sensor collects a part of the energy (reflected or emitted) coming from the object which is then translated to an image of specific density on film. To complicate the problem, the relationship between the radiance sensed by the remote detector and the resultant density of the recording film is difficult to determine for the following reasons.

2.1 NONLINEARITY

The remote sensor is composed of five basic components each of which affects the density of the recorded image. Figure 1 is a block diagram of a typical infrared scanner. The first concern is with nonlinearity in the last three components.

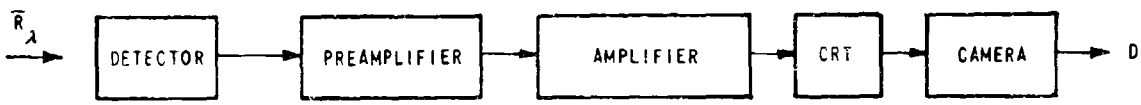

Figure D-1 BLOCK DIAGRAM OF TYPICAL INFRARED SCANNER

An aggravation to this problem is that changing altitude, or time of day a mission is flown or flying over terrain of extremely different average radiance properties requires that the non linear transfer functions of the amplifier, CRT, and camera be manually changed. Fortunately, once set, the combined transfer function for all three parts will only change slowly with time.

2.2 CONTROL TARGETS

A second difficulty is that of calibrating the control targets. In order to discuss this properly, we must first review the fundamentals of target radiance. The review is of special interest here as applied to control targets, but may be applied to any target.

The total radiance (watts/unit solid angle/unit projected area) of an object at a given temperature (T) over the electromagnetic spectrum is given by the equation

$$R_T = \frac{1}{\pi} \int_0^\infty \epsilon_\lambda R_{BB_\lambda} d\lambda + \frac{1}{\pi} \int_0^\infty \rho_\lambda \cdot H_\lambda d\lambda \qquad (1)$$

assuming the surface of the object is diffuse

where

ϵ_λ = object emissivity

R_{BB_λ} = radiation of a black body at the same temperature as the object (watts/unit area/micron)

ρ_λ = object reflectivity

H_λ = irradiance on the object (watts/unit area/micron)

λ = wavelength

If in the wavelength region of interest (3-5 μ for the MIAI scanner) the emissivity of the objects of interest is nearly constant, an average value $\bar{\epsilon}$ can be assigned for the emissivity. The reflectivity of an object must therefore also be nearly constant in that Kirkoff's Law states that reflectivity is equal to one minus emissivity ($\rho = 1-\epsilon$). Thus Equation 1 reduces to:

$$\bar{R}_{3-5} = \frac{\bar{\epsilon}}{\pi} \int_{3\mu}^{5\mu} R_{BB_\lambda} d\lambda + \frac{(1-\bar{\epsilon})}{\pi} \int_{3\mu}^{5\mu} H_\lambda d\lambda \qquad (2)$$

Now then, the integral of $R_{BB}d\lambda$ is merely the area $\bar{A}_{BB}$ under the black body radiation curve for a specific temperature over the 3-5 micron spectral region and the integral of $H_\lambda d\lambda$ is the area ($\bar{A}_H$) under the irradiance curve (also in the 3-5 micron band) so that Equation 2 can be written as:

$$\bar{R}_{3-5} = \frac{\bar{\epsilon}}{\pi} \bar{A}_{BB} + \frac{(1-\bar{\epsilon})}{\pi} \bar{A}_H \qquad (3)$$

Thus the radiance which a remote sensor detects in the 3-5 micron region of the spectrum is a function of the object's average emissivity (and reflectance), its temperature, and the total energy falling upon its surface in the spectral band considered. Although black body radiation curves are known and the average surface temperature of ground objects (control targets) can be measured, instrumentation for measuring irradiance in the 3-5 micron region of the spectrum is costly. Thus the emitted component of the control target radiance may be known but not the reflected.

2.3 DC LOSS

The preamplifier has a time constant on the order of a few scans of the detector, so that the bias is automatically adjusted thus keeping the brightness of the CRT spot within the dynamic range of the recording film. One may think of this as an automatic exposure control on an aerial camera. Because of this, the absolute densities of images do not relate directly to the absolute radiances of the objects. Although a pleasing, well exposed picture is produced, this problem is by far the greatest deterrent to using present scanners for quantitative analyses. It is true that separate recording of the D.C. level would eliminate the difficulty, but this would require major modifications to the scanner.

3. THE SOLUTIONS

Basically we must relate film density to ground radiance in order to use the remote sensor data to measure terrain emissivity, reflectivity or temperature. As with the multiband camera, this can be accomplished by determining the transfer functions of each individual sensor component, and external attenuations, or more simply by using a relative analysis of the unknown to a known object radiance on the ground. The latter approach is preferred because it is inherently simplier than the former. In either case, the transfer function between radiance at the detector and film image density must be determined.

The problem of nonlinearity is solved by use of a calibrating signal generator, the control target problem is solved by use of three rather than the customary two control targets, for photographic systems and the D.C. loss is solved by use of a grass substandard, as described below.

3.1 NONLINEARITY

We built a signal generator for the MIAI scanner which could be plugged into the amplifier in place of the detector and preamplifier to generate a density step wedge on the film output. This generator is described in Appendix E.

The step wedge which should have preceded each data pass, was to be scanned on microdensitometer to obtain the transfer function between preamplifier voltage output (or video amplifier input voltage) and film density for each pass. Because the lens of the recording camera has a transmission loss from the on axis position to the format edge several microdensitometer scans were to be made to obtain the transfer function as a function of image off-axis position in the format. The true shape of this function could not be established precisely, because the step wedge generator was not utilized on a sufficient number of flights during the tests. However, Figure 2 has been included for illustrative purposes.

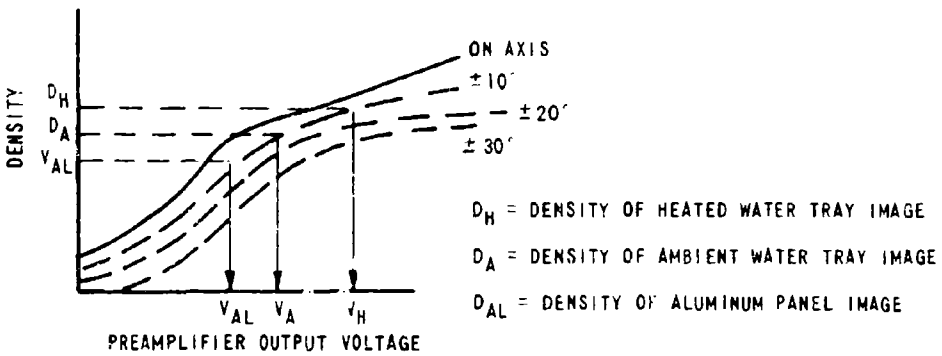

Figure D-2 ILLUSTRATION OF REDUCED STEP WEDGE DATA

The density of the image of any target may be measured and the preamplifier voltage determined from the appropriate curve of figure D-2 above.

3.2 CONTROL TARGETS

At the site of the ground reflection panels for the multi-band camera, we constructed two 20 foot x 20 foot x 4 inch water trays, one of which was heated. Also a 20 foot x 20 foot aluminum target and a dense grass target were constructed. By use of the water and aluminum target densities and the procedure indicated below, the radiance of any target which lies in the same scan as the control targets may be found.

The measured radiance of an object can be expressed* as follows:

$$\bar{R} = \alpha V_T + R_0 \qquad (5)$$

where V_T = the voltage output of the preamplifier

α = a constant

and R_0 = a radiance value which is dependent upon the past history of the radiance level sensed by the scanner.

Thus, we have the following set of equations:

$$\bar{R}_H = \alpha V_H + R_0$$

$$\bar{R}_u = \alpha V_u + R_0$$

$$\bar{R}_{AL} = \alpha V_{AL} + R_0$$

where the subscripts H, u, and AL refer to heated water, unheated water, and aluminum, respectively. The voltages are determined from the densities using figure D-2 above. So long as the three control targets are all in the same scan lines α and R_0 are the same for all three equations. From Equation 3

* Tests using the 3-5 micron detector and preamplifier of the CAL Bendix scanner suggests this expression is quite valid.

$$\bar{R}_H = \frac{1}{\pi}\left[\bar{\epsilon}\, A_{BB_H} + (1-\bar{\epsilon})\,\bar{A}_H\right]$$
$$\bar{R}_u = \frac{1}{\pi}\left[\bar{\epsilon}\, A_{BB_u} + (1-\bar{\epsilon})\,\bar{A}_H\right]$$
$$\bar{R}_{AL} = \frac{1}{\pi}\left[\bar{\epsilon}_{AL}\, A_{BB_{AL}} + (1-\bar{\epsilon}_{AL})\,\bar{A}_H\right]$$

From a measurement of the surface temperatures of the heated water target, the unheated water target, and the aluminum target, the black body radiation values are determined from the black body radiation curves (i.e., A_{BB_H}, A_{BB_u} and $A_{BB_{AL}}$) for each of these temperatures. The emissivity of water is approximately 0.98 across the 3-5 micron spectral region and that for aluminum is approximately 0.02. Equating the two sets of equations we have:

$$\alpha V_H + R_o = \frac{1}{\pi}\left[\bar{\epsilon}\, A_{BB_H} + (1-\bar{\epsilon})\,\bar{A}_H\right]$$
$$\alpha V_u + R_o = \frac{1}{\pi}\left[\bar{\epsilon}\, A_{BB_u} + (1-\bar{\epsilon})\,\bar{A}_H\right]$$
$$\alpha V_{AL} + R_o = \frac{1}{\pi}\left[\bar{\epsilon}_{AL}\, A_{BB_{AL}} + (1-\bar{\epsilon})\,\bar{A}_H\right]$$

The unknowns are A_H, R_o, and α. The three equations can be solved simultaneously for these unknowns. By substituting both R_o and α into the first set of equations the Radiances of the targets can be plotted as a function of the output voltage of the preamplifier, as shown in Figure D-3, solid line.

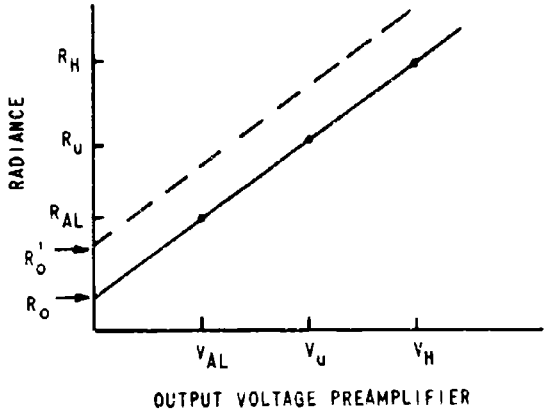

Figure D-3 RADIANCE-VOLTAGE CALIBRATION CURVE

Thus, for any target in the same scan as the water and aluminum targets, the radiance may be found by (1) measuring the density of the image, (2) determining the voltage from Figure D-2, and (3) determining radiance from Figure D-3, solid line.

3.3 D.C. Loss

For any other terrain feature of interest in the scene, but not on the same scan lines as the control target, the R_o factor of Equation 5 may well have changed considerably. Therefore, a constant radiance target is necessary running throughout the length of the area of interest. A small stream or creek would make an excellent target, however these are generally not present. In natural terrain grass is generally present over the entire area of interest. If a multi-band camera system is flown simultaneously with the infrared scanner the vigor and percentage of grass cover can be evaluated by measuring the reflectance properties in the near infrared and the red portion of the spectrum. Those images having the same properties in these bands can then be selected for use as standard targets for the far infrared.

The density of the image of the grass area within the same scan lines as the three control target are now measured and the corresponding voltage obtained from the appropriate curve of Figure D-2. From the density of images of similar grass areas in other scans on the infrared record, the apparent voltage output of the preamplifier can be obtained from the appropriate calibration curve of Figure D-2. By using the differences in voltages for these grass samples to adjust the voltage values derived from the film densities of any other objects of interest in the same scan lines as the remote grass area, the radiances for these objects can now be determined directly from Figure D-3, the Radiance/Voltage output calibration curve for the data pass. Thus the procedure for obtaining the radiance of terrain features in the three to five micron spectral band is complete.

4. SOIL PROPERTIES AND FAR INFRARED RADIANCE

Investigators, using a qualitative analysis, namely interpretation of far infrared records, have observed film density differences in terrain features of interest. They have attributed these density differences caused by total radiance differences, to temperature or emissivity differences between the terrain features. This practice is highly arbitrary, in that very little is known about the emissivities of terrain features, and the irradiance at the time such films are recorded. The quantitative analysis approach allows us to investigate the contributions of emissivity, reflectivity and irradiance to the total radiance sensed by the scanner, with a minimum of assumption necessary.

Emissivity Measure

To obtain an emissivity measure of a terrain feature in the scene, we must measure the average surface temperature of the feature. This can be done with a radiometer or surface thermistors.

We must assume that the irradiance on the feature is equal to that on the standard grass target, which should be quite valid provided the two are in close proximity on the ground and no cloud shadows are present. We can determine the absolute level of the irradiance (A_H) as described previously. It is now possible to measure the terrain features emissivity using the following equation.

$$\epsilon = \frac{\pi R_T - A_H}{\bar{q}_{BB} - A_\mu} \qquad (6)$$

where

R_T = the radiance of the feature derived from its image film density

A_μ = the irradiance derived from the density of the image of grass control target

$\bar{R}_{BB}$ = the black body radiation derived from the black body radiation curve for the appropriate temperature

5. TEMPERATURE MEASURE

To obtain the surface temperature of a terrain feature we must have a measure of its average emissivity. This can be obtained by selecting several samples of the terrain feature of interest in the field and using the procedures described above to measure an average emissivity from film density values. Using this average emissivity value for the terrain feature of interest, the value of R_o derived from the density of the image of the grass control target and the total radiance of the feature derived from its image density, the black body radiation of other examples of the same type of terrain feature can be computed from the following equation:

$$\bar{R}_{BB} = \frac{\bar{L}}{\bar{\epsilon} R_o - R_H} - R_H \qquad (7)$$

Black body radiation curves can then be used to determine the surface temperature of the feature.

Moisture Effects

Of particular importance with respect to terrain sensing in the far infrared spectral region is the theory that soil moisture content can be evaluated from records taken at different times of the day. The rate of change of temperature for a moist soil should be different from that of a less moist soil because of the differences in the specific heats of the soils.

Depending upon the precision with which the temperature measure of a soil surface can be obtained from the procedure described above and the magnitude of the change of surface temperature which will occur between a pre and post sunset mission it would be feasible to investigate this theory from

the data to be collected in Puerto Rico. However, because of a problem encountered by the air crew on applying the step wedge to the film before each pass, suitable data for the analysis were not acquired.

Appendix E

MIAI SIGNAL GENERATING CALIBRATOR

SIGNAL GENERATING CALIBRATOR

The calibrator is a solid state pulse generator which can be triggered by an external negative pulse. Trigger amplitudes may vary between 6 and 20 volts. The output is a selectable positive or negative going pulse whose full scale amplitude may be varied between 10 millivolts and 200 millivolts. A decade precision attenuator is included to obtain 0.1 full scale amplitude increments.

Figure 1 shows a schematic of the unit. The output pulse has a nominal pulse width of 2.5 milliseconds, and peak amplitude of 4.0 volts, as shown in Figure 2. The pulse width may be varied to any width between 10 sec and 2.6 sec. The unit uses a self-contained battery supply which has an operating life in excess of 10 hours.

Because the calibrator will be used as an input to a capacitor coupled video amplifier, the output of the video amplifier will be corrupted by the time constants in the coupling networks, and a droop in the pulse will exist. The amount of the droop represents the degradation of the video signal during a one half scan line period, and will result in a change in the gray level over the half line period.

Operation

To use the calibrator, proceed as follows:

1. Connect the desired trigger signal to the TRIG. INPUT of the calibrator.
2. Connect the calibrator OUTPUT to the input of the video amplifier.

3. Turn calibrator power to ON position.

4. Set output polarity switch to the desired output polarity, (+ or -).

5. Set attenuator to full scale position, 10.0.

6. Adjust level control to obtain the desired full scale output, as observed on the monitor scope.

7. Initiate calibration routine (start camera, etc.), then decrease attenuator from 10.0 to 0 in equal time increments.

8. When calibration has been completed, turn power OFF and disconnect calibrator.

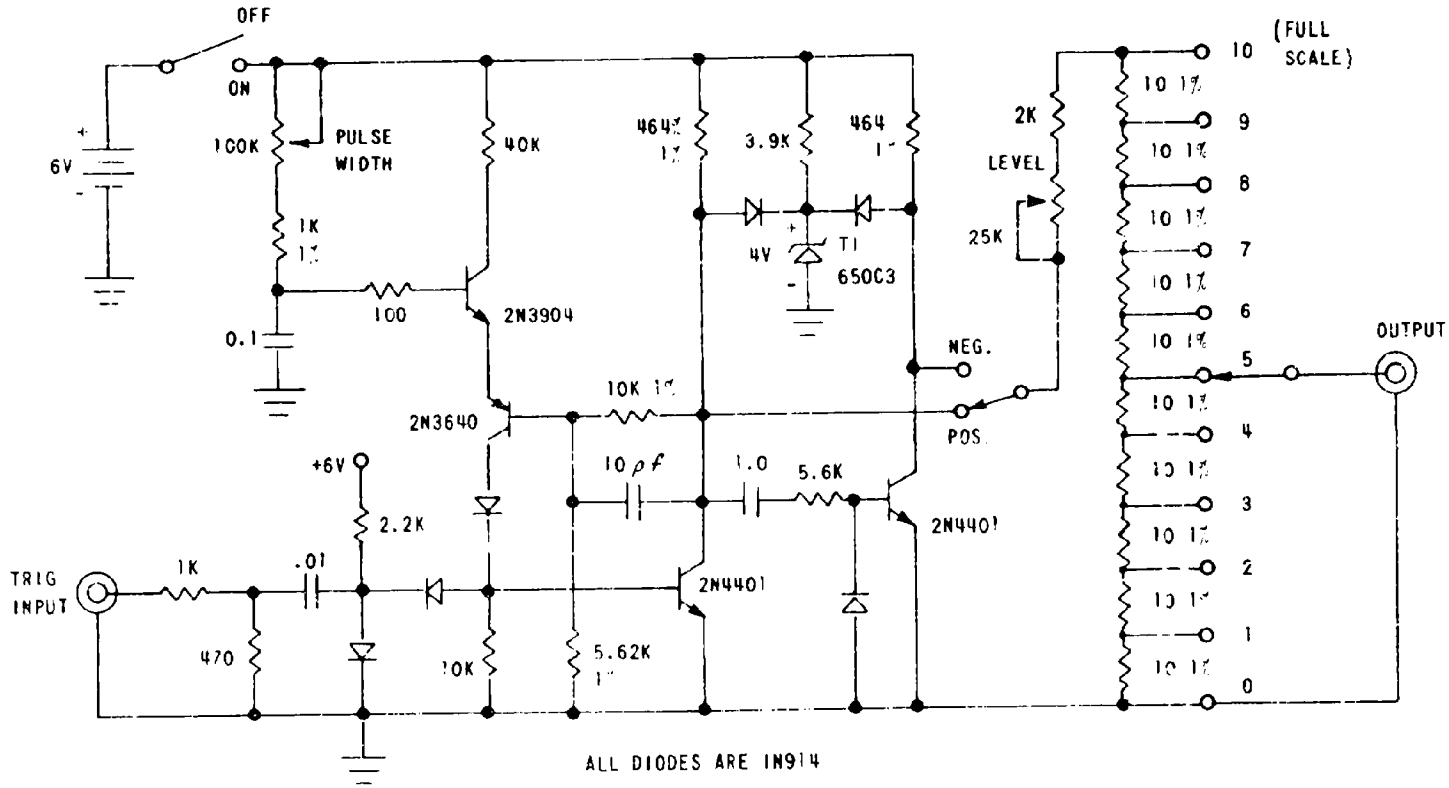

Figure E-1 PULSE GENERATOR SCHEMATIC

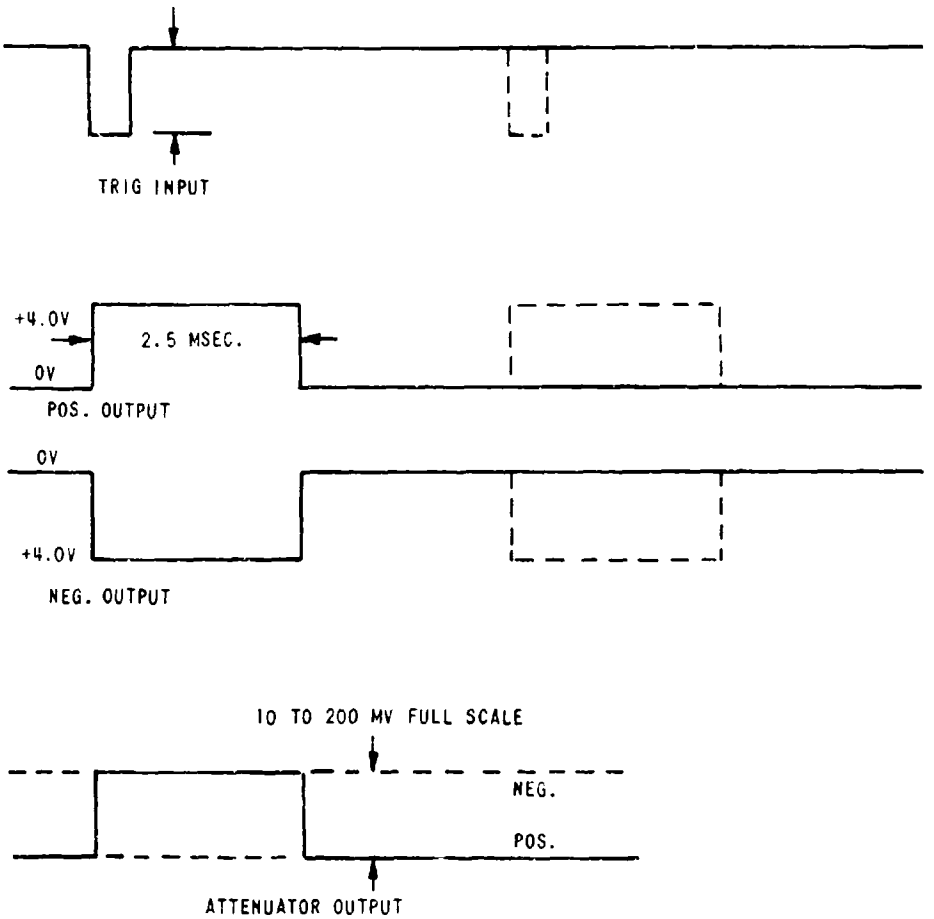

Figure E-2 PULSE GENERATOR OUTPUTS

UNCLASSIFIED
Security Classification

DOCUMENT CONTROL DATA - R & D

(Security classification of title, body of abstract and indexing annotation must be entered when the overall report is classified)

1. ORIGINATING ACTIVITY (Corporate author)
Cornell Aeronautical Laboratory, Inc.
Buffalo, New York 14221

2a. REPORT SECURITY CLASSIFICATION
UNCLASSIFIED

2b. GROUP
N/A

3. REPORT TITLE
A PROGRAM TO ACQUIRE ENVIRONMENTAL FIELD DATA IN FOUR AREAS IN A HUMID SUBTROPIC ENVIRONMENT

4. DESCRIPTIVE NOTES (Type of report and inclusive dates)
Scientific Final, 1 May 1968 - 31 August 1969, Approved 12 November 1969

5. AUTHOR(S) (First name, middle initial, last name)
John E. Walker

6. REPORT DATE	7a. TOTAL NO. OF PAGES	7b. NO. OF REFS
November 1969	163	39

8a. CONTRACT OR GRANT NO	9a. ORIGINATOR'S REPORT NUMBER(S)
F 19628-68-C-0339	VT-2636-O-1
b. Project, Task, Work Unit Nos. 7628-03-01	
c. DoD Element: 6240539F	9b. OTHER REPORT NO(S) (Any other numbers that may be assigned this report)
d. DoD Subelement: 681000	AFCRL-69-0393

10. DISTRIBUTION STATEMENT
Distribution of this document is unlimited. It may be released to the Clearing House, Department of Commerce, for sale to the general public.

11. SUPPLEMENTARY NOTES	12. SPONSORING MILITARY ACTIVITY
TECH, OTHER	Air Force Cambridge Research Laboratories (CRL) L.G. Hanscom Field, Bedford, Mass. 01730

13. ABSTRACT

Multiband remote sensing provides a means of obtaining signatures for natural earth objects and backgrounds. The Air Force Cambridge Research Laboratories (AFCRL) collected multiband data from four humid tropical environments in Puerto Rico. The Cornell Aeronautical Laboratory Incorporated (CAL) collected field data and performed a limited quantitative analysis toward the objective of defining terrain signatures. Irradiance spectral reflectance, surface temperature, soil moisture, soil granularity, air temperature, humidity, wind speed and direction measurements and ground photographs were obtained. The limited analysis resulted in the development of bi band methodology for determining whether variations in film image density of soil is caused by surface moisture or surface structure. If the ratio of the average exposures (low/high) of two images of soil in the blue region of the spectrum (.50) is equal to or greater than their exposure ratios in the near infrared (0.80) the difference is attributable to surface structure; if less, then the cause is surface moisture. The results also suggest that for surface structure, the absolute value of the ratio can be related to the amount of textual difference between the surfaces. It is concluded that an electro-optical multiband analysis system using bi band techniques can be developed to facilitate the Air Force engineers task of terrain analysis and at the same time provide him with the tools necessary to extend the utility of multiband remote sensing to obtain spectral signatures for other earth objects and backgrounds.

DD FORM 1 NOV 65 1473

UNCLASSIFIED
Security Classification

14 KEY WORDS	LINK A		LINK B		LINK C	
	ROLE	WT	ROLE	WT	ROLE	WT
Environmental Field Data						
Humid Environment						
Spectral Reflectance						
Vegetation						
Soils						
Water						
Remote Sensing						
Multiband						
Infrared						